Line-fitting method of model order reduction for elastic multibody systems

Dissertation

zur Erlangung des akademischen Grades

Doktoringenieur (Dr.-Ing.)

von Dipl.-Ing. Valery Makhavikou

geb. am 30.05.1986 in Mogilev, Weißrussland

genehmigt durch die Fakultät Maschinenbau

der Otto - von - Guericke - Universität Magdeburg

Gutachter:

Prof. Dr.-Ing. Roland Kasper

Prof. Dr.-Ing. Andrés Kecskeméthy

Dr.-Ing. Dmitry Vlasenko

Promotionskolloquium am 24.07.2015

Acknowledgments

I would like to express my special gratitude to Prof. Dr. Roland Kasper, my research supervisor, for his professional advices, constructive critiques, patient guidance, and willingness to generously invest his time in this research. My grateful thanks are also extended to Dr. Dmitry Vlasenko for planning and controlling the investigation, for his help in analysis of results obtained during this study, and for the establishment of joint projects of the Otto-von-Guericke University and the Schaeffler Technologies AG & Co. KG in the field of elastic multibody simulation. I wish to acknowledge the Schaeffler company for the financial support of the research and for finite element models used in this thesis. I am sincerely grateful to the Otto-von-Guericke University for the financial support and creation of all necessary conditions for the efficient conduction of scientific work. Finally, I would like to express my special thanks to my wife and parents for their valuable support and encouragement throughout this study.

Abstract

Computer aided simulation is an important part of development of modern technical products. Simulation enables optimization of system design and identification of possible operational problems without manufacturing the product. Many modern technical systems operate at high speeds and include lightweight components. Such systems can undergo deformation effects that considerably influence system dynamics and, consequently, must be taken into account in a process of system modeling and simulation.

The subject of this research relates to simulation of elastic multibody systems. The elastic multibody system is a system of rigid and elastic bodies interconnected by joints or coupling elements, in which the bodies may undergo large rigid body motion and small deformations. In this work the modeling of multibody dynamics is made with the help of a floating frame approach. Dynamics of an elastic body is formulated using a finite element method, which results in the transformation of partial differential equations of motion into a set of ordinary differential equations. In order to describe the elastic behavior accurately, it is necessary to use a fine discretization, which leads to finite element models having a large number of elastic coordinates. For this reason, efficient simulation of finite element models of industrial applications often becomes difficult or even infeasible. In order to enable simulation of multibody systems containing large models of elastic bodies, elastic coordinates are reduced by means of model order reduction methods. Reduced order models preserve important dynamic information of original models and make the simulation of elastic multibody system more efficient from a computational point of view.

Over the last decades a variety of reduction techniques have been developed. The set of classical reduction methods includes condensation, modal truncation, and component mode synthesis. The category of modern reduction approaches consists of techniques based on the singular value decomposition using Gramian matrices and moment matching via Krylov subspaces.

The main scientific contribution of this thesis is a new method of linear model order reduction. The proposed method solves the problem of classical reduction approaches: a lack of possibility to tune a reduced order model for certain transfer functions and certain frequency ranges. In addition, the new approach satisfies the following requirements: high accuracy, preservation of stability of reduced order models, small order and stiffness of reduced order models, and the possibility of application in the context of elastic multibody systems. The proposed method differs from the modern reduction approaches and has its

own advantages.

The proposed reduction approach relies on the idea of line fitting of model transfer functions. The method is evaluated using several application examples. The reduced order models are validated in the time and frequency domains and the results are compared with the results of the classical Craig-Bampton approach. It is shown that the proposed method generates reduced order models with higher accuracy, smaller order, and smaller stiffness. The computational cost of a coordinate transformation matrix is higher then in the Craig-Bampton method, but it remains acceptable for moderately dimensional finite element models.

Kurzfassung

Die computergestützte Simulation ist ein wichtiger Bestandteil bei der Entwicklung von modernen technischen Produkten. Simulationen ermöglichen eine Optimierung des Systemdesigns sowie eine Identifizierung möglicher Betriebsprobleme vor der Herstellung eines Produkts. Viele moderne technische Systeme arbeiten mit hohen Geschwindigkeiten und bestehen aus diversen Leichtbauteilen. Solche Systeme können Deformationseffekten unterliegen, die die Systemdynamik deutlich beeinflussen. Deswegen müssen sie bei der Systemmodellierung und Simulation mit berücksichtigt werden.

Der Fokus dieser wissenschaftlichen Arbeit ist auf die Simulation von elastischen Mehrkörpersystemen gerichtet. Ein solches System besteht aus starren und elastischen Körpern, die über Gelenke bzw. Verbindungselemente miteinander verbunden sind. Weiterhin unterliegen diese Körper großen Starrkörperbewegungen sowie kleinen Deformationen. In dieser Arbeit wird die Modellierung der Mehrkörperdynamik mit Hilfe der Methode des bewegten Bezugssystems durchgeführt. Die Dynamik eines elastischen Körpers wird unter Verwendung der Finite-Elemente-Methode beschrieben. Diese überführt die partiellen Differentialgleichungen mit denen elastische Systeme beschrieben werden in einen Satz von gewöhnlichen Differentialgleichungen. Um das elastische Verhalten genau zu beschreiben, ist es notwendig eine feine Diskretisierung zu verwenden. Dies resultiert in einer großen Anzahl von elastischen Koordinaten. Aus diesem Grund wird es oft schwierig oder teilweise sogar unmöglich, eine effiziente FEM Simulation durchzuführen. Um die Simulation von elastischen Mehrkörpersystemen mit relativ großen Modellen zu ermöglichen, wird die Anzahl elastischer Koordinaten mit Hilfe eines Ordnungsreduktionsverfahrens stark verringert. Das reduzierte Modell enthält die wichtigen dynamischen Informationen des Originalmodells und ermöglicht eine recheneffiziente Simulation von großen elastischen Mehrkörpersystemen.

In den letzten Jahrzehnten wurde eine Vielzahl von Ordnungsreduktionsverfahren entwickelt. Klassische Reduktionsverfahren umfassen die Kondensation, die Modale Reduktion und die Komponenten-Modus-Synthese. Die modernen Reduktionsansätze setzen sich aus den Verfahren Gramscher Matrizen und den Krylov-Unterraummethoden zusammen.

Der wissenschaftliche Hauptbeitrag dieser Arbeit ist eine neue Methode der linearen Ordnungsreduktion. Das vorgeschlagene Verfahren löst das Problem der klassischen Reduktionsansätze. Dazu zählt die fehlende Möglichkeit zur Abstimmung des reduzierten Mod-

ells für bestimmte Übertragungsfunktionen und bestimmte Frequenzbereiche. Darüber hinaus erfüllt der neue Ansatz die folgenden Anforderungen: hohe Genauigkeit, Erhaltung der Stabilität, niedrige Ordnung, hohe Steifigkeit und die Möglichkeit der Anwendung im Rahmen elastischer Mehrkörpersysteme. Das vorgeschlagene Verfahren unterscheidet sich von den modernen Reduktionsansätzen und besitzt diverse Vorteile.

Das vorgeschlagene Reduktionsverfahren basiert auf der Idee der Kurvenanpassung von Übertragungsfunktionen. Die Methode wird anhand mehrerer Anwendungsbeispiele bewertet. Die reduzierten Modelle werden im Zeit- und Frequenzbereich geprüft. Die Ergebnisse werden mit den Ergebnissen des klassischen Craig-Bampton Ansatzes verglichen. Es wird gezeigt, dass die vorgeschlagene Methode reduzierte Modelle generiert, die eine höhere Genauigkeit, eine niedrigere Ordnung und kleinere numerische Steifigkeit besitzen. Der Rechenaufwand einer Koordinatentransformationsmatrix ist höher als bei der Craig-Bampton Methode, aber annehmbar für FE-Modelle mit moderater Dimension.

Contents

List of Figures

List of Tables

Notation

Roman Symbols

$\mathbf{A}$	rotation matrix
$\mathbf{I}$	identity matrix
$\mathbf{q}$	vector of elastic coordinates
$\mathbf{S}$	matrix of space dependent shape functions
$\mathbf{x}$	position coordinates for an origin of body frame
$\mathbf{z_I}$	vector of generalized velocity coordinates of a body
$\mathbf{z_{II}}$	vector of generalized acceleration coordinates of a body
$\mathbf{z}$	vector of generalized position coordinates of a body
m	mass of a body

Greek Symbols

$\boldsymbol{\alpha}$	vector of angular acceleration
$\boldsymbol{\omega}$	vector of angular velosity
$\boldsymbol{\sigma}$	stress vector
$\boldsymbol{\theta}$	vector of rotational parameters of body frame
$\boldsymbol{\varepsilon}$	strain vector

Abbreviations

CMS	Component Mode Synthesis
DoF	Degree of Freedom
EMBS	Elastic Multibody System
FEM	Finite Element Method

MAC Modal Assurance Criterion

NRED Normalized Relative Eigenfrequency Difference

ODE Ordinary Differential Equation

PDE Partial Differential Equation

ROM Reduced Order Model

SVD Singular Value Decomposition

Mathematical Symbols

$\hat{}$ (hat) denotes reduced order coordinates

$\tilde{}$ (tilde) transform a three dimensional vector to a skew-symmetric matrix

1 Introduction

1.1 Research area

Simulation is an essential part of development of modern technical products because it enables evaluation of system behavior without its construction. Computer aided analysis helps to optimize product design and performance, to identify possible operating problems.

In recent decades the interest to light-weight, high-speed and precise mechanical systems has been greatly increased. Some parts of such products usually undergo deformation effects, which must be taken into account during a process of system modeling and simulation.

In this thesis we focus on the simulation of elastic multibody systems (EMBS). The term EMBS denotes a group of interconnected rigid and elastic bodies that may undergo large rotational and translational motions. Elastic bodies are solid bodies that return to their initial shapes after applied stresses are removed. EMBS appear in applications of many engineering fields: robotics, biomechanics, vehicle and aircraft dynamics.

Modeling of EMBS is based on methods of multibody system dynamics and theory of elasticity. The most efficient way to describe dynamics of elastic multibody systems undergoing small deformations is a floating frame formulation. According to this method the total motion of elastic body is divided into two parts: rigid body motion represented by the motion of body reference frame and deformations with respect to this frame.

Dynamic formulation of elastic body leads to a set of time- and space-dependent partial differential equations (PDEs). These equations can be solved analytically only for models having simple geometries. In other cases, the set of PDEs is approximated by a set of ordinary differential equations (ODEs) that are obtained by means of spatial discretization techniques. The most used approach for this purpose is a finite element method (FEM). In many applications a large number of elastic coordinates have to be employed to properly describe body deformations. Complex finite element models are usually described by more than half a million of ODEs. Simulation of such models on standard computers is not feasible. In the case of small deformations, it is possible to solve the problem using model order reduction techniques. These methods approximate the large set of ODEs by a small number of equations that keep important dynamic properties of the original system. The quality of approximation depends on a choice of model order reduction method.

The main scientific contribution of the thesis is a new linear model order reduction method for elastic multibody simulation. In the next sections we review previous and current studies relevant to this topic, formulate demands on model order reduction methods, and identify a drawback of classical reduction approaches. The method proposed in the thesis satisfies the stated demands and addresses the problem of classical reduction approaches.

1.2 State of the art

In the past three decades, the interest to elastic multibody applications caused extensive research of approaches for modeling and simulation of elastic multibody systems. The past studies can be separated into two large groups: modeling of elastic multibody dynamics and model order reduction. The information about the modeling and simulation of EMBS is presented in the textbooks [77, 79] and review articles [78, 89]. Description of basic model reduction methods can be found in the books [70, 6, 74]. An overview of classical reduction techniques is presented in [5]. Additional references on the studies relevant to the thesis topic are given further in the text.

1.2.1 Modeling elastic multibody dynamics

The modeling techniques of EMBS can be divided into two groups: *global reference frame formulation* and *intermediate reference frames formulation*. In the global reference frame formulation the motion of multibody system is described with respect to an inertial reference frame. This approach simplifies representation of inertia forces, but calculation of internal forces (stiffness and damping forces) becomes more complicated. The inertia forces can be found as a product of mass matrix and a vector of accelerations. It is not necessary to calculate Coriolis and centrifugal forces because they are already taken into account in the vector of inertia forces. However, the representation of internal forces is highly nonlinear in terms of global coordinates. This fact makes impossible using model order reduction methods together with the global reference frame formulation. The most suitable applications for this formulation are large deformation problems having a small order.

In the intermediate reference frame formulation the motion of flexible bodies in a multibody system is described using additional reference frames. The intermediate reference frame is attached to a flexible component and describe its rigid body motion. In this case, the motion of component relative to the intermediate reference frame is mainly a component's deformation. The approach enables representation of inertial forces as a linear function of intermediate frame coordinates. The most widely-used intermediate frame is attached to an entire flexible body and is called a *floating reference frame*. One of the important advantages of the floating frame formulation is a possibility to apply model reduction methods.

The motion of bodies using floating frames can be described by absolute or relative coordinates. These formulations result in different equations of motion. In the absolute coordinate formulation, the coordinates of body frames are written with respect to the global reference frame. Joints constrain system degrees of freedom and introduce algebraic equations to equations of motion. The unknown forces arising in joints are represented in terms of Lagrangian multipliers. Using absolute coordinate formulation it is simple to generate equations of motions, but the solution of differential algebraic equations requires a larger computational cost. The formulation suits to modeling of both open and closed-loop multibody systems [80, 4].

In the relative coordinate approach, the position and orientation of each body in a multibody system are defined with respect to a preceding body using degrees of freedom of joint connecting the bodies [19, 61]. This leads to a minimal set of generalized coordinates and automatically incorporates joint forces in the equations of motion. Numerical methods for solving this type of equations are more computationally efficient. However, the generation of equations of motion is more complicated: the relative coordinate approach requires additional step to define a tree structure of the system; for closed-loop EMBS it is necessary to define a location of cut-joint constraint.

Reviews of solution methods for the absolute and relative coordinates formulations can be found in [75, 27, 38].

Since there exits no unique manner of defining a floating frame it can be attached to a body in a number of different ways. These approaches can be divided into two categories. The methods of the first group attach the coordinate system to material points of the body. The most common procedure to do this is to set six nodal deflections to zero. These conditions attach a reference frame to the body and eliminate rigid body degrees of freedom in this coordinate system. As the body frame is allowed to move with respect to the inertial frame, attaching the moving frame to the body does not exclude any of the rigid body degrees of freedom in the inertial coordinate system. This formulation is referred to as *fixed axes* [80, 1, 68].

The second group of floating frames consists of coordinate systems that follow a body in an optimal manner. This category includes a frame oriented along the *principal axes* of inertia [62], *mean-axes* frame [60], and a *Buckens frame* [76, 77, 60]. In contrast to the fixed axes frames, coordinate systems of this type impose reference conditions on all points of the body. In the principle axes formulation the moving reference frame is enforced to coincide with the instantaneous principal axes of the deformable body. This method provides six conditions based on two basic concepts: the origin of the reference frame must remain at a instantaneous mass center, and three products of inertia must remain zeros. In this case, the coupling between flexible and rigid body motion is weaker and equations of motions become more simple. The mean-axes conditions are six constraints that enforce a frame to follow a body in such a way that the kinetic energy associated with the deformation stays at a minimum. The mean axes frame conditions simplify equations of

motion by transforming a generalized mass matrix to a block-diagonal form. The Buckens coordinate system is a frame relative to which the sum of squares of displacements, with respect to an observer stationed at the frame, is minimum. This type of moving frames is identical to a mean-axes frame for the applications where deformations are small. The choice of the Buckens frame leads to the smallest elastic deformation possible, which is an important issue for the construction of equations of motion under the assumption of small deformations. The moving frames eliminate the need to select material points for attaching the frame, but it is more difficult to determine their location because of specific frame conditions.

Elastic multibody systems include, in general, two types of bodies: bulky solids that can be treated as rigid bodies and bodies that are subjected to elastic deformations. The rigid bodies have a finite number of degrees of freedom, e.g. a rigid body in space has six DoFs that describe a position and an orientation of the body with respect to a global inertial frame. In contrast to rigid bodies, elastic components have an infinite number of DoFs that describe displacements of each point on the body. The dynamic behavior of such bodies is governed by a set of space and time dependent partial differential equations, analytical solution of which is only in seldom cases possible. It is especially difficult to find the analytical solution for bodies with complex body forms, special boundary conditions, and complicated material properties [43]. In order to solve the problem, various discretization methods were developed to approximate the solution of PDEs by a finite number of coordinates, e.g. the Rayleigh–Ritz method, the finite element method [11, 34, 20], the finite difference method [7], and the boundary element method [13]. All these methods generate so called shape functions that describe deformation shapes of a body in the multibody system. The difference between the methods lies in the way, in which the shape functions are constructed.

The deformation shapes have to satisfy boundary conditions imposed on the body [77, 76]. For bodies with simple geometries and simple boundary conditions the deformation shapes can be found using the Rayleigh–Ritz method. The analysis of more complex models is usually carried out by discretization methods as the FEM.

The commonly used discretization approach in elastic multibody dynamics is the FEM. It provides a systematic way for the construction of shape functions of geometrically complex models with boundary conditions. The approach has some important advantages for EMBS in comparison with the finite difference method and the boundary element method. The general procedure of finite difference approach is to replace derivatives by finite differences. It follows that the method can use only cubes as discretization elements; therefore, the approximation of body geometry, especially for curved areas, is worse. In addition, in the classical finite difference approach a local refinement of mesh is not possible and it has to be made throughout the entire geometry. This leads to models with larger number of nodes in comparison to the FEM models and makes difficulties for the analysis of stresses. One more useful property of FEM is a sparse structure of

matrices that require less memory space. The main advantage of finite difference method is the simplicity of application.

The difference between the boundary element method and FEM concerns the discretization. In the FEM the complete domain must be discretized, while the boundary element method requires discretization of only surfaces. It follows that the discretization effort is much smaller and changes in meshing are much easier to perform. Due to no further approximation is imposed on the solution at interior points, the boundary element method usually possesses advantages when dealing with stress problems. However, the solution matrix resulting from the boundary element formulation is non-symmetric and fully populated, therefore it is more expensive to store the matrices in the computer memory. Besides, treatment of thin structure and non-linear problems is difficult. Nowadays, the boundary element method is under the focus of intensive approach, but the FEM is more established and developed.

The mass matrix of FE model can be constructed using different formulations. In a *lumped mass formulation*, see [46, 67], the total mass of a body is divided between nodes of the model. This produces a diagonal mass matrix and reduces a numerical cost required to solve equations of motion. The drawback of the approach is that the inertia properties of the body are violated [79]. The *consistent mass matrix* is obtained using space dependent shape functions of finite elements. This formulation provides better approximation of body inertia and, as a result, better accuracy for higher frequencies and modes [42].

Equations of motion of elastic bodies require calculation of volume integrals that express dynamic properties of bodies. Finite element programs provide only a part of integrals required for the construction of equations motion using the floating frame approach. In order to obtain a complete set of volume integrals, special preprocessor modules are usually utilized [84, 69]. The calculation of volume integrals for the consistent mass approach can be found in [43, 55, 77, 82]. This process for the lumped mass formulation is considered in [3, 91]. The time-invariant data required for the construction of equations of motion can be computed in advance and stored in a Standard Input Data format that is proposed in [88].

The important aspect in modeling of deformations is connected with a choice of suitable type of analysis. The fundamental principle of linear analysis is the assumption that the change of stiffness is small enough, so it is possible to use the initial stiffness of the model throughout the entire process of deformation. The linear analysis provides an acceptable approximation for the most problems that engineers deal with. If the stiffness of deformable component changes significantly under operating conditions, nonlinear analysis becomes necessary [25]. The cause of nonlinear behavior can be different. A number of factors influence stiffness of deformable body: body shape, material properties, large loads, and presence of constraints. If changes of stiffness originate only changes in shape, nonlinear behavior is defined as *geometric nonlinearity*. This type includes large deformations problems, where deformations exceed approximately 10% of the smallest dimension

of body [63]. If changes of stiffness occur due to only changes in material properties under operating conditions, the problem type belongs to a category of *material nonlinearities*. A linear material model assumes stress to be proportional to strain, and once the load has been removed the model will always return to its original shape. If the loads are high enough to cause permanent deformations, then a nonlinear material model must be used. In certain cases, stiffness of a structure can also change due to large applied loads. The influence of stiffening effect is accounted by a geometric stiffness matrix that is added to the regular stiffness matrix. The stiffening effects (also called stress stiffening, geometric stiffening, or incremental stiffening) normally need to be considered for thin structures for which bending stiffness is very small compared to axial stiffness, such as cables, thin beams, and shells [63]. A typical example in this field is a rotating beam under the influence of large centrifugal forces [41, 76]. The geometric stiffness matrix can be generated using the methods from [71, 76, 10] and the data exported from commercial FE software.

1.2.2 Model order reduction

Finite element models of elastic bodies contain a large number of degrees of freedom, varying from several thousand to several million depending on a model geometry and accuracy demands. Due to the high computational cost dynamic analysis of such systems is practically not feasible. In order to solve the problem, engineers resort to the help of model order reduction methods, which can greatly reduce the computational cost of simulation. The main idea of reduction approaches is to approximate the initial FE model by a model with much smaller number of DoFs so that the reduced model retains important dynamic characteristics of the initial model. The computational burdens are also reduced because reduction techniques remove high-frequency components of elastic body motion enabling the use of a larger integration time step. The possibility to apply model order reduction methods to elastic bodies is one of the most important advantages of the floating frame formulation in the context of EMBS [89].

The set of classical reduction approaches applied in elastic multibody dynamics consists of the methods based on modal truncation, condensation, and component mode synthesis. The classical approaches are implemented in many simulation software and remain state of the art techniques for model order reduction. More recently, a few alternative reduction methods have come from the field of control theory, namely, techniques based on the singular value decomposition using Gramian matrices and moment matching via Krylov subspaces. These methods are aimed at the approximation of input-output behavior of dynamical systems. Each of these reduction procedures has its specific advantages and disadvantages. The review and comparison of the most popular methods can be found in [16, 44, 43].

One of the oldest reduction methods is a static condensation. The approach was introduced in [37] and it is called at present as Guyan method. According to this approach,

all DoFs of elastic body are partitioned into the sets of master and slave DoFs. Assuming that there are no forces applied to the slave DoFs, the method expresses the slave DoFs using the master DoFs and generates a reduced order model depended only on the master coordinates. The Guyan reduction leads to the exact representation of static deformations and to the relative good approximation of low eigenfrequencies and respective eigenvectors. However, the Guyan approach utilizes only the stiffness matrix of the body and ignores the influence of mass matrix on a spectrum of the model. Since the influence of inertia becomes significant for high frequencies, the method results in reduced order models with an erroneous high frequency spectrum.

The next method of the group of condensation approaches is a dynamic condensation method [49]. The method is similar to the Guyan procedure, but it utilizes the inertia information of the body. The dynamic condensation method was originally developed for reducing the systems that undergo a harmonic or periodical excitation. The accuracy of the reduced order model is limited to the spectrum defined around the frequency chosen for the initialization of the method.

The most often used reduction approach is a modal truncation method, which was firstly presented in the context of EMBS in [80]. The method relies on the eigenvalue decomposition of the system and employs a limited number of vibration modes of the body to represent deformation shapes. The high-frequency modes usually carry slight energy and do not influence significantly the overall motion of the system. Using low-frequency deformation modes of the body, the modal truncation method builds a low-dimensional approximation of equations of motion. A linear combination of retained deformation modes has to capture as accurately as possible the deformation shapes of the body under operational conditions. The choice of dominant deformation modes is not a trivial task. The issue is considered in [31, 32, 26], where a few approaches are proposed to determine relevant deformation modes for input-output behavior of elastic body.

The deformation shapes can be accurately described by a large set of eigenmodes or by a much smaller set of eigenmodes supplemented with several correction modes. The correction modes account for effects of truncated eigenmodes and depend on the distribution of forces acting on the body. Since the spatial distribution of forces is not taken into account in the modal truncation approach, a relative large number of modes is needed to sufficiently approximate elastic body deformations [91]. The further studies of modal reduction were aimed at taking into account the distribution of applied external forces and computing of necessary correction modes.

The important traditional reduction technique is the component mode synthesis (CMS) [40, 9, 23]. The method was developed in times of low computational power for practical finite element analysis. The technique substructures a whole FE model into components, reduces components accounting boundary conditions, and assembles the parts to form a reduced model of the whole structure. Nowadays a single elastic body corresponds to a substructure, therefore the coupling of body components is no longer necessary.

The methods based on CMS approach can be divided into three categories: fixed-interface, free-interface, and residual-flexible free interface methods. The proper choice of category is task dependent. The group of fixed-interface methods is recommended for models where the interest is focused on a low-frequency spectrum of the model. For applications where it is compulsory to have better approximation of middle and high frequency spectrum, the free-interface or residual-flexible free interface groups of methods should be exploited [43, 22]. In this thesis we consider the fixed-interface category of methods in more detail because the spectrum of interest for majority of EMBS lies in the low-frequency domain.

The most commonly used model reduction technique based on the CMS approach is the Craig-Bampton method [22]. The method approximates deformation shapes using a combination of fixed interface normal modes and constraint modes. The former set of modes are dynamic modes that improve the accuracy of reduced model in a low-frequency domain, while the constraint modes account for static deformations of the model due to the influence on the interface coordinates. Unlike the Guyan reduction procedure the Craig-Bampton method utilizes both stiffness and mass characteristics of the model. Besides, as opposed to the modal truncation it takes into account distribution of external forces to compute correction modes for exact modeling of static deformations. The method provides an accurate approximation for low and medium eigenfrequencies and corresponding eigenforms. The main drawback of the approach is that the accuracy of reduced model highly depends on the number and position of interface coordinates. This fact complicates generation of reduced order models that satisfy specified accuracy demands. In additon, the number of fixed-interface normal modes required for the acceptable accuracy is difficult to estimate a priori. Another issue with the computed fixed-interface normal modes is that they can be nearly orthogonal to the applied loads and, therefore, do not participate significantly in the solution. It follows that the correct choice of interface coordinates and fixed-interface modes requires much experience and insight into the specific problem. The CMS methods can be hardly automated.

The next large group of reduction methods is composed of mathematical methods from system and control theory. These methods take a frequency response as a characteristic quantity to describe the original system. According to these approaches, the reduced order model is defined based on matching certain parameters of reduced and original models or eliminating less important states of the system. The methods provide more accurate reduced order models than the modal reduction.

The basic idea of Krylov subspace method is to approximate a transfer function matrix by matching its values and derivatives at some frequency points. The frequency points are called expansion points or shifts. For each expansion point the transfer function matrix is transformed into a power series, coefficients of which are called moments. In order to match values and derivatives of transfer function matrix, it is necessary to match the moments of original and reduced models at the expansion points. Due to numerical instability the explicit calculation of moments is not feasible, but the moment-matching conditions

can be satisfied implicitly by the projection of equations of motion onto Krylov-subspaces. Initially, the Krylov subspace method was developed for state-space systems [36, 30, 50], i.e. first order systems. The reduction of second order system can be performed by converting the model into the state-space model and then applying reduction approaches for first order systems, but in this case, the reduced model will be also of first order type. Integration of such reduced models into a second order multibody system becomes impossible. This makes necessary using reduction techniques that provide models of second order type. At present, the Krylov subspace method has several adaptations that can be applied directly to second order systems. The basis of second order Krylov subspace can be generated with a second order Arnoldi algorithm [8, 73]. The algorithm constructs iteratively a basis of Krylov subspace using inverse, addition, and multiplication matrix operations. The total Krylov subspace is defined by concatenating of subspaces obtained for each expansion point. Due to the iterative nature the approach enables reduction of large scale models. Besides, the approximation quality of frequency response is high, particularly around expansion points. Nevertheless, there are also some drawbacks of the Krylov subspace method. Stability of the reduced model is not guaranteed even if the full order model is stable [48]. Because of the local nature of the reduction procedure, it is difficult to develop global error bounds. The method generates reduced systems of large order when systems with many inputs are under consideration. According to [28, 66], one of the directions of current research is the reduction of inputs and outputs before the application of Krylov subspace method.

Another group of reduction methods includes approaches based on SVD or Gramian matrices. The fundamental idea of the methods lies in using energy interpretation of input output system behavior. The reduction is performed by eliminating those states of the system, which require a large amount of energy to be reached and/or produce small amount of energy to be observed. These states insignificantly contribute to system dynamics and can be neglected. The basic approach for representing the input and output amount of energy involves the controllability and observability Gramian matrices. Eigenvalues of Gramian matrices indicate how strongly the states can be controlled or observed. The measure of energy for each state of the system is determined by Hankel singular values, which are calculated as the square roots of the eigenvalues for the product of the controllability and observability Gramian matrices. The unimportant states of the systems are identified by small Hankel singular values.

One of the reduction approaches based on the idea of energy interpretation is a balanced truncation method. The method was firstly proposed in [58]. The approach in its basic form can be applied only to first order systems. The advantage of balanced truncation reduction is an immediately available error bound that is expressed by proper norms of the difference of transfer function matrices for reduced and original systems [5, 6, 47]. Besides, the method preserves system stability. Using the balanced truncation approach only the load distribution, the frequency range of interest and a measure for the required

accuracy have to be provided by the user, therefore the method is especially attractive for optimization problems [65]. However, the calculation of Gramian matrices requires solution of Lyapunov equations, which is possible only for bodies with a few thousands degrees of freedom [29]. At present, there are some approaches that adapt the balanced truncation method to second order systems, see [57, 83], and provide very accurate reduced order models. However, for second order systems the global error bound is lost and stability of reduced order system is not guaranteed [66]. A matter of current research concerning the balanced truncation approach is handling of large scale systems [15, 14].

1.3 Problem statement and aim of the thesis

From the user's point of view the following aspects of model order reduction are of special interest:

- accuracy of reduced model,
- possibility to emphasize a certain frequency range of interest,
- computational efficiency of reduction method,
- estimation of error introduced by a reduction process,
- preservation of model stability,
- possibility to automate the reduction process,
- fast simulation of reduced model.

Fidelity of reduced model can be described by the following parameters: an error of displacement for all nodes of the body, error of displacement for nodes of interest, error of eigenfrequencies and eigenvectors, and error of transfer function matrices. None of these parameters provides complete information about the quality of reduced model, therefore combination of them is usually utilized to validate the reduced model. The fastest way to assess the reduced model is using of eigenfrequency and eigenvector related tests. The tests reveal whether these fundamental characteristics are well-approximated. However, it is impossible to validate the motion of a single point on the body using these tests. The problem can be solved by analyzing frequency response transfer functions. The analysis gives comprehensive information about reduced system behavior, but calculation of reference results is computationally expensive. After these tests showed acceptable results, the reduced model can be also validated in the time domain.

Since technical products operate in certain frequency ranges, the possibility to tune the reduced order model for the operating frequencies is of great importance for the user.

The computational efficiency of reduction method is defined by a number of operations and memory consumption required for generation of coordinate transformation matrix.

The error introduced by reduction can be identified using validation tests described above or, for some reduction methods, using error estimators that define permissible error bounds prior to the reduction process.

Preservation of stability is an important property of reduction approach because it ensures that the reduced model does not cause any type of failure (e.g., instability, excessive vibrations, large stresses) to the EMBS. Special criteria are used to ascertain whether this property is preserved.

The fully or partially automated reduction process decreases the user's involvement and speeds up producing of reduced order models.

The demand of fast simulation imposes restrictions on the stiffness and number of degrees of freedom of reduced structure.

The use of model order reduction methods in the context of EMBS imposes on them additional restrictions:

- reduced models have to preserve a second order structure of equations of motion;
- reduction method has to generate a coordinate transformation matrix that excludes rigid body motion from equations of motion. The rigid body motion in the floating frame formulation is accounted by the motion of a coordinate system attached to the body.

The classical reduction methods are implemented in many simulation software and remain state of the art techniques for model order reduction. In this thesis we are focused on the solution of one of the principal problems of classical reduction techniques: a lack of possibility to tune a reduced model for certain transfer paths (functions) and certain frequency ranges. Solution of the problem is important because it enables generation of accurate reduced models having a small order. The goal of the thesis is to fill in this gap by a new model order reduction approach that, in addition, satisfies the following requirements: high accuracy of reduced models, preservation of stability, fast simulation of reduced models, and the possibility of using the method in the context of EMBS. The new method differs from more recent approaches, namely, the Krylov subspace method and the balanced truncation, and has its own advantages. The stability of Krylov subspace method is not guaranteed and reduction of systems with large number of inputs leads to large reduced order models. The balanced truncation technique preserves stability of second order systems only in special cases and its application is limited to FE models with a relative small number of degrees of freedom.

The main idea of new approach is to reduce error of transfer functions in reference frequency points. For this reason, hereinafter the method is referred to as a *line-fitting approach*.

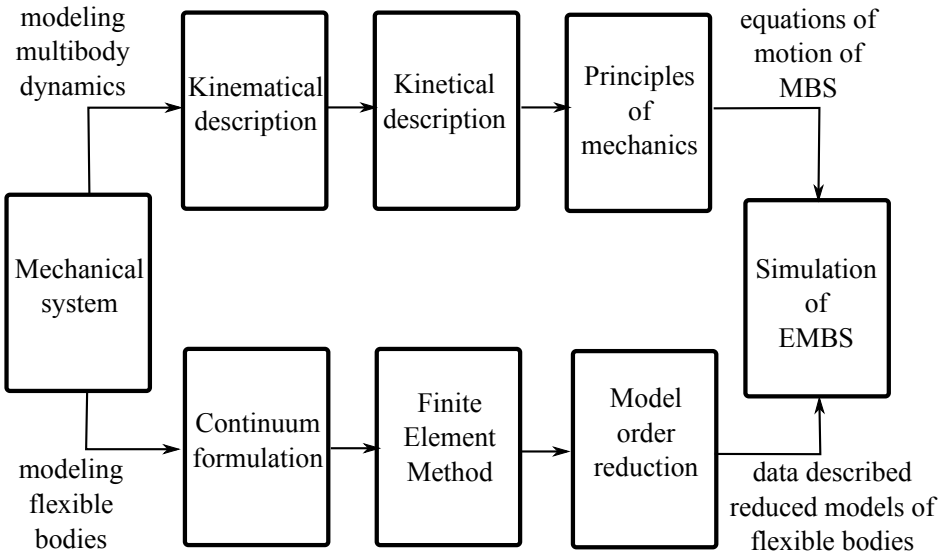

Figure 1.1: Process of elastic multibody simulation.

1.4 Scopes of the thesis and outline

In this thesis we describe a new linear structure preserving model order reduction method for elastic multibody simulation. The application of the method is limited to mechanical systems that undergo linear elastic deformations. In this contribution we show the benefits of the developed method in comparison with the classical and widely-used Craig-Bampton approach. The thorough comparison of line-fitting method with other reduction techniques falls outside the scope of the thesis.

The thesis has the following structure. We begin with fundamentals of theory for elastic multibody simulation in Chapter 2. The information in this chapter is presented in accordance with the procedure of simulation of elastic multibody systems, see Fig. 1.1. The first section of the chapter is devoted to modeling of elastic body motion using a floating frame formulation. Within this section the following aspects are covered: description of deformations using the Ritz approach and finite element method, kinematics and kinetics of a free elastic body for the floating frame of reference formulation and the Ritz approximation, derivation of equations of motion of a single unconstrained elastic body by Jourdain's principle, derivation of motion integrals and their evaluation using FE preprocessors. In addition, different types of floating frames are considered and some of possible ways to introduce damping into equations of motion are discussed. The second section of the theoretical chapter explains the concept of model order reduction based on projection. We describe the classical reduction techniques, namely, the static and dynamic condensation, modal truncation, and the Craig-Bampton method. After that validation tests of reduced models are presented and discussed. The set of tests includes an eigenfrequency related criterion NRED, eigenvector related criterion MAC, and frequency response analysis. Modeling of constraints, derivation of equations of motion of whole EMBS, and solution methods are discussed in the final section of the chapter.

The description of line-fitting model order reduction approach is given in the separate Chapter 3.

Application examples are presented in Chapter 4. There are two models under consideration: a bar and a bearing cage. The former model has a simple form and its finite element model has a small number of degrees of freedom, while the latter one has a complex shape and a large number of elastic coordinates. In this chapter we apply the line-fitting method to the both models, evaluate properties of reduced order models in time and frequency domains, and compare the results with results of traditional Craig-Bampton approach.

The goal of Chapter 5 is comprehensive evaluation of the line-fitting method. The analysis is performed based on the theoretical description of the approach in Chapter 3 and the numerical results presented in Chapter 4.

Finally, Chapter 6 highlights the most important results of this thesis and suggests further work on the subject.

2 Fundamentals of elastic multibody systems

2.1 Modeling of elastic body motion

2.1.1 Floating frame approach

The floating frame formulation is the most widely used approach for modeling elastic multibody systems. According to this formulation the motion of deformable body is a superposition of large nonlinear motion of body frame and small elastic deformations with respect to the body frame. There are a number of methods to fix a floating frame to a body. The different types of body frames and associated with them reference conditions are discussed in detail in Section 2.1.6.

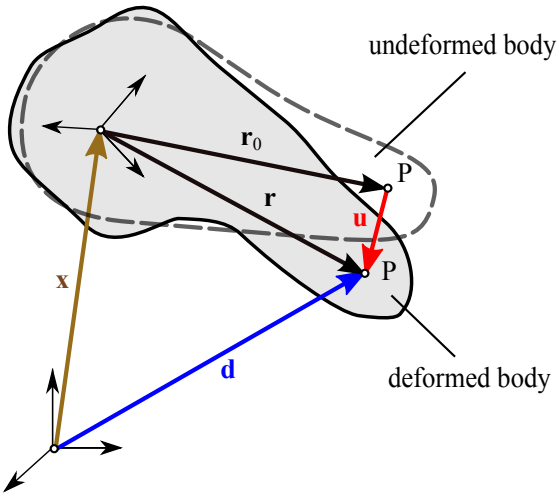

Figure 2.1: Description of flexible body using the floating frame of reference formulation.

The motion of a deformable body is represented by the motion of its points. Fig. 2.1 describes motion of an arbitrary point P of the deformable body. The position $\mathbf{d}(t)$ of point P in the global inertial frame is defined as

$$\mathbf{d}\,(t) = \mathbf{x}\,(t) + \mathbf{r}\,(t) = \mathbf{x}\,(t) + \mathbf{A}\,(t) \cdot \bar{\mathbf{r}}\,(t) = \mathbf{x}\,(t) + \mathbf{A}\,(t) \cdot (\bar{\mathbf{r}}_\mathbf{0} + \bar{\mathbf{u}}\,(t)), \qquad (2.1)$$

where $\mathbf{x}$ denotes a position of origin of body reference frame in the global coordinate system, the vector $\mathbf{r}$ defines a local position of the point P in the global frame, $\mathbf{A}$ is a

body rotation matrix, the vectors $\bar{\mathbf{r}}$ and $\bar{\mathbf{r}}_\mathbf{0}$ correspond to deformed and undeformed local positions of the point P in the body frame, and the vector $\bar{\mathbf{u}}$ represents a displacement of P due to deformation. Displacement vectors of all points define a *displacement field* of the body.

For the deformable body the vector $\bar{\mathbf{u}}$ is time- and space- dependent. As the body has an infinite number of points modeling its dynamics requires an infinite set of coordinates. In order to reduce the number of coordinates to a finite set, approximation approaches such as Rayleigh-Ritz and the finite element method are used.

2.1.2 Approximation of displacement field

Rayleigh-Ritz method

Separation of variables of the displacement field $\bar{\mathbf{u}}$ in Eq. 2.1 leads to infinite series in the following form:

$$\bar{\mathbf{u}}(\bar{\mathbf{r}}_\mathbf{0}, t) = \begin{bmatrix} \bar{u}_1 \\ \bar{u}_2 \\ \bar{u}_3 \end{bmatrix} = \begin{bmatrix} \sum_{k=1}^{\infty} f_{1k}(\bar{\mathbf{r}}_0) \cdot q_{1k}(t) \\ \sum_{k=1}^{\infty} f_{2k}(\bar{\mathbf{r}}_0) \cdot q_{2k}(t) \\ \sum_{k=1}^{\infty} f_{3k}(\bar{\mathbf{r}}_0) \cdot q_{3k}(t) \end{bmatrix} \tag{2.2}$$

The time dependent coefficients q_{1k}, q_{2k}, q_{3k} are called coordinates, and the space dependent functions f_{1k}, f_{2k}, f_{1k} are called *base functions*. It is necessary that the base functions satisfy body boundary conditions, the infinite series converge to limit functions $\bar{u}_1, \bar{u}_2, \bar{u}_3$, and the limit functions accurately represent the displacement field.

The Rayleigh-Ritz method approximates the displacement field by truncating the infinite series of Eq. 2.2 and results in the following representation:

$$\begin{bmatrix} \bar{u}_1 \\ \bar{u}_2 \\ \bar{u}_3 \end{bmatrix} \approx \begin{bmatrix} \sum_{k=1}^{l} f_{1k}(\bar{\mathbf{r}}_0) \cdot q_{1k}(t) \\ \sum_{k=1}^{m} f_{2k}(\bar{\mathbf{r}}_0) \cdot q_{2k}(t) \\ \sum_{k=1}^{n} f_{3k}(\bar{\mathbf{r}}_0) \cdot q_{3k}(t) \end{bmatrix} = \mathbf{S} \cdot \mathbf{q} \tag{2.3}$$

with $\mathbf{S}$ being a *shape matrix* containing the base functions and $\mathbf{q}$ being a vector of time dependent coordinates. The coordinates $\mathbf{q}$ lack a physical meaning. The base functions in $\mathbf{S}$ define predicted deformation shapes for the body.

In order to the approximation of deformations $\bar{\mathbf{u}}$ from Eq. 2.3 converges towards the solution of partial differential equations, the base functions must be *admissible*. It means that they have to form a complete set of functions and satisfy the boundary conditions

[76]. Completeness is achieved if the exact displacements, and their derivatives, can be matched arbitrarily closely if enough coordinates appear in the assumed displacement field [79].

One of the main problems connected with the Rayleigh–Ritz method is the difficulty to find the base functions, when deformable bodies have complex geometrical shapes. In addition, for systems with constrains the set of base functions must be adjusted for the boundary conditions. The base functions are defined in a body reference frame, therefore the choice of functions is also affected by the choice of the body frame. These problems can be eliminated using the finite element method.

Finite element method

The finite element method is a numerical approach for solving partial differential equations having a set of boundary conditions. Along with the Rayleigh-Ritz approach, the finite element method reduces the number of coordinates required for the description of deformations to a finite set.

The idea of the method is to discretize a deformable body into small regions called *elements* and to describe the deformation of the whole body by deformations of elements. The elements are connected at the points called *nodes*, see Fig. 2.2.

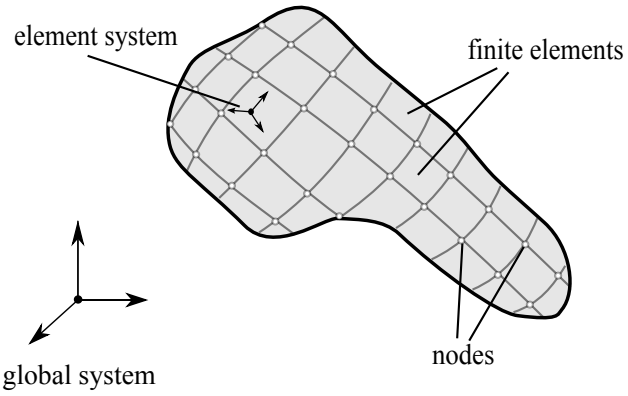

Figure 2.2: Finite element discretization of deformable body.

In the finite element method the deformation of elements is defined by interpolation polynomials and nodal coordinates. The displacement field of the element is described with respect to an element coordinate system as

$$\bar{\mathbf{u}}_\mathbf{e}(\bar{\mathbf{r}}_{\mathbf{e0}}, t) = \mathbf{N}_\mathbf{e}(\bar{\mathbf{r}}_{\mathbf{e0}}) \cdot \mathbf{q}_\mathbf{e}(t), \tag{2.4}$$

where $\mathbf{N_e}$ is a space dependent interpolation matrix, $\mathbf{q_e}$ is a time dependent vector of nodal coordinates and the vector $\bar{\mathbf{r}}_{\mathbf{e0}}$ defines an undeformed position of a point within the element in the element reference frame.

The displacement field of the whole body can be represented via deformations of elements as follows. The displacement $\bar{\mathbf{u}}_\mathbf{e}$ is expressed in the global frame by a rotation matrix $\mathbf{A_e}$ as

$$\mathbf{u_e}(\bar{\mathbf{r}}_{\mathbf{e0}}, \mathbf{t}) = \mathbf{A_e} \cdot \bar{\mathbf{u}}_\mathbf{e}(\bar{\mathbf{r}}_{\mathbf{e0}}, t) = \mathbf{A_e} \cdot \mathbf{N_e}(\bar{\mathbf{r}}_{\mathbf{e0}}) \cdot \mathbf{q_e}(t). \tag{2.5}$$

The vector $\bar{\mathbf{r}}_{\mathbf{e0}}$ can be also written in another form as

$$\bar{\mathbf{r}}_{\mathbf{e0}} = \mathbf{A}_\mathbf{e}^\mathbf{T} \cdot (\mathbf{d_0} - \mathbf{x_e}), \tag{2.6}$$

where $\mathbf{d_0}$ and $\mathbf{x_e}$ are an undeformed position of arbitrary point P within the element and a position of origin of element system in the global coordinate system, respectively, see Fig. 2.3.

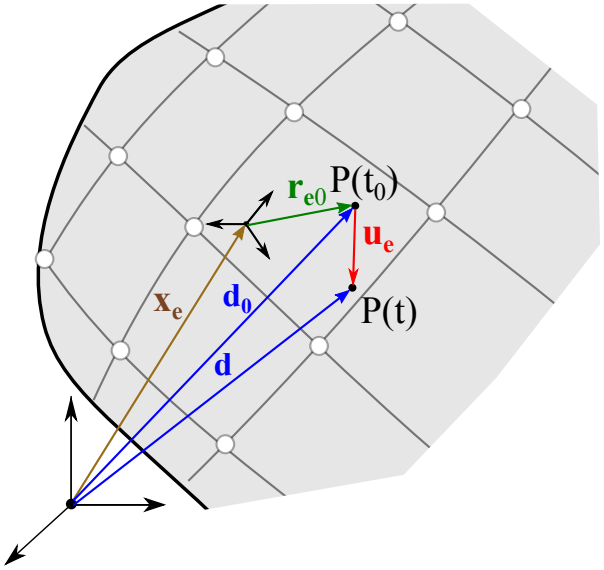

Figure 2.3: Deformation of finite element with respect to a global frame.

The set of nodal coordinates for the FE model can be represented by a vector

$$\mathbf{q}\,(t) = \begin{bmatrix} \vdots \\ \mathbf{q}^k(t) \\ \vdots \end{bmatrix}, \; k = 1, \ldots, n_{nodes} \tag{2.7}$$

of dimension N with $\mathbf{q}^k(t)$ being a vector of degrees of freedom of k-th node. The element nodal coordinates $\mathbf{q_e}(t)$ and the body nodal coordinates $\mathbf{q}(t)$ are connected by a matrix $\mathbf{C_e} \in \mathbb{R}^{n_q^e \times N}$:

$$\mathbf{q_e}(t) = \mathbf{C_e} \cdot \mathbf{q}(t). \tag{2.8}$$

Here n_q^e is the number of nodal coordinates of element e. The matrix $\mathbf{C_e}$ is calculated as

$$\mathbf{C_e} = \mathbf{T_e} \cdot \mathbf{B_e}. \tag{2.9}$$

The matrix $\mathbf{B_e} \in \mathbb{R}^{n_q^e \times N}$ is a Boolean transformation matrix and it serves to express connectivity of the element e. The matrix $\mathbf{T_e} \in \mathbb{R}^{n_q^e \times n_q^e}$ is a transformation matrix that consists of elements of matrix $\mathbf{A_e}^T$ and transforms the element nodal coordinates from the global coordinate system to the local element system. Using Eq. 2.5, Eq. 2.8, Eq. 2.9 and summing over all elements leads the formulation of displacement field of the body in the global frame:

$$\mathbf{u}(\mathbf{d_0},t) = \sum_{e=1}^{n_E} \mathbf{A_e} \cdot \bar{\mathbf{N}}_\mathbf{e}(\mathbf{d_0}) \cdot \mathbf{T_e} \cdot \mathbf{B_e} \cdot \mathbf{q}(t) = \mathbf{S}(\mathbf{d}_0) \cdot \mathbf{q}(t) \tag{2.10}$$

In contrast to the Rayleigh-Ritz approach, the finite element method avoids specifying of base functions for the whole body. The base functions of the body are assembled from the base functions of elements. There are different types of finite elements that can be used to represent bodies with complex forms.

Boundary conditions can be imposed direct on the nodal coordinates $\mathbf{q}$.

2.1.3 Kinematics

Position

Using the inertial coordinate system of finite element model as a body coordinate system and combining Eq. 2.1 with Eq. 2.10 the position of arbitrary point of the elastic body can be described as follows:

$$\begin{aligned} \mathbf{d}(\bar{\mathbf{r}}_0, t) &= \mathbf{x}(t) + \mathbf{A}(t) \cdot (\bar{\mathbf{r}}_\mathbf{0} + \bar{\mathbf{u}}(\bar{\mathbf{r}}_0, t)) = & (2.11) \\ & \mathbf{x}(t) + \mathbf{A}(t) \cdot (\bar{\mathbf{r}}_\mathbf{0} + \mathbf{S}(\bar{\mathbf{r}}_0) \cdot \mathbf{q}(t)). & (2.12) \end{aligned}$$

In three-dimensional analysis, at least six coordinates are required to define configuration of body frame. One of the methods is to define three coordinates for a position of origin of the frame and three coordinates for an orientation of the frame with respect to the inertial coordinate system. The orientation parameters $\boldsymbol{\theta}$ can be identified using *Euler angles*, *Rodrigues parameters*, or four dependent *Euler parameters*. The drawback of the three-variable representation is singularity at certain orientations of the reference frame in space. Formulation of rotation matrix $\mathbf{A}$ using orientation parameters can be found in Chapter 6.

The global point position of Eq. 2.11 is written in terms of generalized reference and elastic coordinates

$$\mathbf{z} = \begin{bmatrix} \mathbf{x} \\ \boldsymbol{\theta} \\ \mathbf{q} \end{bmatrix}. \tag{2.13}$$

The translational coordinates $\mathbf{x}$ of the frame origin are defined in the global inertial frame, the rotational coordinates $\boldsymbol{\theta}$ describe the orientation of body frame in space and are not tied to any coordinate system, the elastic coordinates $\mathbf{q}$ are expressed with respect to the body coordinate system.

Velocity

Differentiating Eq. 2.11 with respect to time yields

$$\dot{\mathbf{d}} = \dot{\mathbf{x}} + \dot{\mathbf{A}}\bar{\mathbf{r}} + \mathbf{A}\mathbf{S}\dot{\mathbf{q}}. \tag{2.14}$$

Here $\dot{\mathbf{d}}$ is an absolute velocity of the point, $\bar{\mathbf{r}}$ is a point position vector with respect to the body coordinate system, and $\dot{\mathbf{q}}$ defines a vector of generalized elastic velocities.

The derivative of matrix $\mathbf{A}$ can be found using its orthogonality property. Since $\mathbf{A}\mathbf{A}^T = \mathbf{I}$, one obtains

$$\dot{\mathbf{A}}\mathbf{A}^T + \mathbf{A}\dot{\mathbf{A}}^T = \mathbf{0},$$

which can be rewritten as

$$\dot{\mathbf{A}}\mathbf{A}^T = -(\dot{\mathbf{A}}\mathbf{A}^T)^T.$$

The matrix $\dot{\mathbf{A}}\mathbf{A}^T$ is equal to the negative of its transpose, therefore it is a skew symmetric matrix. It follows that

$$\dot{\mathbf{A}}\mathbf{A}^T = \tilde{\boldsymbol{\omega}} \tag{2.15}$$

with $\tilde{\boldsymbol{\omega}}$ being a skew symmetric matrix defined by a vector $\boldsymbol{\omega}$. The matrix $\tilde{\boldsymbol{\omega}}$ has the form

$$\tilde{\boldsymbol{\omega}} = \begin{bmatrix} 0 & -\omega_3 & \omega_2 \\ \omega_3 & 0 & -\omega_1 \\ -\omega_2 & \omega_1 & 0 \end{bmatrix} \tag{2.16}$$

The vector $\boldsymbol{\omega} = \begin{bmatrix} \omega_1 & \omega_2 & \omega_3 \end{bmatrix}^T$ is the *angular velocity vector* defined in the global coordinate system. Thus,

$$\dot{\mathbf{A}} = \tilde{\boldsymbol{\omega}}\mathbf{A} \tag{2.17}$$

It follows that the vector $\dot{\mathbf{A}}\bar{\mathbf{r}}$ can be written as

$$\tilde{\boldsymbol{\omega}}\mathbf{A}\bar{\mathbf{r}} = \tilde{\boldsymbol{\omega}}\mathbf{r} = -\tilde{\mathbf{r}}\boldsymbol{\omega} = \tilde{\mathbf{r}}^T\boldsymbol{\omega} \tag{2.18}$$

Substituting Eq. 2.18 in Eq. 2.14 the velocity vector $\dot{\mathbf{d}}$ takes the form

$$\dot{\mathbf{d}} = \dot{\mathbf{x}} + \tilde{\mathbf{r}}^T\boldsymbol{\omega} + \mathbf{A}\mathbf{S}\dot{\mathbf{q}} = \begin{bmatrix} \mathbf{I} & \tilde{\mathbf{r}}^T & \mathbf{A}\mathbf{S} \end{bmatrix} \cdot \begin{bmatrix} \dot{\mathbf{x}} \\ \boldsymbol{\omega} \\ \dot{\mathbf{q}} \end{bmatrix}. \tag{2.19}$$

This can be written in another form as

$$\dot{\mathbf{d}} = \mathbf{L}\mathbf{z}_\mathbf{I}, \tag{2.20}$$

where

$$\mathbf{L} = \begin{bmatrix} \mathbf{I} & \tilde{\mathbf{r}}^T & \mathbf{AS} \end{bmatrix} \text{ and } \mathbf{z}_\mathbf{I} = \begin{bmatrix} \dot{\mathbf{x}} \\ \boldsymbol{\omega} \\ \dot{\mathbf{q}} \end{bmatrix}. \tag{2.21}$$

The vector $\mathbf{z}_\mathbf{I}$ defines generalized velocity coordinates.

Acceleration

The absolute acceleration of the point can be found by the differentiation of Eq. 2.20 with respect to time. This results in

$$\ddot{\mathbf{d}} = \dot{\mathbf{L}}\mathbf{z}_\mathbf{I} + \mathbf{L}\dot{\mathbf{z}}_\mathbf{I}. \tag{2.22}$$

Differentiating of the matrix $\mathbf{L}$ yields

$$\dot{\mathbf{L}} = \begin{bmatrix} \mathbf{0} & \dot{\tilde{\mathbf{r}}}^T & \dot{\mathbf{A}}\mathbf{S} \end{bmatrix}, \tag{2.23}$$

where the second term can be identified using the relation $\mathbf{r} = \mathbf{A}\bar{\mathbf{r}}$ and Eq. 2.17 as

$$\dot{\tilde{\mathbf{r}}}^T = -\dot{\tilde{\mathbf{r}}} = -\tilde{\dot{\mathbf{r}}} = -(\widetilde{\dot{\mathbf{A}}\bar{\mathbf{r}} + \mathbf{A}\dot{\bar{\mathbf{r}}}}) = -(\widetilde{\tilde{\boldsymbol{\omega}}\mathbf{A}\bar{\mathbf{r}} + \mathbf{A}\mathbf{S}\dot{\mathbf{q}}}), \tag{2.24}$$

and the third term can be written as $\dot{\mathbf{A}}\mathbf{S} = \tilde{\boldsymbol{\omega}}\mathbf{A}\mathbf{S}$. As a result, the product $\dot{\mathbf{L}}\mathbf{z}_\mathbf{I}$ yields

$$\dot{\mathbf{L}}\mathbf{z}_\mathbf{I} = \tilde{\boldsymbol{\omega}}\tilde{\boldsymbol{\omega}}\mathbf{A}\bar{\mathbf{r}} + 2\tilde{\boldsymbol{\omega}}\mathbf{A}\mathbf{S}\dot{\mathbf{q}}. \tag{2.25}$$

Thus, the acceleration vector takes the following form

$$\ddot{\mathbf{d}} = \ddot{\mathbf{x}} + \tilde{\mathbf{r}}^T\boldsymbol{\alpha} + \mathbf{A}\mathbf{S}\ddot{\mathbf{q}} + \tilde{\boldsymbol{\omega}}\tilde{\boldsymbol{\omega}}\mathbf{r} + 2\tilde{\boldsymbol{\omega}}\mathbf{A}\mathbf{S}\dot{\mathbf{q}}, \tag{2.26}$$

where $\boldsymbol{\alpha}$ is an angular acceleration vector. In this equation the first term represents an absolute acceleration of the origin of body coordinate system. The second term $\tilde{\mathbf{r}}^T\boldsymbol{\alpha}$ is a tangential acceleration of the point. The tangential acceleration is perpendicular to the vectors $\mathbf{r}$ and $\boldsymbol{\alpha}$. The third component $\mathbf{A}\mathbf{S}\ddot{\mathbf{q}}$ represents an acceleration of the point due to deformations. The fourth part describes a normal acceleration of the point. This component is directed along the line connecting the point and the origin of the body frame. Finally, the latter term represents the Coriolis acceleration. If the body is rigid, the third and fifth components of Eq. 2.26 vanish.

The generalized acceleration coordinates take the form

$$\mathbf{z_{II}} = \dot{\mathbf{z}}_\mathbf{I} = \begin{bmatrix} \ddot{\mathbf{x}} \\ \boldsymbol{\alpha} \\ \ddot{\mathbf{q}} \end{bmatrix}. \tag{2.27}$$

2.1.4 Kinetics

There are a number of methods used to derive equations of motion of elastic body: D'Alembert's principle, Hamilton's principle, Jourdain's principle, Newton-Euler formalism. All of them lead to the same system of equations. Direct application of Newton's second law becomes difficult for large multibody systems. In contrast to Newton's second law, the first three approaches are variational principles, which employ scalar quantities such as kinetic energy, potential energy, virtual work, and virtual power. These methods make possible finding equations of motion for complex multibody systems. In this work we utilize Jourdain's variational principle to derive equations of motion because it is a straightforward approach for systems where generalized velocity coordinates are not equal to a derivative of generalized position coordinates.

According to Jourdain's principle the sum of virtual power of all forces acting on the body must be zero. It follows that the sum of virtual power of inertial, internal, and external forces equals zero:

$$\delta P_{inert} + \delta P_{inter} + \delta P_{ext} = 0. \tag{2.28}$$

Virtual power of inertia forces

The virtual power of inertia forces takes the following form

$$\delta P_{inert} = \int_V -\rho \delta \dot{\mathbf{d}}^T \ddot{\mathbf{d}} dV, \tag{2.29}$$

where $\dot{\mathbf{d}}$ and $\ddot{\mathbf{d}}$ are global velocity and acceleration vectors of an arbitrary point of the body, $\delta\dot{\mathbf{d}}$ indicates a virtual velocity of the point, ρ defines mass density, and V represents a volume of the body.

The virtual velocity $\delta\dot{\mathbf{d}}$ can be expressed in terms of virtual generalized velocity $\delta\mathbf{z_I}$ as

$$\delta\dot{\mathbf{d}} = \mathbf{L}\delta\mathbf{z_I}. \tag{2.30}$$

with $\mathbf{L}$ being the matrix from Eq. 2.21. Using the definition of global acceleration vector $\ddot{\mathbf{d}} = \dot{\mathbf{L}}\mathbf{z_I} + \mathbf{L}\dot{\mathbf{z}}_\mathbf{I}$ from Eq. 2.22, the virtual power of inertia forces can be obtained as follows

$$\delta P_{inert} = -\left(\int_V \rho \left(\delta \mathbf{z_I}\right)^T \mathbf{L}^T \mathbf{L}\dot{\mathbf{z}}_\mathbf{I} dV + \int_V \rho \left(\delta \mathbf{z_I}\right)^T \mathbf{L}^T \dot{\mathbf{L}}\mathbf{z_I} dV \right). \tag{2.31}$$

Since the vector of generalized velocity coordinates $\mathbf{z_I}$ depends only on time, one can write the expression for δP_{inert} as

$$\delta P_{inert} = -\left(\delta \mathbf{z_I}\right)^T \left(\left[\int_V \rho \mathbf{L}^T \mathbf{L} dV \right] \dot{\mathbf{z}}_\mathbf{I} + \left[\int_V \rho \mathbf{L}^T \dot{\mathbf{L}} \mathbf{z_I} dV \right] \right) = \tag{2.32}$$

$$-\left(\delta \mathbf{z_I}\right)^T \left(\mathbf{M} \dot{\mathbf{z}}_\mathbf{I} + \mathbf{h}_v \right), \tag{2.33}$$

where $\mathbf{M}$ is a generalized mass matrix of the elastic body in multibody system and $\mathbf{h}_v$ defines a quadratic velocity vector contained centrifugal and Coriolis forces.

Substituting $\mathbf{L}$ from Eq. 2.21 into the mass matrix expression we can write $\mathbf{M}$ in more detailed form as

$$\mathbf{M} = \int_V \rho \begin{bmatrix} \mathbf{I} \\ \tilde{\mathbf{r}} \\ (\mathbf{AS})^T \end{bmatrix} \begin{bmatrix} \mathbf{I} & \tilde{\mathbf{r}}^T & \mathbf{AS} \end{bmatrix} dV = \tag{2.34}$$

$$\int_V \rho \begin{bmatrix} \mathbf{I} & \tilde{\mathbf{r}}^T & \mathbf{AS} \\ & \tilde{\mathbf{r}}\tilde{\mathbf{r}}^T & \tilde{\mathbf{r}}\mathbf{AS} \\ symmetric & & \mathbf{S}^T\mathbf{S} \end{bmatrix} dV. \tag{2.35}$$

Here the orthogonality property of rotation matrix $\mathbf{A}^T\mathbf{A} = \mathbf{I}$ is used. The mass matrix from Eq. 2.35 can be also represented as follows:

$$\mathbf{M} = \begin{bmatrix} \mathbf{M}_t & \mathbf{M}_{tr} & \mathbf{M}_{te} \\ & \mathbf{M}_r & \mathbf{M}_{re} \\ symmetric & & \mathbf{M}_e \end{bmatrix}. \tag{2.36}$$

The indexes t, r and e indicate translational, rotational and elastic parts of generalized mass matrix. The evaluation of submatrices from Eq. 2.36 requires using the relations that connect values in the body and inertial coordinates systems:

$$\mathbf{r} = \mathbf{A}\bar{\mathbf{r}}, \tag{2.37}$$

$$\tilde{\mathbf{r}} = \mathbf{A}\tilde{\bar{\mathbf{r}}}\mathbf{A}^T. \tag{2.38}$$

In Eq. 2.36 the term

$$\mathbf{M}_t = \int_V \rho \mathbf{I} dV = m\mathbf{I},\ \mathbf{M}_t \in \mathbb{R}^{3\times 3} \tag{2.39}$$

is a diagonal matrix, where m is a mass of the body. The submatrix

$$\mathbf{M}_r = \int_V \rho \tilde{\mathbf{r}}\tilde{\mathbf{r}}^T dV = \mathbf{A} \cdot \int_V \rho \tilde{\bar{\mathbf{r}}}\tilde{\bar{\mathbf{r}}}^T dV \cdot \mathbf{A}^T = \mathbf{A} \cdot \mathbf{J}(\mathbf{q}) \cdot \mathbf{A}^T,\ \mathbf{M}_r \in \mathbb{R}^{3\times 3} \tag{2.40}$$

is an inertia tensor in the global coordinate system. It depends on the elastic coordinates

$\mathbf{q}$. The matrix $\mathbf{J}$ denotes an inertia tensor with respect to the body coordinate system. Next, the term

$$\mathbf{M}_e = \int_V \rho \mathbf{S}^T \mathbf{S} dV,\ \mathbf{M}_e \in \mathbb{R}^{N \times N} \tag{2.41}$$

corresponds to a finite element mass matrix of the body. The component

$$\mathbf{M}_{tr} = \int_V \rho \tilde{\mathbf{r}}^T dV = \int_V \rho \mathbf{A} \tilde{\bar{\mathbf{r}}}^T \mathbf{A}^T dV = \mathbf{A} \cdot \int_V \rho \tilde{\bar{\mathbf{r}}}^T dV \cdot \mathbf{A}^T = m \mathbf{A} \cdot \tilde{\bar{\mathbf{c}}}^T \cdot \mathbf{A}^T \tag{2.42}$$

is 3×3 matrix with

$$\bar{\mathbf{c}} = \bar{\mathbf{c}}(\mathbf{q}) = \frac{1}{m} \int_V \rho \bar{\mathbf{r}} dV \tag{2.43}$$

being a vector of mass center of the body with respect to the body frame. Analogous to the inertia tensor of the body, the position of mass center also depends on the elastic coordinates $\mathbf{q}$. Finally, the matrices

$$\mathbf{M}_{te} = \int_V \rho \mathbf{A} \mathbf{S} dV = \mathbf{A} \cdot \int_V \rho \mathbf{S} dV = \mathbf{A} \cdot \mathbf{C}_t,\ \mathbf{C}_t \in \mathbb{R}^{3 \times N}, \tag{2.44}$$

$$\mathbf{M}_{re} = \int_V \rho \tilde{\mathbf{r}} \mathbf{A} \mathbf{S} dV = \int_V \rho \mathbf{A} \tilde{\bar{\mathbf{r}}} \mathbf{A}^T \mathbf{A} \mathbf{S} dV = \mathbf{A} \cdot \int_V \rho \tilde{\bar{\mathbf{r}}} \mathbf{S} dV = \mathbf{A} \cdot \mathbf{C}_r,\ \mathbf{C}_r \in \mathbb{R}^{3 \times N} \tag{2.45}$$

describe coupling terms of rigid body motion and elastic deformations. It is necessary to note that only the matrices $\mathbf{M}_t$ and $\mathbf{M}_e$ are constant, while other terms of the generalized mass matrix depend on the generalized coordinates of the body and, as a result, they are implicit functions of time.

In order to evaluate volume integrals of the quadratic velocity vector $\mathbf{h}_v$ from Eq. 2.33, we separate it into translational, rotational, and elastic components $\mathbf{h}_v = \begin{bmatrix} \mathbf{h}_{vt}^T & \mathbf{h}_{vr}^T & \mathbf{h}_{ve}^T \end{bmatrix}^T$ and exploit the expressions for $\mathbf{L}$ and $\dot{\mathbf{L}}\mathbf{z}_\mathbf{I}$ from Eq. 2.21 and Eq. 2.25. The translational part $\mathbf{h}_{vt}$ can be obtained as

$$\mathbf{h}_{vt} = \int_V \rho \left(\tilde{\boldsymbol{\omega}} \tilde{\boldsymbol{\omega}} \mathbf{r} + 2 \tilde{\boldsymbol{\omega}} \mathbf{A} \mathbf{S} \dot{\mathbf{q}} \right) dV = m \mathbf{A} \tilde{\boldsymbol{\omega}} \left(\tilde{\boldsymbol{\omega}} \bar{\mathbf{c}} + 2 \dot{\bar{\mathbf{c}}} \right). \tag{2.46}$$

The simplification of $\mathbf{h}_{vt}$ is accomplished by using the relations

$$\int_V \rho \tilde{\boldsymbol{\omega}} \tilde{\boldsymbol{\omega}} \mathbf{r}\, dV = \int_V \rho \mathbf{A} \tilde{\boldsymbol{\omega}} \tilde{\boldsymbol{\omega}} \bar{\mathbf{r}}\, dV = \mathbf{A} \tilde{\boldsymbol{\omega}} \tilde{\boldsymbol{\omega}} m \cdot \frac{1}{m} \int_V \rho \bar{\mathbf{r}}\, dV = m \mathbf{A} \tilde{\boldsymbol{\omega}} \tilde{\boldsymbol{\omega}} \bar{\mathbf{c}} \tag{2.47}$$

and

$$\int_V 2 \rho \tilde{\boldsymbol{\omega}} \mathbf{A} \mathbf{S} \dot{\mathbf{q}} dV = \int_V 2 \rho \mathbf{A} \tilde{\boldsymbol{\omega}} \mathbf{S} \dot{\mathbf{q}} dV = 2 \mathbf{A} \tilde{\boldsymbol{\omega}} m \dot{\bar{\mathbf{c}}} \tag{2.48}$$

where

$$\dot{\bar{\mathbf{c}}} = \frac{1}{m} \int_V \rho \dot{\bar{\mathbf{r}}} dV \tag{2.49}$$

is a local velocity of mass center in the body frame.

The rotational component of the quadratic velocity vector takes the form

$$\mathbf{h}_{vr} = \int_V \rho\tilde{\mathbf{r}}\left(\tilde{\boldsymbol{\omega}}\tilde{\boldsymbol{\omega}}\mathbf{r} + 2\tilde{\boldsymbol{\omega}}\mathbf{A}\mathbf{S}\dot{\mathbf{q}}\right)dV = \mathbf{A}\cdot\tilde{\bar{\boldsymbol{\omega}}}\mathbf{J}\bar{\boldsymbol{\omega}} + \mathbf{A}\cdot\mathbf{G}_r\bar{\boldsymbol{\omega}}, \tag{2.50}$$

where $\mathbf{G}_r$ is a component of Coriolis forces

$$\mathbf{G}_r = 2\int_V \rho\tilde{\bar{\mathbf{r}}}\dot{\tilde{\bar{\mathbf{r}}}}^T dV \tag{2.51}$$

and $\mathbf{J}$ is the tensor of inertia from Eq. 2.40. The extraction of $\mathbf{J}$ in the first term of Eq. 2.50 is performed using the relation

$$\int_V \rho\tilde{\mathbf{r}}\tilde{\boldsymbol{\omega}}\tilde{\boldsymbol{\omega}}\mathbf{r}dV = \mathbf{A}\tilde{\bar{\boldsymbol{\omega}}}\left(\int_V \rho\tilde{\bar{\mathbf{r}}}\tilde{\bar{\mathbf{r}}}^T dV\right)\bar{\boldsymbol{\omega}}, \tag{2.52}$$

where the following operations with skew-symmetric matrices are carried out

$$\tilde{\mathbf{r}}\tilde{\boldsymbol{\omega}} = \tilde{\boldsymbol{\omega}}\tilde{\mathbf{r}} + \widetilde{(\tilde{\mathbf{r}}\boldsymbol{\omega})}, \tag{2.53}$$

$$\begin{aligned}\tilde{\mathbf{r}}\tilde{\boldsymbol{\omega}}\tilde{\boldsymbol{\omega}}\mathbf{r} = -\tilde{\mathbf{r}}\tilde{\boldsymbol{\omega}}\tilde{\mathbf{r}}\boldsymbol{\omega} = -\left(\tilde{\boldsymbol{\omega}}\tilde{\mathbf{r}} + \widetilde{(\tilde{\mathbf{r}}\boldsymbol{\omega})}\right)\tilde{\mathbf{r}}\boldsymbol{\omega} = \\ -\tilde{\boldsymbol{\omega}}\tilde{\mathbf{r}}\tilde{\mathbf{r}}\boldsymbol{\omega} - \widetilde{(\tilde{\mathbf{r}}\boldsymbol{\omega})}\tilde{\mathbf{r}}\boldsymbol{\omega} = -\tilde{\boldsymbol{\omega}}\tilde{\mathbf{r}}\tilde{\mathbf{r}}\boldsymbol{\omega} = \tilde{\boldsymbol{\omega}}\tilde{\mathbf{r}}\tilde{\mathbf{r}}^T\boldsymbol{\omega}\end{aligned} \tag{2.54}$$

and the relations $\tilde{\mathbf{r}} = \mathbf{A}\tilde{\bar{\mathbf{r}}}\mathbf{A}^T, \tilde{\boldsymbol{\omega}} = \mathbf{A}\tilde{\bar{\boldsymbol{\omega}}}\mathbf{A}^T$ are used.

The derivation of $\mathbf{G}_r$ in Eq. 2.50 is accomplished as follows:

$$\int_V 2\rho\tilde{\mathbf{r}}\tilde{\boldsymbol{\omega}}\mathbf{A}\mathbf{S}\dot{\mathbf{q}}dV = 2\int_V \rho\mathbf{A}\tilde{\bar{\mathbf{r}}}\tilde{\bar{\boldsymbol{\omega}}}\dot{\bar{\mathbf{r}}}dV = \mathbf{A}\cdot 2\int_V \rho\tilde{\bar{\mathbf{r}}}\dot{\tilde{\bar{\mathbf{r}}}}^T dV\bar{\boldsymbol{\omega}} \tag{2.55}$$

The elastic part $\mathbf{h}_{ve}$ of the quadratic velocity vector takes the form:

$$\begin{aligned}\mathbf{h}_{ve} = \int_V \rho\left(\mathbf{A}\mathbf{S}\right)^T\left(\tilde{\boldsymbol{\omega}}\tilde{\boldsymbol{\omega}}\mathbf{r} + 2\tilde{\boldsymbol{\omega}}\mathbf{A}\mathbf{S}\dot{\mathbf{q}}\right)dV = \\ \int_V \rho\left(\mathbf{A}\mathbf{S}\right)^T\tilde{\boldsymbol{\omega}}\tilde{\boldsymbol{\omega}}\mathbf{r}dV + \int_V \rho\left(\mathbf{A}\mathbf{S}\right)^T 2\tilde{\boldsymbol{\omega}}\mathbf{A}\mathbf{S}\dot{\mathbf{q}}dV\end{aligned} \tag{2.56}$$

The first summand of Eq. 2.56 is given by

$$\int_V \rho\mathbf{S}^T\mathbf{A}^T\mathbf{A}\tilde{\boldsymbol{\omega}}\mathbf{A}^T\mathbf{A}\tilde{\boldsymbol{\omega}}\mathbf{A}^T\mathbf{A}\bar{\mathbf{r}}dV = \int_V \rho\mathbf{S}^T\tilde{\boldsymbol{\omega}}\tilde{\boldsymbol{\omega}}\bar{\mathbf{r}}dV \tag{2.57}$$

Ordinary matrix operations can not factor the rotational velocity $\bar{\boldsymbol{\omega}}$ out of this integrand, therefore the combination of matrix and index notation proposed in [77] is used:

$$\int_V \rho\mathbf{S}^T\tilde{\boldsymbol{\omega}}\tilde{\boldsymbol{\omega}}\bar{\mathbf{r}}dV = \left[\bar{\boldsymbol{\omega}}^T\mathbf{O}_{ek}\bar{\boldsymbol{\omega}}\right], k = 1..N. \tag{2.58}$$

Here the brackets mean that all components form a vector of length N. The matrix

$\mathbf{O}_{ek} \in \mathbb{R}^{3\times 3}$ is given as

$$\mathbf{O}_{ek} = \int_V \rho \tilde{\mathbf{S}}_{*k} \tilde{\bar{\mathbf{r}}} dV \tag{2.59}$$

with $\mathbf{S}_{*k}$ being the k-th column of shape matrix $\mathbf{S}$, see [77].

The second summand of Eq. 2.56 can be rewritten as

$$\begin{aligned} \int_V \rho \left(\mathbf{AS}\right)^T 2\tilde{\boldsymbol{\omega}} \mathbf{AS}\dot{\mathbf{q}} dV = 2\int_V \rho \mathbf{S}^T \tilde{\bar{\boldsymbol{\omega}}} \mathbf{S}\dot{\mathbf{q}} dV = \\ 2\int_V \rho \mathbf{S}^T \widetilde{(\mathbf{S}\dot{\mathbf{q}})}^T \bar{\boldsymbol{\omega}} dV = 2\int_V \rho \mathbf{S}^T \dot{\tilde{\bar{\mathbf{r}}}}^T dV \bar{\boldsymbol{\omega}} = \mathbf{G}_e \bar{\boldsymbol{\omega}}, \end{aligned} \tag{2.60}$$

where $\mathbf{G}_e \in \mathbb{R}^{N\times 3}$ takes the form

$$\mathbf{G}_e = 2\int_V \rho \mathbf{S}^T \dot{\tilde{\bar{\mathbf{r}}}}^T dV. \tag{2.61}$$

Summarizing the evaluation of generalized quadratic forces yields

$$\mathbf{h}_v = \begin{bmatrix} \mathbf{h}_{vt} \\ \mathbf{h}_{vr} \\ \mathbf{h}_{ve} \end{bmatrix} = \begin{bmatrix} \mathbf{A} m \tilde{\bar{\boldsymbol{\omega}}} \cdot \left(\tilde{\bar{\boldsymbol{\omega}}} \bar{\mathbf{c}} + 2\dot{\bar{\mathbf{c}}}\right) \\ \mathbf{A} \cdot \left(\tilde{\bar{\boldsymbol{\omega}}} \mathbf{J} \bar{\boldsymbol{\omega}} + \mathbf{G}_r \bar{\boldsymbol{\omega}}\right) \\ \left[\bar{\boldsymbol{\omega}}^T \mathbf{O}_{ek} \bar{\boldsymbol{\omega}}\right] + \mathbf{G}_e \bar{\boldsymbol{\omega}} \end{bmatrix}. \tag{2.62}$$

The components $\bar{\mathbf{c}}$, $\dot{\bar{\mathbf{c}}}$, $\mathbf{J}$, $\mathbf{G}_r$, $\mathbf{O}_{ek}$, and $\mathbf{G}_e$ are defined in Eq. 2.43, Eq. 2.49, Eq. 2.40, Eq. 2.51, Eq. 2.59, and Eq. 2.61, respectively.

Virtual power of internal forces

The virtual power due to elastic forces is defined as

$$\delta P_{inter} = -\int_V \delta \dot{\boldsymbol{\varepsilon}}^T \cdot \boldsymbol{\sigma} dV, \tag{2.63}$$

where $\boldsymbol{\sigma}$ and $\dot{\boldsymbol{\varepsilon}}$ are *stress* and *strain rate* vectors, respectively. Further, the relation between the strain vector $\boldsymbol{\varepsilon}$ and the displacement field $\bar{\mathbf{u}}$ is required.

According to the finite element method, the displacement field is approximated by a shape matrix $\mathbf{S}$ and time-depended nodal coordinates $\mathbf{q}$ as $\bar{\mathbf{u}}(\mathbf{d}_0, t) = \mathbf{S}(\mathbf{d}_0) \cdot \mathbf{q}(t)$, see Section 2.1.2. Once the displacement field is given, the strain vector $\boldsymbol{\varepsilon}(\mathbf{d}_0, t)$ is obtained by applying the differential displacement-strain operator ∇ [79, 51]:

$$\boldsymbol{\varepsilon}(\mathbf{d}_0, t) = \nabla \cdot \bar{\mathbf{u}} = \nabla \cdot \mathbf{S}(\mathbf{d}_0) \cdot \mathbf{q}(t), \tag{2.64}$$

where

$$\nabla = \begin{bmatrix} \frac{\partial}{\partial x_1} & 0 & 0 \\ 0 & \frac{\partial}{\partial x_2} & 0 \\ 0 & 0 & \frac{\partial}{\partial x_3} \\ \frac{\partial}{\partial x_2} & \frac{\partial}{\partial x_1} & 0 \\ 0 & \frac{\partial}{\partial x_3} & \frac{\partial}{\partial x_2} \\ \frac{\partial}{\partial x_3} & 0 & \frac{\partial}{\partial x_1} \end{bmatrix}. \tag{2.65}$$

The differentiations in this relation are done with respect to the axes of the body coordinate system that is initially parallel to the global reference frame.

Six elements of strain vector form a symmetric matrix in $\mathbb{R}^{3\times3}$. Here the strain is presented in a vector form

$$\boldsymbol{\varepsilon} = \begin{bmatrix} \varepsilon_{11} & \varepsilon_{22} & \varepsilon_{33} & 2\varepsilon_{12} & 2\varepsilon_{13} & 2\varepsilon_{23} \end{bmatrix}^T \in \mathbb{R}^6. \tag{2.66}$$

In the elastic multibody dynamics it is generally assumed the linear strain-displacement relationship, which is described by Eq. 2.64. However, there are some applications that require taking into account a nonlinear term. Additional non-linear strain is obtained by a differential operator $\hat{\nabla}$:

$$\hat{\nabla}(\bar{\mathbf{u}}) = \begin{bmatrix} \frac{\partial u_1}{\partial x_1}\frac{\partial}{\partial x_1} & \frac{\partial u_2}{\partial x_1}\frac{\partial}{\partial x_1} & \frac{\partial u_3}{\partial x_1}\frac{\partial}{\partial x_1} \\ \frac{\partial u_1}{\partial x_2}\frac{\partial}{\partial x_2} & \frac{\partial u_2}{\partial x_2}\frac{\partial}{\partial x_2} & \frac{\partial u_3}{\partial x_2}\frac{\partial}{\partial x_2} \\ \frac{\partial u_1}{\partial x_3}\frac{\partial}{\partial x_3} & \frac{\partial u_2}{\partial x_3}\frac{\partial}{\partial x_3} & \frac{\partial u_3}{\partial x_3}\frac{\partial}{\partial x_3} \\ \frac{\partial u_1}{\partial x_1}\frac{\partial}{\partial x_2} + \frac{\partial u_1}{\partial x_2}\frac{\partial}{\partial x_1} & \frac{\partial u_1}{\partial x_1}\frac{\partial}{\partial x_2} + \frac{\partial u_2}{\partial x_2}\frac{\partial}{\partial x_1} & \frac{\partial u_1}{\partial x_1}\frac{\partial}{\partial x_2} + \frac{\partial u_3}{\partial x_2}\frac{\partial}{\partial x_1} \\ \frac{\partial u_1}{\partial x_2}\frac{\partial}{\partial x_3} + \frac{\partial u_1}{\partial x_3}\frac{\partial}{\partial x_2} & \frac{\partial u_1}{\partial x_2}\frac{\partial}{\partial x_3} + \frac{\partial u_2}{\partial x_3}\frac{\partial}{\partial x_2} & \frac{\partial u_1}{\partial x_2}\frac{\partial}{\partial x_3} + \frac{\partial u_3}{\partial x_3}\frac{\partial}{\partial x_2} \\ \frac{\partial u_1}{\partial x_3}\frac{\partial}{\partial x_1} + \frac{\partial u_1}{\partial x_1}\frac{\partial}{\partial x_3} & \frac{\partial u_1}{\partial x_3}\frac{\partial}{\partial x_1} + \frac{\partial u_2}{\partial x_1}\frac{\partial}{\partial x_3} & \frac{\partial u_1}{\partial x_3}\frac{\partial}{\partial x_1} + \frac{\partial u_3}{\partial x_1}\frac{\partial}{\partial x_3} \end{bmatrix}. \tag{2.67}$$

The nonlinear strain takes the form

$$\boldsymbol{\varepsilon} = \nabla \cdot \bar{\mathbf{u}} + \frac{1}{2}\hat{\nabla} \cdot \bar{\mathbf{u}}. \tag{2.68}$$

The strain rate $\dot{\boldsymbol{\varepsilon}}$ can be obtained differentiating Eq. 2.68 as[47]:

$$\dot{\varepsilon} \;=\; \nabla\dot{\bar{\mathbf{u}}} + \frac{1}{2}\left(\dot{\hat{\nabla}}\bar{\mathbf{u}} + \hat{\nabla}\dot{\bar{\mathbf{u}}}\right) = \nabla\dot{\bar{\mathbf{u}}} + \hat{\nabla}\dot{\bar{\mathbf{u}}}. \tag{2.69}$$

Using the relation $\dot{\bar{\mathbf{u}}} = \mathbf{S} \cdot \dot{\mathbf{q}}$ and Eq. 2.69 the virtual strain rate takes the form

$$\delta\dot{\boldsymbol{\varepsilon}} = \left(\nabla\mathbf{S} + \hat{\nabla}\mathbf{S}\right)\delta\dot{\mathbf{q}}. \tag{2.70}$$

According to the generalization of Hooke's law, the strain and stress vectors are connected by an elasticity matrix $\mathbf{E} \in \mathbb{R}^{6\times6}$ as

$$\boldsymbol{\sigma} = \mathbf{E} \cdot \boldsymbol{\varepsilon}. \tag{2.71}$$

Substituting Eq. 2.70 and the stress expression of Eq. 2.71 into Eq. 2.63 yields

$$\delta P_{inter} = -\left(\delta\dot{\mathbf{q}}\right)^T \left(\mathbf{K}_{eL}\cdot\mathbf{q} + \mathbf{K}_{eN}(\mathbf{q})\cdot\mathbf{q}\right), \tag{2.72}$$

where $\mathbf{K}_{eL}$ and $\mathbf{K}_{eN}(\mathbf{q})$ are linear and nonlinear components of *stiffness matrix* related to the elastic coordinates of finite element model and defined as

$$\mathbf{K}_{eL} = \int_V (\nabla\mathbf{S})^T \mathbf{E} \nabla\mathbf{S} dV \tag{2.73}$$

$$\mathbf{K}_{eN} = \int_V (\nabla\mathbf{S})^T \mathbf{E} \hat{\nabla}\mathbf{S} dV + \frac{1}{2}\int_V (\hat{\nabla}\mathbf{S})^T \mathbf{E} \hat{\nabla}\mathbf{S} dV. \tag{2.74}$$

It follows that the virtual power of elastic forces is obtained by

$$\delta P_{inter} = -\delta\mathbf{z_I}^T \mathbf{K}\mathbf{z}, \tag{2.75}$$

where

$$\mathbf{K} = \begin{bmatrix} \mathbf{0} & \mathbf{0} & \mathbf{0} \\ \mathbf{0} & \mathbf{0} & \mathbf{0} \\ \mathbf{0} & \mathbf{0} & \mathbf{K}_{eL} + \mathbf{K}_{eN}(\mathbf{q}) \end{bmatrix} \tag{2.76}$$

is a *generalized stiffness matrix* of the elastic body.

Virtual power of external forces

The virtual power of an external force acting at an arbitrary point of the body can be defined as

$$\delta P_{ext} = \delta\dot{\mathbf{d}}^T \cdot \mathbf{f}, \tag{2.77}$$

where $\mathbf{f} \in \mathbb{R}^3$ is an external force expressed in the global coordinate system, the vector $\dot{\mathbf{d}}$ defines a global velocity of the point where the force is applied. The virtual velocity $\delta\dot{\mathbf{d}}$ can be expressed in terms of generalized velocity coordinates $\mathbf{z_I}$ as

$$\delta\dot{\mathbf{d}} = \mathbf{L}\delta\mathbf{z_I} \tag{2.78}$$

with $\mathbf{L}$ being the matrix from Eq. 2.21. It follows that the virtual power of external forces is given by

$$\delta P_{ext} = \delta\mathbf{z_I}^T \mathbf{L}^T \mathbf{f} = \delta\mathbf{z_I}^T \begin{bmatrix} \mathbf{I} \\ \tilde{\mathbf{r}} \\ (\mathbf{AS})^T \end{bmatrix} \cdot \mathbf{f}. \tag{2.79}$$

The gravity force can be considered as a concentrated load at the center of gravity or a

volume force. The virtual power of a volume force is defined as

$$\delta P_{ext} = \int_V \delta \mathbf{z_I}^T \begin{bmatrix} \mathbf{I} \\ \tilde{\mathbf{r}} \\ (\mathbf{AS})^T \end{bmatrix} \mathbf{b} dV = \delta \mathbf{z_I}^T \left(\int_V \begin{bmatrix} \mathbf{I} \\ \tilde{\mathbf{r}} \\ (\mathbf{AS})^T \end{bmatrix} \mathbf{b} dV \right), \tag{2.80}$$

where $\mathbf{b}$ is a load per unit volume. For the gravity force the relation $\mathbf{b} = \rho \cdot \mathbf{g}$ can be used, where $\mathbf{g}$ denotes the gravity acceleration.

Moments can be represented using pairs of concentrated forces with the property $\mathbf{f}_1 = -\mathbf{f}_2$.

Similar to the consideration of volume forces, the virtual power of generalized surface force associated with a surface load $\mathbf{p}$ per unit area dD is defined as

$$\delta P_{ext} = \delta \mathbf{z_I}^T \int_D \begin{bmatrix} \mathbf{I} \\ \tilde{\mathbf{r}} \\ (\mathbf{AS})^T \end{bmatrix} \mathbf{p} dD. \tag{2.81}$$

If the body is subjected to several external forces, then their effects must be added. The generalized external force can be expressed as

$$\mathbf{h}_{ext} = \int_V \begin{bmatrix} \mathbf{I} \\ \tilde{\mathbf{r}} \\ (\mathbf{AS})^T \end{bmatrix} \mathbf{b} dV + \begin{bmatrix} \mathbf{I} \\ \tilde{\mathbf{r}} \\ (\mathbf{AS})^T \end{bmatrix} \cdot \mathbf{f} + \int_D \begin{bmatrix} \mathbf{I} \\ \tilde{\mathbf{r}} \\ (\mathbf{AS})^T \end{bmatrix} \mathbf{p} dD. \tag{2.82}$$

The virtual power of external forces takes the form

$$\delta P_{ext} = \delta \mathbf{z_I}^T \cdot \mathbf{h}_{ext}. \tag{2.83}$$

2.1.5 Equations of motion of free elastic body

Substituting the expressions for the virtual power of inertia forces from Eq. 2.33, internal forces from Eq. 2.75, and external forces from Eq. 2.83 into Jourdain's principle of Eq. 2.28 yields

$$\delta \mathbf{z_I}^T \left(\mathbf{M} \dot{\mathbf{z}}_\mathbf{I} + \mathbf{K}\mathbf{z} + \mathbf{h}_v - \mathbf{h}_{ext} \right) = \mathbf{0}. \tag{2.84}$$

Incorporation of damping into the equations of motion is considered in Section 2.1.8.

If components of generalized velocity coordinates $\mathbf{z_I}$ are independent, then Eq. 2.84 holds true only upon condition that the term in the parentheses equals zero. It follows the equations of motion of free elastic body are given as

$$\mathbf{M} \dot{\mathbf{z}}_\mathbf{I} + \mathbf{K}\mathbf{z} + \mathbf{h}_v - \mathbf{h}_{ext} = \mathbf{0}. \tag{2.85}$$

These equations are called *generalized Newton-Euler equations* of motion [79]. Here $\mathbf{M}$

and $\mathbf{K}$ are generalized mass and stiffness matrices of the body, $\mathbf{h}_v$ and $\mathbf{h}_{ext}$ represent the generalized quadratic velocity vector and the generalized vector of external forces. The equation can be rewritten in a detailed form as

$$\underbrace{\begin{bmatrix} m\cdot\mathbf{I} & m\cdot\mathbf{A}\cdot\tilde{\bar{\mathbf{c}}}^T\cdot\mathbf{A}^T & \mathbf{A}\cdot\mathbf{C}_t \\ & \mathbf{A}\cdot\mathbf{J}(\mathbf{q})\cdot\mathbf{A}^T & \mathbf{A}\cdot\mathbf{C}_r \\ symmetric & & \mathbf{M}_e \end{bmatrix}}_{\mathbf{M}}\cdot\dot{\mathbf{z}}_\mathbf{I}+\underbrace{\begin{bmatrix}\mathbf{0}&\mathbf{0}&\mathbf{0}\\ \mathbf{0}&\mathbf{0}&\mathbf{0}\\ \mathbf{0}&\mathbf{0}&\mathbf{K}_{eL}+\mathbf{K}_{eN}(\mathbf{q})\end{bmatrix}}_{\mathbf{K}}\cdot\mathbf{z}=$$

$$-\underbrace{\begin{bmatrix}\mathbf{A}m\tilde{\bar{\boldsymbol{\omega}}}\cdot\left(\tilde{\bar{\boldsymbol{\omega}}}\bar{\mathbf{c}}+2\dot{\bar{\mathbf{c}}}\right)\\ \mathbf{A}\cdot\left(\tilde{\bar{\boldsymbol{\omega}}}\mathbf{J}\bar{\boldsymbol{\omega}}+\mathbf{G}_r\bar{\boldsymbol{\omega}}\right)\\ \left[\bar{\boldsymbol{\omega}}^T\mathbf{O}_{ek}\bar{\boldsymbol{\omega}}\right]+\mathbf{G}_e\bar{\boldsymbol{\omega}}\end{bmatrix}}_{\mathbf{h}_v}+\underbrace{\left(\int_V\begin{bmatrix}\mathbf{I}\\ \tilde{\mathbf{r}}\\ (\mathbf{AS})^T\end{bmatrix}\mathbf{b}dV+\begin{bmatrix}\mathbf{I}\\ \tilde{\mathbf{r}}\\ (\mathbf{AS})^T\end{bmatrix}\cdot\mathbf{f}+\int_D\begin{bmatrix}\mathbf{I}\\ \tilde{\mathbf{r}}\\ (\mathbf{AS})^T\end{bmatrix}\mathbf{p}dD\right)}_{\mathbf{h}_{ext}} \tag{2.86}$$

The components of generalized mass matrix are summarized in Table 2.1.

Table 2.1: Components of generalized mass matrix.

Notation	Definition
$m\in\mathbb{R}$	mass of body
$\mathbf{I}\in\mathbb{R}^{3\times3}$	identity matrix
$\mathbf{A}\in\mathbb{R}^{3\times3}$	rotation matrix from the body frame to the inertial coordinate system
$\bar{\mathbf{c}}\in\mathbb{R}^3$	position of center of mass defined w.r.t. the body frame, Eq. 2.43
$\mathbf{C}_t\in\mathbb{R}^{3\times N}$	matrix coupled translational and elastic coordinates, Eq. 2.44
$\mathbf{C}_r\in\mathbb{R}^{3\times N}$	matrix coupled rotational and elastic coordinates, Eq. 2.45
$\mathbf{J}(\mathbf{q})\in\mathbb{R}^{3\times3}$	tensor of inertia defined w.r.t. the body frame, Eq. 2.40
$\mathbf{M}_e\in\mathbb{R}^{N\times N}$	finite element mass matrix defined w.r.t. the body frame, Eq. 2.41

The submatrices $\mathbf{K}_{eL}$ and $\mathbf{K}_{eN}$ of generalized stiffness matrix $\mathbf{K}$ are given in Eq. 2.73 and Eq. 2.74. The formulation of generalized quadratic velocity vector requires computing of additional terms described in Table 2.2.

Table 2.2: Components of generalized quadratic velocity vector.

Notation	Definition
$\dot{\bar{\mathbf{c}}}\in\mathbb{R}^3$	local velocity of mass center in the body frame, Eq. 2.49
$\mathbf{G}_r\in\mathbb{R}^{3\times3}$	component of Coriolis forces, Eq. 2.51
$\mathbf{O}_{ek}\in\mathbb{R}^{3\times3}$	elastic part of centrifugal forces, Eq. 2.59
$\mathbf{G}_e\in\mathbb{R}^{3\times N}$	elastic component of Coriolis forces, Eq. 2.61

The external concentrated and volume generalized forces $\mathbf{h}_{ext}$ are given in Eq. 2.82.

If the body is assumed to be rigid, the components associated with the generalized elastic coordinates in Eq. 2.86 vanish. This leads to the classical Newton-Euler equations of rigid

body motion. In addition, if the motion of the reference frame is constrained to be zero, Eq. 2.86 is reduced to the classical structural equations.

The generalized mass matrix form Eq. 2.86 has a rank deficiency of six, therefore it is not solvable until reference conditions are defined.

2.1.6 Definition of body coordinate system

It is assumed in the floating frame formulation that the displacement field $\bar{\mathbf{u}}$ describes deformation of the body with respect to the body reference frame. The global motion of body is the superposition of motion of body reference frame and deformations with respect to the body frame. If the assumed displacement field $\bar{\mathbf{u}}$ contains rigid body modes, they have to be eliminated to define a displacement field describing only deformations. This can be done by imposing a set of reference conditions, which are introduced by a set of linear algebraic equations. As the number of rigid body modes equals six, it is necessary to impose six reference conditions.

Since there are no unique manner of defining rigid and elastic motions, the floating frame can be selected in a number of different ways. These methods can be divided into two categories. The methods of the first group attach a coordinate system to material points of the body. This formulation is referred to as *nodal-fixed axes.* The second group of floating frames consists of coordinate systems that follow a body in an optimal manner. This category includes a frame oriented along the *principal axes* of inertia, a *mean-axes* (Tisserand) frame, and a *Buckens frame.* In contrast to nodal-fixed frames, coordinate systems of this type impose reference conditions on all nodes of the body. The moving frames eliminate the need to select material points for attaching the floating frame, but it is more difficult to determine the frame location and orientation because of specific frame conditions.

Nodal-fixed frames

If points of the body possess rotational degrees of freedom, the body coordinate system can be attached to one point. In this case, the reference conditions are given as

$$\begin{cases} \bar{\mathbf{u}}\left(\bar{\mathbf{r}}_{\mathbf{0}}^{P}, t\right) = \mathbf{0} \\ \bar{\boldsymbol{\vartheta}}\left(\bar{\mathbf{r}}_{\mathbf{0}}^{P}, t\right) = \mathbf{0}, \end{cases} \tag{2.87}$$

where $\bar{\boldsymbol{\vartheta}}$ defines rotational coordinates of the point P and $\bar{\mathbf{r}}_{\mathbf{0}}^{P}$ is an undeformed position of the point P.

Alternatively, the body coordinate system can be defined by three points P_1, P_2 and P_3. It is assumed that the origin of the frame is always located at the point P_1, the point P_2 remains along the x axis, and the point P_3 lies on the xy plane, see Fig. 2.4.

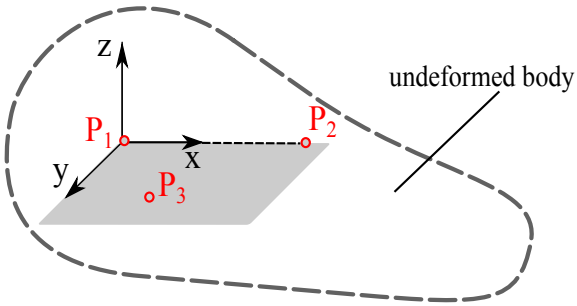

Figure 2.4: Attachment of body coordinate system by three points.

This yields six reference conditions

$$\begin{cases} \bar{\mathbf{u}}\left(\bar{\mathbf{r}}_0^{P_1}, t\right) = \mathbf{0} \\ \bar{u}_y\left(\bar{\mathbf{r}}_0^{P_2}, t\right) = 0 \\ \bar{u}_z\left(\bar{\mathbf{r}}_0^{P_2}, t\right) = 0 \\ \bar{u}_z\left(\bar{\mathbf{r}}_0^{P_3}, t\right) = 0, \end{cases} \tag{2.88}$$

where $\bar{\mathbf{r}}_0^{P_1}$,$\bar{\mathbf{r}}_0^{P_2}$, and $\bar{\mathbf{r}}_0^{P_3}$ are undeformed positions of points P_1,P_2, and P_3 respectively. If the body coordinate system differs from the coordinate system of finite element model, the undeformed locations of body points $\bar{\mathbf{r}}_0$ and shape functions $\mathbf{S}$ have to be redefined with respect to the new body frame.

The reference conditions of Eq. 2.88 can be simplified in the case of fixation of body frame to nodes of the body. If nodes possess three DoFs, the displacement field $\bar{\mathbf{u}}$ for an arbitrary node K takes the form

$$\bar{\mathbf{u}}\left(\bar{\mathbf{r}}_0^K, t\right) = \mathbf{q}^K(t) \in \mathbb{R}^3, \tag{2.89}$$

where $\mathbf{q}^K$ is a vector of degrees of freedom for the node K. Then Eq. 2.88 can be rewritten as

$$\begin{cases} \mathbf{q}^{K_1}(t) = \mathbf{0} \in \mathbb{R}^3 \\ q_y^{K_2}(t) = 0 \in \mathbb{R} \\ q_z^{K_2}(t) = 0 \in \mathbb{R} \\ q_z^{K_3}(t) = 0 \in \mathbb{R} \end{cases} \tag{2.90}$$

with K_1, K_2, and K_3 being nodes of the body.

The reference conditions of Eq. 2.90 can be automatically taking into account in equations of motion and there is no need to include them to the system of equations. The dependency of the vector of unconstrained elastic coordinates $\mathbf{q}_u$ and the initial vector of nodal deformations $\mathbf{q}$ can be written as

$$\mathbf{q} = \mathbf{B} \cdot \mathbf{q}_u, \tag{2.91}$$

where $\mathbf{B}$ is a linear transformation that arises from imposing the constrains of Eq. 2.90

and consists of zeros and ones. The displacement field $\bar{\mathbf{u}}$ can be represented as

$$\bar{\mathbf{u}} = \mathbf{S} \cdot \mathbf{B} \cdot \mathbf{q}_u = \mathbf{S}_u \cdot \mathbf{q}_u, \tag{2.92}$$

where $\mathbf{S}_u$ is a shape matrix that satisfies the reference conditions. Substituting Eq. 2.92 into Eq. 2.11 leads to the equations of motion in terms of independent generalized coordinates.

The conditions of Eq. 2.88 attach the reference frame to the body. The rigid-body motion in this coordinate system is eliminated. Since the body frame is allowed to move with respect to an inertial frame, attaching the moving frame to the points does not exclude any of the rigid-body modes in the inertial coordinate system.

Principal axes frame

In this formulation the moving reference frame is enforced to coincide with the instantaneous principal axes of a deformable body. This method provides six conditions based on two requirements: the origin of the reference frame must remain at the instantaneous mass center, and three products of inertia must remain zeros:

$$\begin{cases} \mathbf{c} = \mathbf{0} \\ \mathbf{J}_{ij} = 0, \quad i \neq j, i = 1..3, j = 1..3. \end{cases} \tag{2.93}$$

Here $\mathbf{c}$ is the vector of mass center from Eq. 2.43 and $\mathbf{J}$ is the inertia tensor defined in Eq. 2.40.

In this case, the coupling between flexible and rigid body motion is weaker and equations of motions become easier: the tensor of inertia $\mathbf{J}$ becomes a diagonal matrix, and the sub-matrices $\mathbf{M}_{tr}$ and $\mathbf{M}_{te}$ of Eq. 2.42 and Eq. 2.44 vanish because the vector of mass center is equal to zero. Deriving expressions for products of inertia in terms of nodal coordinates can be found in [77, 62]. In contrast to the nodal fixed frame formulations, the reference conditions of principal axes frames increase the number of equations to be solved by six.

Mean-axes frame

The mean-axis conditions are six constraints that enforce the body frame to follow the motion of nodes in such a way that the following conditions are satisfied

$$\begin{cases} \mathbf{C}_t \cdot \dot{\mathbf{q}} = \mathbf{0} \\ \mathbf{C}_r(\mathbf{q}) \cdot \dot{\mathbf{q}} = \mathbf{0} \end{cases} \tag{2.94}$$

with $\mathbf{C}_t$ and $\mathbf{C}_r$ being the matrices defined in Eq. 2.44 and Eq. 2.45, respectively. According to [76], if the origin of body frame is located in a mass center of undeformed body, the first equation from Eq. 2.94 enforces the frame to follow an instantaneous mass center

$$\mathbf{C}_t \cdot \dot{\mathbf{q}} = m \cdot \dot{\bar{\mathbf{c}}} = \mathbf{0} \Rightarrow \bar{\mathbf{c}} = \mathbf{0}. \tag{2.95}$$

Similar to the principle axes approach, the first condition of Eq. 2.94 eliminates the terms $\mathbf{M}_{tr}$ and $\mathbf{M}_{te}$ from the generalized mass matrix of Eq. 2.35. The second equation from Eq. 2.94 defines orientation of the floating frame and removes the term $\mathbf{M}_{re}$. It follows that the generalized mass matrix $\mathbf{M}$ takes a block-diagonal form. The inertia tensor remains a non-diagonal matrix. Due to the conditions of Eq. 2.94 the mean-axes frame has a property that the kinetic energy associated with the deformation stays at a minimum [17].

Buckens frame

The Buckens frame is a special case of mean-axes frame. The mean-axes constrains of Eq. 2.94 are valid even for large deformations of the body. If small deformations are assumed, the products of elastic coordinates $\mathbf{q}$ can be neglected in the equations of motion. The Taylor expansion of $\mathbf{C}_r$ up to the first order terms yields

$$\mathbf{C}_r(\mathbf{q}) = \mathbf{C}_{r0} + \mathbf{C}_{r1}(\mathbf{q}), \tag{2.96}$$

where the indexes 0 and 1 define zero and the first order terms of the Taylor expansion, respectively.

Assuming small deformations, the second condition of mean-axes frame can be simplified as

$$\mathbf{C}_r(\mathbf{q}) \cdot \dot{\mathbf{q}} = \mathbf{C}_{r0} \cdot \dot{\mathbf{q}} = \mathbf{0} \tag{2.97}$$

that leads to Buckens frame conditions

$$\begin{cases} \mathbf{C}_t \cdot \dot{\mathbf{q}} = \mathbf{0} \\ \mathbf{C}_{r0} \cdot \dot{\mathbf{q}} = \mathbf{0}. \end{cases} \tag{2.98}$$

The term $\mathbf{C}_t$ is defined in Eq. 2.44, while $\mathbf{C}_{r0}$ is given by

$$\mathbf{C}_{r0} = \int_V \rho \tilde{\tilde{\mathbf{r}}}_0 \mathbf{S} dV. \tag{2.99}$$

Similarly to the mean-axes frame constrains, the Buckens frame conditions transform generalized mass matrix to a block-diagonal form. In addition, according to [87] the

Buckens frame ensures that the sum of the squares of elastic displacements with respect to the body frame is a minimum:

$$\frac{1}{2}\int_V \bar{\mathbf{u}}^T \cdot \bar{\mathbf{u}}\, dm = \min. \tag{2.100}$$

It means that the Buckens coordinate system leads to the smallest elastic displacements possible. This may be important when the assumption of small deformation for modeling elastic body motion is used. In the general case the Buckens frame constraints must be added to equations of motion, but under certain conditions they are automatically satisfied. One of the approaches to take into account the Buckens frame conditions during the simulation is proposed in [2]. The other way to satisfy these reference conditions is connected with using eigenmodes of unconstrained body. The requirements of Buckens frame can be automatically satisfied, if columns of shape matrix $\mathbf{S}$ from Eq. 2.10 are mass orthogonal to rigid body modes and the position of body frame in the undeformed state of the body coincides with the mass center, see [77].

2.1.7 Approximation of motion integrals by finite element programs

The dynamic properties of elastic body are defined by the volume integrals introduced in Section 2.1.4. Most of them depend on generalized elastic coordinates and, therefore, must be updated at each step of integration. In order to reduce computational costs during simulation, the volume integrals are expressed by generalized elastic coordinates and precomputed time-invariant system matrices. These matrices can be found as follows.

Every volume integral $\mathbf{Z}$ is expressed as a sum of terms $\mathbf{Z}_0$, $\mathbf{Z}_1$, and $\mathbf{Z}_2$ that are constant, linearly, and quadratically depended on the elastic coordinates $\mathbf{q}$, respectively:

$$\mathbf{Z}(\mathbf{q}) = \mathbf{Z}_0 + \mathbf{Z}_1(\mathbf{q}) + \mathbf{Z}_2(\mathbf{q}). \tag{2.101}$$

Assuming small deformations, the quadratic component $\mathbf{Z}_2$ is negligibly small, therefore

$$\mathbf{Z}(\mathbf{q}) = \mathbf{Z}_0 + \mathbf{Z}_1(\mathbf{q}). \tag{2.102}$$

Using this representation, it is possible to find constant components for all volume integrals. This process is described in detail in [56, 76]. Table 2.3 contains a set of time-invariant system matrices required for the calculation of the volume integrals of elastic body.

The principle of retrieving constant matrices from volume integrals can be illustrated by processing the inertia tensor. Using the relation $\bar{\mathbf{r}} = \bar{\mathbf{r}}_0 + \mathbf{S} \cdot \mathbf{q}$ of Eq. 2.11, the inertia

Table 2.3: Time-invariant components of volume integrals.

Notation	Calculation
$m \cdot \mathbf{I}$	$\int_V \rho \mathbf{I}\, dV$
$m \cdot \bar{\mathbf{c}}_0$	$\int_V \rho \bar{\mathbf{r}}_0\, dV$
$\mathbf{J}_0$	$\int_V \rho \tilde{\bar{\mathbf{r}}}_0 \cdot \tilde{\bar{\mathbf{r}}}_0^T\, dV$
$\mathbf{C1}$	$\int_V \rho \mathbf{S}\, dV$
$\mathbf{C2}$	$\int_V \rho \tilde{\bar{\mathbf{r}}}_0 \cdot \mathbf{S}\, dV$
$\mathbf{C3}$	$\int_V \rho \mathbf{S} \cdot \mathbf{S}^T\, dV$
$\mathbf{C4}_k$	$\int_V \rho \tilde{\bar{\mathbf{r}}}_0 \cdot \tilde{\mathbf{S}}_{*k}\, dV$
$\mathbf{C5}_k$	$\int_V \rho \tilde{\mathbf{S}}_{*k} \cdot \mathbf{S}\, dV$
$\mathbf{C6}_{kl}$	$\int_V \rho \tilde{\mathbf{S}}_{*k} \cdot \tilde{\mathbf{S}}_{*l}\, dV$

tensor $\mathbf{J}$ of Eq. 2.40 takes the form

$$\begin{aligned}\mathbf{J}(\mathbf{q}) &= \int_V \rho \tilde{\bar{\mathbf{r}}} \cdot \tilde{\bar{\mathbf{r}}}^T dV = \int_V \rho \tilde{\bar{\mathbf{r}}}_0 \cdot \tilde{\bar{\mathbf{r}}}_0^T dV + \int_V \rho \left(\tilde{\bar{\mathbf{r}}}_0 \cdot \widetilde{(\mathbf{S}\cdot\mathbf{q})}^T + \widetilde{(\mathbf{S}\cdot\mathbf{q})} \cdot \tilde{\bar{\mathbf{r}}}_0^T \right) dV \\ &\quad + \int_V \rho \widetilde{(\mathbf{S}\cdot\mathbf{q})} \cdot \widetilde{(\mathbf{S}\cdot\mathbf{q})}^T dV. \end{aligned} \tag{2.103}$$

The first summand of this equation corresponds to the matrix $\mathbf{J}_0$ from Table 2.3. The third part depends quadratically on generalized coordinates $\mathbf{q}$, therefore it vanishes by small deformations. Using the relation

$$\mathbf{S} \cdot \mathbf{q} = \mathbf{S}_{*1} \cdot q_1 + ... + \mathbf{S}_{*N} \cdot q_N \tag{2.104}$$

the coordinates $\mathbf{q}$ can be taken out of the brackets of the second summand of Eq. 2.103 by the transformation

$$\begin{aligned}\int_V \rho \left(\tilde{\bar{\mathbf{r}}}_0 \cdot \widetilde{(\mathbf{S}\cdot\mathbf{q})}^T + \widetilde{(\mathbf{S}\cdot\mathbf{q})} \cdot \tilde{\bar{\mathbf{r}}}_0^T \right) dV &= \sum_{k=1}^{N} \int_V \rho \left(\tilde{\bar{\mathbf{r}}}_0 \cdot \tilde{\mathbf{S}}_{*k}^T + \tilde{\mathbf{S}}_{*k} \cdot \tilde{\bar{\mathbf{r}}}_0^T \right) dV q_k = \\ -\sum_{k=1}^{N} \int_V \rho \left(\tilde{\bar{\mathbf{r}}}_0 \cdot \tilde{\mathbf{S}}_{*k} + \tilde{\mathbf{S}}_{*k} \cdot \tilde{\bar{\mathbf{r}}}_0 \right) dV q_k. \end{aligned} \tag{2.105}$$

It follows that the inertia tensor $\mathbf{J}$ is constructed by the generalized coordinates $\mathbf{q}$ and the time-invariant matrices as

$$\mathbf{J}(\mathbf{q}) = \mathbf{J}_0 - \sum_{k=1}^{N} \int_V \rho \left(\tilde{\bar{\mathbf{r}}}_0 \cdot \tilde{\mathbf{S}}_{*k} + \tilde{\mathbf{S}}_{*k} \cdot \tilde{\bar{\mathbf{r}}}_0 \right) dV q_k = \underbrace{\mathbf{J}_0 - \sum_{k=1}^{N} \left(\mathbf{C4}_k + \mathbf{C4}_k^T \right) q_k}_{\mathbf{J}_1(\mathbf{q})}. \tag{2.106}$$

Let us consider formulation of other terms of generalized mass matrix in terms of the time-invariant components. According toTable 2.1, the following terms must be considered: position of center of mass $\bar{\mathbf{c}}$, coupling terms $\mathbf{C}_t$ and $\mathbf{C}_r$, and the finite element matrix $\mathbf{M}_e$.

The vector of center of mass can be rewritten as

$$\bar{\mathbf{c}} = \bar{\mathbf{c}}_0 + \bar{\mathbf{c}}_1(\mathbf{q}) = \bar{\mathbf{c}}_0 + \frac{1}{m} \cdot \mathbf{C1} \cdot \mathbf{q}. \tag{2.107}$$

The term of coupling of translational and elastic coordinates takes the form

$$\mathbf{C}_t = \mathbf{C1}. \tag{2.108}$$

The matrix $\mathbf{C}_r$ in terms of the time-invariant components is given as

$$\mathbf{C}_r = \mathbf{C}_{r0} + \mathbf{C}_{r1}(\mathbf{q}) = \mathbf{C2} + \sum_{k=1}^{N} \mathbf{C5}_k \cdot q_k. \tag{2.109}$$

Finally, the finite element mass matrix $\mathbf{M}_e$ coincides with the component $\mathbf{C3}$.

The terms of generalized quadratic velocity vector from Table 2.2 must be also represented using constant components of motion integrals. The set of terms to be considered includes the velocity of mass center $\dot{\bar{\mathbf{c}}}$, components of Coriolis force $\mathbf{G}_r$ and $\mathbf{G}_e$, and the component of elastic part of centrifugal force $\mathbf{O}_{ek}$.

Using Eq. 2.49 and $\dot{\tilde{\mathbf{r}}} = \mathbf{S}\dot{\mathbf{q}}$, the velocity of mass center takes the following form

$$\dot{\bar{\mathbf{c}}} = \frac{1}{m} \cdot \mathbf{C1} \cdot \dot{\mathbf{q}}. \tag{2.110}$$

The component $\mathbf{G}_r$ from Eq. 2.51 can also be written as

$$\mathbf{G}_r = 2 \int_V \rho \tilde{\tilde{\mathbf{r}}} \widetilde{\mathbf{S}\dot{\mathbf{q}}}^T dV. \tag{2.111}$$

Using the relation $\tilde{\tilde{\mathbf{r}}} = \tilde{\tilde{\mathbf{r}}}_0 + \widetilde{\mathbf{S}\mathbf{q}}$ and Eq. 2.104, the integrand of the equation takes the form

$$\begin{aligned} \tilde{\tilde{\mathbf{r}}} \widetilde{\mathbf{S}\dot{\mathbf{q}}}^T &= \tilde{\tilde{\mathbf{r}}}_0 \cdot \widetilde{\mathbf{S}\dot{\mathbf{q}}}^T + \widetilde{\mathbf{S}\mathbf{q}} \cdot \widetilde{\mathbf{S}\dot{\mathbf{q}}}^T = \\ &\quad - \sum_{k=1}^{N} \tilde{\tilde{\mathbf{r}}}_0 \cdot \widetilde{\mathbf{S}_{*k}} \cdot \dot{q}_k - \sum_{k=1}^{N} \sum_{l=1}^{N} \widetilde{\mathbf{S}_{*k}} \cdot \widetilde{\mathbf{S}_{*l}} \cdot q_k \cdot \dot{q}_l. \end{aligned} \tag{2.112}$$

Thus, the component $\mathbf{G}_r$ can be expressed in terms of the time invariant matrices as

$$\mathbf{G}_r = -2 \sum_{k=1}^{N} \mathbf{C4}_k \cdot \dot{q}_k - 2 \sum_{k=1}^{N} \sum_{l=1}^{N} \mathbf{C6}_{kl} \cdot q_k \cdot \dot{q}_l. \tag{2.113}$$

Similarly, the matrix $\mathbf{G}_e$ from Eq. 2.61 can be rewritten as

$$\mathbf{G}_e = 2 \int_V \rho \mathbf{S}^T \widetilde{\mathbf{S}\dot{\mathbf{q}}}^T dV = 2 \sum_{k=1}^{N} \int_V \rho \mathbf{S}^T \left(\widetilde{\mathbf{S}}_{*k} \right)^T dV \cdot \dot{q}_k = 2 \sum_{k=1}^{N} \mathbf{C5}_k^T \cdot \dot{q}_k.$$

Finally, the terms $\mathbf{O}_{ek}$ from Eq. 2.59 are obtained as follows

$$\mathbf{O}_{ek} = \int_V \rho \tilde{\mathbf{S}}_{*k} \tilde{\bar{\mathbf{r}}} dV = \int_V \rho \tilde{\mathbf{S}}_{*k} \tilde{\bar{\mathbf{r}}}_0 dV + \sum_{l=1}^{N} \int_V \rho \tilde{\mathbf{S}}_{*k} \tilde{\mathbf{S}}_{*l} dV \cdot q_l = \mathbf{C4}_k + \sum_{l=1}^{N} \mathbf{C6}_{kl} \cdot q_l.$$

The FE programs can export the component **C3**. The remaining components must be computed in special preprocessors. The data needed for the construction of equations of motion of elastic body can be defined by the finite element stiffness matrix $\mathbf{K}_e$, the mass matrix $\mathbf{M}_e$, information about boundary conditions, and the undeformed positions of nodes $\bar{\mathbf{r}}_\mathbf{0}$. The construction process for consistent mass matrix formulation is presented in [55, 76, 82]. In this thesis we consider a principle of evaluation of motion integrals by example of **C1** and **C4**.

If the FE model undergoes only translational rigid body motion, the linear velocity of all nodes of the model is the same

$$\mathbf{v}(t) = \dot{\mathbf{u}}(\bar{\mathbf{r}}_\mathbf{0}, t) = \mathbf{S}(\bar{\mathbf{r}}_\mathbf{0}) \cdot \dot{\mathbf{q}}(t). \tag{2.114}$$

The vector of generalized velocities is composed of velocities of each node

$$\dot{\mathbf{q}}(t) = \begin{bmatrix} \mathbf{v}(t) \\ \vdots \\ \mathbf{v}(t) \end{bmatrix} = \underbrace{\begin{bmatrix} \mathbf{I} \\ \vdots \\ \mathbf{I} \end{bmatrix}}_{\mathbf{S}_t} \mathbf{v}(t). \tag{2.115}$$

Here $\mathbf{I}$ is 3×3 identity matrix. Substituting this equations in the previous one yields the orthogonality relation

$$\mathbf{S} \cdot \mathbf{S}_t = \mathbf{I}. \tag{2.116}$$

In the case the FE model undergoes rotational rigid body motion, the linear velocity of each nodes are defined as

$$\dot{\mathbf{u}}(\bar{\mathbf{r}}_\mathbf{0}, t) = \tilde{\boldsymbol{\omega}} \bar{\mathbf{r}}_\mathbf{0} = -\widetilde{\bar{\mathbf{r}}}_\mathbf{0} \boldsymbol{\omega} = \mathbf{S}(\bar{\mathbf{r}}_\mathbf{0}) \cdot \dot{\mathbf{q}}(t). \tag{2.117}$$

The vector of generalized velocities takes the form

$$\dot{\mathbf{q}}(t) = \begin{bmatrix} \tilde{\boldsymbol{\omega}} \bar{\mathbf{r}}_\mathbf{0} \\ \vdots \\ \tilde{\boldsymbol{\omega}} \bar{\mathbf{r}}_\mathbf{0} \end{bmatrix} = \underbrace{\begin{bmatrix} -\widetilde{\bar{\mathbf{r}}}_\mathbf{0} \\ \vdots \\ -\widetilde{\bar{\mathbf{r}}}_\mathbf{0} \end{bmatrix}}_{\mathbf{S}_r} \boldsymbol{\omega}. \tag{2.118}$$

The last two equations result in

$$-\widetilde{\bar{\mathbf{r}}}_\mathbf{0} = \mathbf{S} \cdot \mathbf{S}_r. \tag{2.119}$$

For the construction of volume integrals it is necessary to introduce an auxiliary matrix $\mathbf{S}_e$ that is defined as

$$\mathbf{S}_e = \mathbf{B} \tag{2.120}$$

with $\mathbf{B}$ being a matrix that accounts for boundary conditions imposed on the elastic coordinates $\mathbf{q}$, see Eq. 2.91. If model reduction methods are applied, the matrix $\mathbf{S}_e$ is defined as

$$\mathbf{S}_e = \mathbf{B} \cdot \mathbf{V}, \tag{2.121}$$

where $\mathbf{V}$ is a coordinate transformation matrix.

The component $\mathbf{C1}$ can be written for the system with boundary conditions and reduced coordinates as follows:

$$\mathbf{C1} = \int_V \rho \mathbf{S} \cdot \mathbf{S}_e \, dV. \tag{2.122}$$

Using the relation of Eq. 2.116 this equation can be written in another form

$$\mathbf{C1} = \int_V \rho \mathbf{S} \cdot \mathbf{S}_e \, dV = \mathbf{S}_t^T \cdot \left[\int_V \rho \mathbf{S}^T \cdot \mathbf{S} \, dV \right] \cdot \mathbf{S}_e = \mathbf{S}_t^T \cdot \mathbf{M}_e \cdot \mathbf{S}_e. \tag{2.123}$$

The calculation of the term $\mathbf{C4}_k$ requires using the second relation defined in Eq. 2.119:

$$\mathbf{C4}_k = \int_V \rho \tilde{\bar{\mathbf{r}}}_0 \cdot \tilde{\mathbf{S}}_{*k} \, dV = \mathbf{S}_r^T \cdot \int \rho \mathbf{S}^T \cdot \tilde{\mathbf{S}}_{*k} \, dV. \tag{2.124}$$

Here the matrix $\tilde{\mathbf{S}}_{*k}$ has to be transformed as

$$\tilde{\mathbf{S}}_{*k} = -\begin{bmatrix} \tilde{\mathbf{e}}_1 \cdot \mathbf{S}_{*k} & \tilde{\mathbf{e}}_2 \mathbf{S}_{*k} & \tilde{\mathbf{e}}_3 \mathbf{S}_{*k} \end{bmatrix} = -\begin{bmatrix} \tilde{\mathbf{e}}_1 \cdot \mathbf{S} \cdot \mathbf{I}_{*k} & \tilde{\mathbf{e}}_2 \cdot \mathbf{S} \cdot \mathbf{I}_{*k} & \tilde{\mathbf{e}}_3 \cdot \mathbf{S} \cdot \mathbf{I}_{*k} \end{bmatrix}, \tag{2.125}$$

where $\mathbf{e}_i \in \mathbb{R}^{3\times 1}$ are unit vectors and $\mathbf{I}_{*k}$ is the k-th column of identity matrix $\mathbf{I} \in \mathbb{R}^{N\times N}$. Using the matrix $\mathbf{S}_e$, the i-th column of matrix $\mathbf{C4}_k$ takes the form

$$[\mathbf{C4}_k]_{*i} = -\mathbf{S}_r^T \cdot \mathbf{X}_i \cdot [\mathbf{S}_e]_{*k}, \tag{2.126}$$

where $\mathbf{X}_i = \int_V \rho \mathbf{S}^T \cdot \tilde{\mathbf{e}}_i \cdot \mathbf{S} \, dV$.

In order to identify the mass matrix $\mathbf{M}_e$ in this equation, the matrix $\tilde{\mathbf{e}}_i$ must be pulled out of the integral. This can be carried out only for isoparametric finite elements [47]. For the isoparametric elements the locations of material points on the elements, as well as their displacements are interpolated by the same shape functions. These elements do not use rotational parameters as nodal coordinates[79]. The pulling out the matrix $\tilde{\mathbf{e}}_i$ yields

$$\mathbf{X}_i = diag(\tilde{\mathbf{e}}_i) \cdot \int_V \rho \mathbf{S}^T \cdot \mathbf{S} \, dV = diag(\tilde{\mathbf{e}}_i) \cdot \mathbf{M}_e. \tag{2.127}$$

The calculation of matrix $\mathbf{X}_i$ for nonisoparametric elements is problematic, therefore the approximation approach proposed in [55] is usually applied:

$$asym(\mathbf{X}_i) := \frac{1}{2} \cdot \left(\mathbf{X}_i - \mathbf{X}_i^T \right). \tag{2.128}$$

The final expression for the term $\mathbf{C4}_k$ is given as

$$[\mathbf{C4}_k]_{*i} = -\mathbf{S}_r^T \cdot asym(\mathbf{X}_i) \cdot [\mathbf{S}_e]_{*k}, i = 1..3. \tag{2.129}$$

The calculation of volume integrals from Table 2.3 using the finite element data is shown in Table 2.4.

Table 2.4: Calculation of volume integrals using data imported from finite element tools.

Notation	Calculation
$m \cdot \mathbf{I}$	$\mathbf{S}_t^T \cdot \mathbf{M}_e \cdot \mathbf{S}_t$
$m \cdot \bar{\mathbf{c}}_0$	$\mathbf{S}_r^T \cdot \mathbf{M}_e \cdot \mathbf{S}_t$
$\mathbf{J}_0$	$\mathbf{S}_r^T \cdot \mathbf{M}_e \cdot \mathbf{S}_r$
$\mathbf{C1}$	$\mathbf{S}_t^T \cdot \mathbf{M}_e \cdot \mathbf{S}_e$
$\mathbf{C2}$	$\mathbf{S}_r^T \cdot \mathbf{M}_e \cdot \mathbf{S}_e$
$\mathbf{C3}$	$\mathbf{S}_e^T \cdot \mathbf{M}_e \cdot \mathbf{S}_e$
$[\mathbf{C4}_k]_{*i}$	$-\mathbf{S}_r^T \cdot asym(diag(\tilde{\mathbf{e}}_i) \cdot \mathbf{M}_e) \cdot [\mathbf{S}_e]_{*k}$
$[\mathbf{C5}_k]_{i*}$	$-[\mathbf{S}_e]_{*k}{}^T \cdot asym(diag(\tilde{\mathbf{e}}_i) \cdot \mathbf{M}_e) \cdot \mathbf{S}_e$
$[\mathbf{C6}_{kl}]_{ij}$	$[\mathbf{S}_e]_{*k}{}^T \cdot diag(\tilde{\mathbf{e}}_i) \cdot \mathbf{M}_e \cdot diag(\tilde{\mathbf{e}}_j) \cdot [\mathbf{S}_e]_{*l}$

The external forces in Eq. 2.86 can be represented using concentrated nodal forces formulation of which does not require the shape matrix $\mathbf{S}$.

2.1.8 Damping definition

For some applications damping effects must be taken into account. The most simple and widely used method to incorporate damping forces into equations of motion is to use a proportional to velocities representation $\mathbf{Dz_I}$ with a constant matrix $\mathbf{D}$. This leads to the following equations of motion for linearly damped models

$$\mathbf{Mz_{II}} + \mathbf{Dz_I} + \mathbf{Kz} + \mathbf{h}_v - \mathbf{h}_{ext} = \mathbf{0}. \tag{2.130}$$

Here the damping matrix $\mathbf{D}$ takes the form

$$\mathbf{D} = \begin{bmatrix} \mathbf{0} & \mathbf{0} & \mathbf{0} \\ \mathbf{0} & \mathbf{0} & \mathbf{0} \\ \mathbf{0} & \mathbf{0} & \mathbf{D}_e \end{bmatrix}, \mathbf{D} \in \mathbb{R}^{(6+N)\times(6+N)}, \tag{2.131}$$

where $\mathbf{D}_e \in \mathbb{R}^{N\times N}$ defines a finite element damping matrix.

In principle, the damping matrix $\mathbf{D}_e$ can be constructed by damping matrices of finite elements analogous to the mass and stiffness matrices. However, material damping properties of certain elements are often not defined well enough to employ the same procedure.

The damping matrix can be constructed by Caughey's series as

$$\mathbf{D}_e = \mathbf{M}_e \cdot \sum_{k=0}^{r} a_k \left(\mathbf{M}_e^{-1} \cdot \mathbf{K}_{eL}\right)^k, \tag{2.132}$$

where r defines a quantity of summands in the series, see [18]. In special case $r = 1$, the damping matrix is called *Rayleigh damping* and is defined as

$$\mathbf{D}_e = a_0 \mathbf{M}_e + a_1 \mathbf{K}_{eL}. \tag{2.133}$$

The damping matrix formulated by Caughey's series allows the definition of unknown coefficients a_i using a modal damping matrix. According to [21, 11] the coefficients of modal damping matrix are defined as

$$\boldsymbol{\phi}_i^T \mathbf{D}_e \boldsymbol{\phi}_j = \begin{cases} 0, & i \neq j \\ 2\omega_i \xi_i, & i = j, \end{cases} \tag{2.134}$$

where the pair $(\boldsymbol{\phi}_i, \omega_i)$ denote the i -th eingenvector and eigenfrequency of the system and ξ_i defines a corresponded modal damping factor.

Using the Eq. 2.133 and Eq. 2.134 the modal damping factor ξ_i can be expressed as shown in [21] as

$$\xi_i = \frac{1}{2}\left(\frac{a_0}{\omega_i} + a_1 \omega_i\right). \tag{2.135}$$

Thus, Rayleigh damping can be defined by choosing ξ_i for two modes and solving for a_0 and a_1. The constants a_0 and a_1 produce specified modal damping factors for two given modes. The advantage of Rayleigh damping lies in a simple calculation, while the drawback is that it does not permit to define realistic damping for all modes of interest.

2.2 Model order reduction of elastic bodies

Modern finite element models may have millions degrees of freedom, which significantly slow down a simulation process. The large number of elastic coordinates $\mathbf{q}_e$ can be reduced by model order reduction techniques. The main idea of these methods is to build a low-dimensional model that preserves important properties of the original model. In this section we consider model order reduction approaches based on projection, as well as demands on the methods when using in the context of elastic multibody systems.

2.2.1 Basics of model order reduction

Let us consider the elastic part of equations of motion of deformable body

$$\mathbf{M}_e \cdot \ddot{\mathbf{q}} + \mathbf{D}_e \cdot \dot{\mathbf{q}} + \mathbf{K}_e \cdot \mathbf{q} = \mathbf{h}_e. \tag{2.136}$$

Here $\mathbf{h}_e$ denotes a vector of external forces. It is necessary for some reduction methods to represent the vector $\mathbf{h}_e$ as a product of time dependent load vector $\mathbf{u}(t) \in \mathbb{R}^p$ and a load distribution matrix $\mathbf{B}_e \in \mathbb{R}^{N \times p}$. In addition, the coordinates of interest $\mathbf{y}(t) \in \mathbb{R}^r$ are cut out from the vector $\mathbf{q}$ by a matrix $\mathbf{C}_e \in \mathbb{R}^{r \times N}$. For these reduction methods the equation of motion are formulated as

$$\begin{aligned} \mathbf{M}_e \cdot \ddot{\mathbf{q}} + \mathbf{D}_e \cdot \dot{\mathbf{q}} + \mathbf{K}_e \cdot \mathbf{q} &= \mathbf{B}_e \cdot \mathbf{u} \\ \mathbf{y} &= \mathbf{C}_e \cdot \mathbf{q}. \end{aligned} \tag{2.137}$$

The reduction techniques based on projection rely on the assumption that a high-dimensional solution vector $\mathbf{q}$ belongs to a subspace $\mathcal{V}$ of smaller dimension $n \ll N$. Let

$$\mathbf{V} = \left[\begin{array}{cccc} \mathbf{v}_1, & \mathbf{v}_2, & \cdots & , \mathbf{v}_n \end{array} \right] \in \mathbb{R}^{N \times n}$$

define a basis of subspace $\mathcal{V}$, then the elastic coordinates $\mathbf{q}$ can be represented as

$$\mathbf{q} \approx \mathbf{V} \cdot \hat{\mathbf{q}}, \tag{2.138}$$

where the vector $\hat{\mathbf{q}}$ is referred to as reduced coordinates. Substituting this relation into equations of motion Eq. 2.137 results in an over-determined system and leave a residuum because an exact solution $\mathbf{q}$ may not be an element of subspace $\mathcal{V}$. The residuum can be eliminated by an orthogonal subspace $\mathcal{W}$ represented by a matrix $\mathbf{W} \in \mathbb{R}^{N \times n}$. This orthogonality condition is called Petrov-Galerkin condition, see [6, 72, 47]. The condition is introduced in the equations of motion by a premultiplication of Eq. 2.137 by the matrix $\mathbf{W}^T$. Thus, the low-dimensional approximation of original model takes the form

$$\begin{aligned} \hat{\mathbf{M}}_e \cdot \ddot{\hat{\mathbf{q}}} + \hat{\mathbf{D}}_e \cdot \dot{\hat{\mathbf{q}}} + \hat{\mathbf{K}}_e \cdot \hat{\mathbf{q}} &= \hat{\mathbf{B}}_e \cdot \mathbf{u} \\ \hat{\mathbf{y}} &= \hat{\mathbf{C}}_e \cdot \hat{\mathbf{q}} \end{aligned} \tag{2.139}$$

with the reduced matrices $\hat{\mathbf{M}}_e = \mathbf{W}^T \cdot \mathbf{M}_e \cdot \mathbf{V}$, $\hat{\mathbf{D}}_e = \mathbf{W}^T \cdot \mathbf{D}_e \cdot \mathbf{V}$, $\hat{\mathbf{K}}_e = \mathbf{W}^T \cdot \mathbf{K}_e \cdot \mathbf{V} \in \mathbb{R}^{n \times n}$, $\hat{\mathbf{B}}_e = \mathbf{W}^T \cdot \mathbf{B}_e \in \mathbb{R}^{n \times p}$, and $\hat{\mathbf{C}}_e = \mathbf{C}_e \cdot \mathbf{V} \in \mathbb{R}^{r \times n}$. If the subspaces $\mathcal{V}$ and $\mathcal{W}$ are identical, the projection is called *orthogonal*, otherwise, it is called *oblique*. The difference of the projection types is visualized by Fig. 2.5.

The reduced equations of motion of a single elastic body in the multibody system are

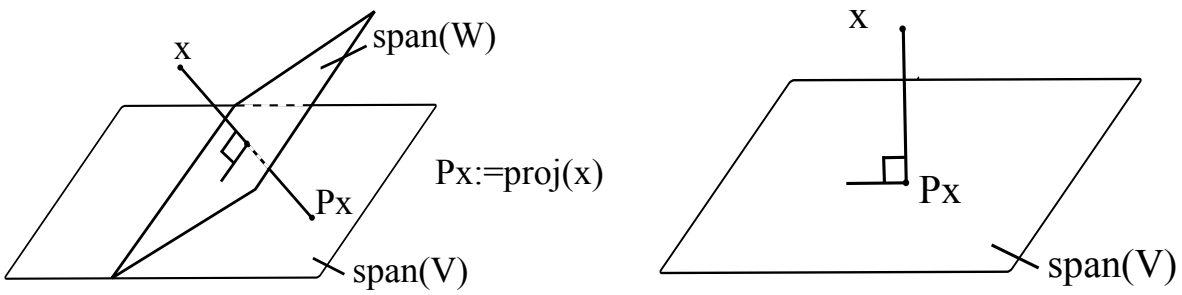

(a) Oblique projection **(b)** Orthogonal projection

Figure 2.5: Types of projection.

written as

$$\begin{bmatrix} \mathbf{M}_t & \mathbf{M}_{tr}(\hat{\mathbf{q}}) & \mathbf{M}_{te} \cdot \mathbf{V} \\ \mathbf{M}_{rt}(\hat{\mathbf{q}}) & \mathbf{M}_r(\hat{\mathbf{q}}) & \mathbf{M}_{re} \cdot \mathbf{V} \\ \mathbf{W}^T \cdot \mathbf{M}_{et} & \mathbf{W}^T \cdot \mathbf{M}_{er} & \hat{\mathbf{M}}_e \end{bmatrix} \begin{bmatrix} \ddot{\mathbf{x}} \\ \boldsymbol{\alpha} \\ \ddot{\hat{\mathbf{q}}} \end{bmatrix} + \begin{bmatrix} \mathbf{0} \\ \mathbf{0} \\ \hat{\mathbf{D}}_e \cdot \dot{\hat{\mathbf{q}}} + \hat{\mathbf{K}}_e \cdot \hat{\mathbf{q}} \end{bmatrix} = \begin{bmatrix} \mathbf{h}_t(\hat{\mathbf{z}}, \hat{\mathbf{z}}_\mathbf{I}) \\ \mathbf{h}_r(\hat{\mathbf{z}}, \hat{\mathbf{z}}_\mathbf{I}) \\ \mathbf{W}^T \cdot \mathbf{h}_e(\hat{\mathbf{z}}, \hat{\mathbf{z}}_\mathbf{I}) \end{bmatrix}, \tag{2.140}$$

where $\ddot{\mathbf{x}}, \boldsymbol{\alpha}$ are the translational and rotational accelerations of the body frame with respect to the global coordinate system. The vectors

$$\hat{\mathbf{z}} = \begin{bmatrix} \mathbf{x} \\ \boldsymbol{\theta} \\ \hat{\mathbf{q}} \end{bmatrix} \text{ and } \hat{\mathbf{z}}_\mathbf{I} = \begin{bmatrix} \mathbf{x} \\ \boldsymbol{\omega} \\ \hat{\mathbf{q}} \end{bmatrix} \tag{2.141}$$

denote reduced generalized position and velocity coordinates, respectively. Other terms of Eq. 2.140 are defined in Section 2.1.4.

The difference of model order reduction methods lies in the way of how they generate the transformation matrices $\mathbf{W}$ and $\mathbf{V}$.

2.2.2 Demands on reduction approaches when using for elastic multibody systems

The general requirements on model order reduction techniques such as high accuracy, computational efficiency, preservation of stability are already discussed in Section 1.3. The use of reduction methods in the context of EMBS imposes on them additional demands. The first requirement is that a reduced order model has to be described by differential equations of second order type. This enables integration of reduced models into multibody systems of second order form. This requirement can be satisfied by using reduction approaches based on projection.

Another issue concerning the usage of reduction methods in the context of EMBS is that it is necessary to ensure that the coordinate transformation matrix $\mathbf{V}$ fulfills boundary conditions imposed by a reference frame. The use of modes that violate the boundary conditions results in a poor representation of deformations [77]. In addition, the linear

combination of columns of $\mathbf{V}$ has to be a subspace that does not contain rigid-body modes. The exclusion of rigid body modes is required by the floating frame formulation. In this formulation the motion of elastic body is decoupled into the rigid body motion approximated by the motion of floating frame and deformations with respect to the moving frame. It follows that the reduction method has to able to produce a coordinate transformation matrix that excludes rigid body motion from the description of deformations.

In order to satisfy the Buckens frame conditions the coordinate transformation matrix $\mathbf{V}$ has to be modified according the formula

$$\mathbf{V_{mod}} = \left(\mathbf{I} - \bar{\mathbf{V}}_\mathbf{0}\bar{\mathbf{V}}_\mathbf{0}^\mathbf{T}\mathbf{M}_e\right)\mathbf{V}, \tag{2.142}$$

where $\bar{\mathbf{V}}_\mathbf{0}$ is a matrix of rigid-body modes normalized by the mass matrix $\mathbf{M}_e$, and $\mathbf{I}$ is an identity matrix of size $N \times N$, see [47, page 135]. This modification does not damage dynamical properties of reduced model. It only rewrites the modes in $\mathbf{V}$ with respect to the center of mass. In order to obtain rigid body modes, it is not necessary to solve an eigenvalue problem. The translational and rotational rigid modes can be found as follows:

$$\mathbf{V_0} = \begin{bmatrix} \mathbf{V}_{0t} & , \mathbf{V}_{0r} \end{bmatrix} = \left[\begin{bmatrix} \vdots \\ [\mathbf{I}]^k \\ \vdots \end{bmatrix}, \begin{bmatrix} \vdots \\ \left[-\tilde{\bar{\mathbf{r}}}_0\right]^k \\ \vdots \end{bmatrix} \right], k = 1, .., N. \tag{2.143}$$

Here the matrix $\mathbf{I}$ is 3×3 identity matrix, the term $[\bar{\mathbf{r}}_\mathbf{0}]^k$ denotes an undeformed position of the k-th node of FE model and $\left[\tilde{\bar{\mathbf{r}}}_\mathbf{0}\right]^k$ corresponds to an associated with $[\bar{\mathbf{r}}_\mathbf{0}]^k$ skew symmetric matrix. It is assumed that a finite element node exhibits only three translational degrees of freedom. The transformation matrix $\mathbf{V_{mod}}$ ensures that the Buckens frame constraints are automatically satisfied and there is no need to add them to equations of motion. It is always possible to transform modes so that the conditions of the Buckens-frame are fulfilled [81].

Linear dependency of columns of $\mathbf{V_{mod}}$ can be removed by the QR decomposition of $\mathbf{V_{mod}}$ and the exclusion of columns that correspond to zero values on the diagonal of matrix $\mathbf{R}$. The remaining modes together with the rigid body modes spans the same solution space as it is spanned by the original modes of $\mathbf{V}$.

2.3 Model reduction techniques

2.3.1 Guyan method

This old reduction approach was proposed by Guyan in [37]. The approach separates model DoFs into internal and boundary subsets. The b-set of boundary DoFs is defined

as a set of coordinates that remain in the system, while an i-set of internal coordinates includes all DoFs that must be eliminated from the system of equations:

$$i \cup b = a, i \cap b = \emptyset. \tag{2.144}$$

Here a defines a set of all DoFs of the system. Let us consider the following undamped system:

$$\mathbf{M}_e \cdot \ddot{\mathbf{q}}(t) + \mathbf{K}_e \cdot \mathbf{q}(t) = \mathbf{h}_e. \tag{2.145}$$

The partition of the system into internal and boundary coordinates yields

$$\begin{bmatrix} \mathbf{M}_{ii} & \mathbf{M}_{ib} \\ \mathbf{M}_{bi} & \mathbf{M}_{bb} \end{bmatrix}_e \begin{bmatrix} \ddot{\mathbf{q}}_i \\ \ddot{\mathbf{q}}_b \end{bmatrix} + \begin{bmatrix} \mathbf{K}_{ii} & \mathbf{K}_{ib} \\ \mathbf{K}_{bi} & \mathbf{K}_{bb} \end{bmatrix}_e \begin{bmatrix} \mathbf{q}_i \\ \mathbf{q}_b \end{bmatrix} = \begin{bmatrix} \mathbf{h}_i \\ \mathbf{h}_b \end{bmatrix}_e. \tag{2.146}$$

Due to the static nature of the method the influence of inertia term is not taken into account. Assuming that there is no force acting on the internal DoFs, i.e. $\mathbf{h}_i = \mathbf{0}$, and solving Eq. 2.146 for $\mathbf{q}_i$ the following relationship is obtained:

$$\mathbf{q} = \begin{bmatrix} \mathbf{q}_i \\ \mathbf{q}_b \end{bmatrix} = \begin{bmatrix} -\mathbf{K}_{ii} \cdot \mathbf{K}_{ib} \\ \mathbf{I}_b \end{bmatrix} \cdot \mathbf{q}_b, \tag{2.147}$$

where $\mathbf{I}_b \in \mathbb{R}^{N_b \times N_b}$ is an identity matrix. According to the Guyan method the low-dimensional subspace is defined by a transformation matrix $\mathbf{V} \in \mathbb{R}^{N \times N_b}$

$$\mathbf{V} = \begin{bmatrix} -\mathbf{K}_{ii} \cdot \mathbf{K}_{ib} \\ \mathbf{I}_b \end{bmatrix}. \tag{2.148}$$

The Guyan reduction leads to the exact representation of static deformations and to a relative good approximation of low frequencies and corresponded modes. For higher frequency modes inertia forces terms become significant that results in inaccurate reduced order models.

2.3.2 Dynamic condensation method

The dynamic condensation method utilizes the inertia information of FE model. The method was developed for reducing systems that undergo a harmonic excitation.

The dynamic behavior of FE model in time domain is described by the system of equations

$$\mathbf{M}_e \cdot \ddot{\mathbf{q}}(t) + \mathbf{K}_e \cdot \mathbf{q}(t) = \mathbf{h}_e(t). \tag{2.149}$$

In contrast to Guyan reduction method, the force vector $\mathbf{h}_e$ is time dependent. Assuming zero initial conditions, the Laplace transformation of Eq. 2.149 leads to the following

equations in the frequency domain:

$$(\mathbf{M}_e \cdot s^2 + \mathbf{K}_e) \cdot \mathbf{q}(s) = \mathbf{h}_e(s). \tag{2.150}$$

The vectors $\mathbf{q}(s)$ and $\mathbf{h}_e(s)$ denote the Laplace transformation of time dependent displacement and force vectors $\mathbf{q}(t)$ and $\mathbf{h}_e(t)$, respectively, i.e.

$$\mathbf{q}(s) = \mathcal{L}\{\mathbf{q}_e\}(s) = \int_0^\infty e^{-st} \cdot \mathbf{q}(t)\, dt \tag{2.151}$$

$$\mathbf{h}_e(s) = \mathcal{L}\{\mathbf{h}_e\}(s) = \int_0^\infty e^{-st} \cdot \mathbf{h}_e(t)\, dt. \tag{2.152}$$

The variable $s = i \cdot \boldsymbol{\omega}$ is a complex number with zero real part. The term $\boldsymbol{\omega}$ represents an angular frequency, which is connected with an excitation frequency f via the relationship $\boldsymbol{\omega}$=$2\pi f$.

Analogously to the Guyan method, the system of Eq. 2.150 is partitioned into the internal and boundary coordinates as

$$\underbrace{(-\mathbf{M}_e \cdot \boldsymbol{\omega}^2 + \mathbf{K}_e)}_{\mathbf{T}(\boldsymbol{\omega})} \cdot \mathbf{q}(\boldsymbol{\omega}) = \mathbf{h}_e(\boldsymbol{\omega}) \tag{2.153}$$

$$\left[\begin{array}{cc} \mathbf{T}_{ii}(\boldsymbol{\omega}) & \mathbf{T}_{ib}(\boldsymbol{\omega}) \\ \mathbf{T}_{bi}(\boldsymbol{\omega}) & \mathbf{T}_{bb}(\boldsymbol{\omega}) \end{array} \right]_e \left[\begin{array}{c} \mathbf{q}_i(\boldsymbol{\omega}) \\ \mathbf{q}_b(\boldsymbol{\omega}) \end{array} \right] = \left[\begin{array}{c} \mathbf{h}_i(\boldsymbol{\omega}) \\ \mathbf{h}_b(\boldsymbol{\omega}) \end{array} \right]_e \tag{2.154}$$

Using the same condition as for the Guyan method, namely, there are no forces applied to the internal DoFs, and solving the system of equations for $\mathbf{q}_b(\boldsymbol{\omega})$ the coordinate transformation matrix is obtained as

$$\mathbf{V} = \begin{bmatrix} -\mathbf{T}_{ii}(\boldsymbol{\omega}) \cdot \mathbf{T}_{ib}(\boldsymbol{\omega}) \\ \mathbf{I}_b \end{bmatrix}. \tag{2.155}$$

The accuracy of models reduced by the dynamic condensation method is limited to the spectrum defined around the frequency chosen for its initialization.

2.3.3 Craig-Bampton method

According to the Craig-Bampton method, all degrees of freedom are also divided into two sets: boundary and internal (also called master and slave). The choice of the boundary set is crucial for the quality of reduced order model. The choice is model dependent and requires advanced engineering experience. However, there are several common criteria that specify positions of boundary degrees of freedom [44]:

- points where large deformation is expected,
- such points that all relevant deformations can be described using only the set of

boundary nodes,

- equally distributed in the structure,
- positions where forces and boundary constraints are to be defined,
- points with the characteristic of having large concentrated mass and at the same time small local stiffness .

The boundary degrees of freedom are denoted with an index b and the internal degrees of freedom with an index i. In this case, the number of all degrees of freedom of FE model can be written as $N = N_b + N_i$.

The coordinate transformation matrix $\mathbf{V}$ of Craig-Bampton method consists of two parts: a retained set of fixed interface normal modes $\mathbf{V}_n$ and a set of constraint modes $\mathbf{V}_c$.

The following partitioned form of undamped Eq. 2.136 is needed in the derivation of deformation modes:

$$\begin{bmatrix} \mathbf{M}_{ii} & \mathbf{M}_{ib} \\ \mathbf{M}_{bi} & \mathbf{M}_{bb} \end{bmatrix}_e \begin{bmatrix} \ddot{\mathbf{q}}_i \\ \ddot{\mathbf{q}}_b \end{bmatrix} + \begin{bmatrix} \mathbf{K}_{ii} & \mathbf{K}_{ib} \\ \mathbf{K}_{bi} & \mathbf{K}_{bb} \end{bmatrix}_e \begin{bmatrix} \mathbf{q}_i \\ \mathbf{q}_b \end{bmatrix} = \begin{bmatrix} \mathbf{h}_i \\ \mathbf{h}_b \end{bmatrix}_e \tag{2.156}$$

The fixed-interface normal modes are obtained by fixing all boundary DoFs and solving the following eigenproblem:

$$(\mathbf{K}_{ii} - \mathbf{\Lambda}\mathbf{M}_{ii})\mathbf{V}_{ii} = \mathbf{0}.$$

Futher, a subset of low-frequency eigenvectors in $\mathbf{V}_{ii}$ is chosen. If N_m is a number of retained columns of $\mathbf{V}_{ii}$, then the complete set of fixed-interface normal modes $\mathbf{V}_n$ is assembled according to the partitioning in Eq. 2.156 as columns of the modal matrix

$$\mathbf{V}_n \equiv \begin{bmatrix} \mathbf{V}_{im} \\ \mathbf{0} \end{bmatrix}.$$

The dimensions of matrix $\mathbf{V}_{im}$ and the null-matrix $\mathbf{0}$ are $N_i \times N_m$ and $N_b \times N_m$, respectively. When normalized with respect to the mass matrix $\mathbf{M}_{ii}$, the modes from $\mathbf{V}_{im}$ satisfy the conditions as

$$\mathbf{V}_{im}^{\mathbf{T}}\mathbf{M}_{ii}\mathbf{V}_{im} = \mathbf{I}_{mm}, \mathbf{V}_{im}^{\mathbf{T}}\mathbf{K}_{ii}\mathbf{V}_{im} = \mathbf{\Lambda}_{mm},$$

where $\mathbf{\Lambda}_{mm}$ is a diagonal matrix of square angular frequencies.

The quantity of retained modes N_m is usually chosen experimentally: if the quality of reduced model is insufficient, it is necessary to increase the number of retained normal modes.

Constraint modes are defined as static deformations of the model when a unit displacement is applied at the boundary coordinates. The remaining coordinates of that set are

restrained, and the remaining degrees of freedom of the structure are force-free. The matrix of constrained modes $\mathbf{V}_c \in \mathbb{R}^{N \times N_b}$ is calculated as follows:

$$\mathbf{V}_c = \begin{bmatrix} -\mathbf{K}_{ii}^{-1}\mathbf{K}_{ib} \\ \mathbf{I}_{bb} \end{bmatrix}.$$

Thereby, the Craig–Bampton transformation matrix $\mathbf{V} \in \mathbb{R}^{N \times (N_b + N_m)}$ takes the following form:

$$\mathbf{V} = \begin{bmatrix} \mathbf{V}_c & \mathbf{V}_n \end{bmatrix}.$$

The vector of reduced coordinates $\hat{\mathbf{q}}$ from Eq. 2.138 can be written as $\hat{\mathbf{q}} = \begin{bmatrix} \mathbf{q}_b \\ \boldsymbol{\eta} \end{bmatrix}$. The vector of modal coordinates $\boldsymbol{\eta}$ represents the contributions of vibration modes towards the nodal displacements.

The normal modes improve the accuracy of reduced model in the low-frequency domain, while the constraint modes describe static deformations of the model due to the influence on the interface coordinates. Unlike the Guyan reduction procedure the Craig-Bampton method utilizes the both stiffness and mass characteristics of the model. Besides, as opposed to the modal truncation, it takes into account distribution of external forces to compute correction modes for exact modeling of static deformations. The method provides an accurate approximation for low and medium eigenfrequencies and corresponded eigenforms. The main drawback of the approach is that the accuracy of reduced model highly depends on the number and position of interface coordinates. This fact complicates generation of reduced order models that satisfy specified accuracy demands. In additon, the number of fixed-interface normal modes required for the acceptable accuracy is difficult to estimate a priori. Another issue with the computed fixed-interface normal modes is that they can be nearly orthogonal to the applied loads and, therefore, do not participate significantly in the solution. It follows that the correct choice of interface coordinates and fixed-interface modes requires much experience and insight into the specific problem.

2.4 Validation tests for reduced models

Although in certain cases the theory of the applied reduction approach indicates the quality of dynamic properties for the reduced model, the application of certain correlation criteria assure that the reduced model's dynamics sufficiently captures the properties of the full model [43]. In order to validate the reduced order model we employ the eigenfrequency related criterion - Normalized Relative Eigenfrequency Difference (NRED), eigenvector related criterion - Modal Assurance Criterion (MAC), and the frequency response analysis to evaluate a relative error of transfer functions.

2.4.1 Eigenfrequency related test

The NRED creation is defined as follows:

$$\mathbf{NRED_i} = \frac{\left|f^i_{red} - f^i_{full}\right|}{|f^i_{red}|},$$

where f^i_{red} and f^i_{full} are i-th eigenfrequencies of reduced and full models, respectively. The lower the value of this criterion is, the better the reduced model captures the dynamic properties of the original model at the predefined frequency range.

2.4.2 Eigenvector related test

The MAC approach deals with the information regarding the angle of compared eigenvectors, as well as their orthogonal coherence. In order to compare eigenvectors of original and reduced models, it is necessary to expand the reduced eigenforms $\mathbf{\Psi}_{red}$ back to the original dimension. It is can be done using the relationship:

$$\mathbf{\Psi}_{exp} = \mathbf{V} \cdot \mathbf{\Psi}_{red},$$

where $\mathbf{V}$ is the coordinate transformation matrix from Eq. 2.138 . Denoting $\mathbf{\Psi}_{full}$ to be a matrix of original model eigenvectors, the modal assurance criterion is defined as:

$$\mathbf{MAC_{i,j}} = \frac{(\mathbf{\Psi}^T_{full_i} \cdot \mathbf{\Psi}_{exp_j})^2}{(\mathbf{\Psi}^T_{full_i}.\mathbf{\Psi}_{full_i})(\mathbf{\Psi}^T_{exp_j}.\mathbf{\Psi}_{exp_j})}. \tag{2.157}$$

The value $\mathbf{MAC_{i,i}} = 1$ corresponds to the absolute correlation. The less this value becomes, the worse the eigenvector correlation is. If diagonal elements of MAC matrix have magnitudes larger or equal than 0.8, the correlation is considered satisfactory [43].

It is necessary to point out that if a model has repeated eigenfrequencies, then any linear combination of the corresponding eigenvectors is also an eigenvector. As the eigenforms are not uniquely defined, the correlation between the vectors using the MAC might be low. This implies that the MAC test becomes an unsuitable tool to assess the quality of reduced order model containing repeated eigenfrequencies.

2.4.3 Frequency response analysis

We perform the frequency response analysis to evaluate a reduction error in the frequency domain. For a single-input single-output system the quality of reduced order model can be checked using a Bode plot of transfer function. For multi-input multi-output systems it is problematically to control all transfer functions separately, therefore the error of reduction is usually evaluated using the Frobenius norm as

$$\epsilon(\omega) = \frac{\|\mathbf{H}(i\omega) - \hat{\mathbf{H}}((i\omega))\|_F}{\|\mathbf{H}(i\omega)\|_F}, \tag{2.158}$$

where $\mathbf{H}$ and $\hat{\mathbf{H}}$ are the transfer matrices of original and reduced systems. The error of transfer functions having small amplitudes has little influence on the value of Eq. 2.158, therefore the function $\epsilon(\omega)$ shows mainly an averaged relative error of transfer functions with large amplitudes.

2.5 Modeling elastic multibody systems

In the previous sections the derivation of equations of motion was limited to a single unconstrained elastic body. In this section the model of elastic body is integrated into a multibody system where the motion of bodies is affected by other system components. The modeling of constrains, derivation of equations of motion of elastic multibody system, and solution methods are discussed in the subsequent sections.

2.5.1 Modeling of constraints

The main types of constraints in EMBS are prescribed trajectories, joints, and contacts. They are introduced to the dynamic formulation of EMBS by algebraic equations

$$\mathbf{g}(\mathbf{z}, t) = \mathbf{0}, \tag{2.159}$$

$$\mathbf{g}(\mathbf{z}) = \mathbf{0}, \tag{2.160}$$

$$\mathbf{g}(\mathbf{z}, t) \geq \mathbf{0}. \tag{2.161}$$

Here $\mathbf{z}$ denotes the vector of system generalized coordinates, t defines time, and $\mathbf{g}$ is a vector of constraints. In this work we consider modeling of prescribed trajectories and joints. The user interested in modeling of contacts is referred to the review article [92].

The Lagrange multiplier method is currently the most widely used technique for incorporating constraints in the floating frame formulation. The method is used with the absolute coordinate formulation, as well as with the relative coordinate formulation to describe loop-closure constraints.

For the absolute coordinate formulation the number of Lagrange multipliers is equal to the number of constraints. The number of system unknown coordinates composed of the vector of system generalized coordinates and the vector of Lagrange multipliers becomes maximal. The dynamic formulation of EMBS leads to a system of DAEs. However, the Lagrange multipliers and associated dependent coordinates can be eliminated prior the solution, in order to obtain a minimal set of coordinates. The set of dependent coordinates can be identified using a constraint Jacobian matrix. This coordinate reduction results

in a system of ODEs. The solution of the independent differential equations defines the independent coordinates. The dependent variables are determined by using constraint equations. The advantage of the Lagrange multiplier method is that the equations of constraints are satisfied with high accuracy and the equations of motion of various EMBS can be constructed in a straightforward way. The drawback of the method is that it results in a system of DAEs with a maximal number of unknown coordinates. The elimination of dependent DoFs and associated Lagrange multipliers requires additional computational efforts and usually generates a stiffer system of equations of motion.

The formulation of constraint equations of joints in a three dimensional analysis requires introducing a joint coordinate system. The joint coordinate systems are attached to so called pilot nodes with six DoFs. The pilot nodes are defined at the center of interface surface of the joint. The nodes on the interface surface are connected with the pilot node by multipoint constraints. The joint contact surface can be modeled as rigid by rigid multipoint constraints, or as flexible by flexible multipoint constraints. The joint constraint equations are formulated using two joint coordinate systems in the same way as it is done in rigid multibody dynamics.

The efficiency of many reduction approaches is limited by the number of interface nodes in which the elastic body is or can be loaded. The forces in joints may be applied on the entire joint surface, which leads to an enormous number of interface DoFs. In this case, interface reduction is required. One of the solutions of the problem is to condense the nodes of a given interface surface into a single node, which represents the motion of the interface surface. The interface reduction is considered in [39, 64].

2.5.2 Equations of motion of elastic multibody systems

Using the Lagrange multiplier method and the augmented formulation of equations of motion, the dynamic behavior of elastic multibody system is defined by the following system of equations

$$\begin{cases} \mathbf{M}(\mathbf{z}) \cdot \dot{\mathbf{z}}_\mathbf{I} + \mathbf{D} \cdot \mathbf{z}_\mathbf{I} + \mathbf{K} \cdot \mathbf{z} + \mathbf{G}^T \cdot \boldsymbol{\lambda} = \mathbf{w}(t, \mathbf{z}, \mathbf{z}_\mathbf{I}) \\ \mathbf{g}(t, \mathbf{z}) = \mathbf{0}. \end{cases} \tag{2.162}$$

Here $\mathbf{M}, \mathbf{D}$, and $\mathbf{K}$ are system mass, damping, and stiffness matrices; $\mathbf{z}$ is a vector of generalized coordinates that is composed of generalized coordinates of each body in the system; the vector $\mathbf{w}$ defines the sum of quadratic velocity and external forces; $\mathbf{g}$ denotes a vector of constraint equations. The constraint forces are introduced to the system of equations by the Lagrange multipliers $\boldsymbol{\lambda}$, and the Jacobian matrix $\mathbf{G}_z$ of the vector of constraints:

$$\mathbf{G} = \frac{\partial \mathbf{g}}{\partial \mathbf{z}} \cdot \mathbf{T}(\mathbf{z}) = \mathbf{G}_z \cdot \mathbf{T}(\mathbf{z}) \tag{2.163}$$

where the matrix $\mathbf{T}$ is from the relation of generalized velocity coordinates and a derivative of generalized position coordinates:

$$\dot{\mathbf{z}} = \mathbf{T} \cdot \mathbf{z_I}. \tag{2.164}$$

Eq. 2.162 is a system of differential equations of motion that can be solved for the vector of system generalized coordinates $\mathbf{z}$ and the vector of Lagrange multipliers $\boldsymbol{\lambda}$. This equation is used as a basis for the development of solution algorithms of multibody dynamics.

2.5.3 Solution of equations of motion for elastic multibody systems

Many techniques are available in the literature for the numerical solution of a mixed set of differential and algebraic equations. Dynamic equations of multibody systems with flexible bodies are usually large-dimensional and stiff. This introduces restrictions on the choice of numerical solution methods. In this section, we outline the most often used approaches in the context of EMBS simulation.

Eq. 2.162 forms a set of index-3 differential algebraic equations. Solution of equations written in this form is possible only in rare cases. Solution approaches for DAEs consist of two groups: transformation of DAEs to ODEs by the elimination of redundant generalized coordinates and Lagrange multipliers [90, 45, 86]; and index reduction methods that reduce the system of equations to index-1 DAEs [33, 12].

There is a large number of integration algorithms for the numerical integration of ODE systems. One-step methods use values of the function and its derivative in a current interval to determine the next value, while multi-step methods attempt to increase the accuracy by using values of previous intervals as well. Explicit methods calculate the next value of the function from the value of the function and its derivative at the current step, while implicit methods find the next value by solving an equation involving both the current value and the next one. Due to the high stiffness of dynamic equations of EMBS, the use of implicit integrators is preferable as they are more stable. Another advantage of implicit solution procedures over the explicit methods is that the time step can be larger than the smallest natural period of the system. However, in this case, the modes with a natural period of the same order or smaller than the chosen time step are not accurately modeled. For this reason, some experience is needed in choosing a time step that provides a response within a required accuracy [89]. There exists a critical number of DoFs above which the explicit procedures are computationally more efficient than the implicit procedures, because the implicit methods require solution of a system of algebraic equations at each time step.

The second type of solution methods is index reduction techniques. The index defines the minimum number of differentiations needed to transform given DAEs into an explicit system of ODEs for all unknown variables. The index of Eq. 2.162 is determined by two

differentiations of constraint equations and one differentiation of Lagrange multipliers. The DAE system of index-2 takes the form

$$\begin{cases} \mathbf{M}(\mathbf{z}) \cdot \dot{\mathbf{z}}_\mathbf{I} + \mathbf{G}^T \cdot \boldsymbol{\lambda} = \mathbf{f} \\ \mathbf{G} \cdot \mathbf{z}_\mathbf{I} + \mathbf{G}_t = \mathbf{0}, \end{cases} \tag{2.165}$$

where $\mathbf{f}$ includes a vector of quadratic velocity force, stiffness and damping forces, and external forces; $\mathbf{G}_t$ defines a derivative of constraint vector $\mathbf{g}$ with respect to time.

The second derivative of constraint equations $\mathbf{g}$ is given by

$$\ddot{\mathbf{g}} = \frac{\partial \dot{\mathbf{g}}}{\partial \dot{\mathbf{z}}} \ddot{\mathbf{z}} + \frac{\partial \dot{\mathbf{g}}}{\partial \mathbf{z}} \dot{\mathbf{z}} + \frac{\partial \dot{\mathbf{g}}}{\partial t}. \tag{2.166}$$

Here the first summand takes the form

$$\frac{\partial \dot{\mathbf{g}}}{\partial \dot{\mathbf{z}}} \ddot{\mathbf{z}} = \frac{\partial \left(\mathbf{G}_z \cdot \dot{\mathbf{z}} + \mathbf{G}_t \right)}{\partial \dot{\mathbf{z}}} \ddot{\mathbf{z}} = \mathbf{G}_z \cdot \ddot{\mathbf{z}}. \tag{2.167}$$

The term $\ddot{\mathbf{z}}$ can be found as

$$\ddot{\mathbf{z}} = \mathbf{T} \cdot \dot{\mathbf{z}}_\mathbf{I} + \dot{\mathbf{T}} \cdot \mathbf{z}_\mathbf{I}. \tag{2.168}$$

The second summand is obtained as follows:

$$\frac{\partial \dot{\mathbf{g}}}{\partial \mathbf{z}} \dot{\mathbf{z}} = \frac{\partial \left(\mathbf{G}_z \cdot \dot{\mathbf{z}} + \mathbf{G}_t \right)}{\partial \mathbf{z}} \dot{\mathbf{z}} = \left(\mathbf{G}_z \cdot \dot{\mathbf{z}} \right)_z \cdot \dot{\mathbf{z}} + \mathbf{G}_{tz} \cdot \dot{\mathbf{z}} \tag{2.169}$$

Finally, the last term of Eq. 2.166 yields

$$\frac{\partial \dot{\mathbf{g}}}{\partial t} = \frac{\partial \left(\mathbf{G}_z \cdot \dot{\mathbf{z}} + \mathbf{G}_t \right)}{\partial t} = \mathbf{G}_{zt} \cdot \dot{\mathbf{z}} + \mathbf{G}_{tt}. \tag{2.170}$$

Using Eq. 2.164 and Eq. 2.168, the second derivative of constraint vector $\mathbf{g}$ is defined as

$$\ddot{\mathbf{g}} = \mathbf{G}_z \cdot \left(\mathbf{T} \cdot \dot{\mathbf{z}}_\mathbf{I} + \dot{\mathbf{T}} \cdot \mathbf{z}_\mathbf{I} \right) + \left(\mathbf{G}_z \cdot \dot{\mathbf{z}} \right)_z \cdot \mathbf{T} \cdot \mathbf{z}_\mathbf{I}. + \mathbf{G}_{tz} \cdot \mathbf{T} \cdot \mathbf{z}_\mathbf{I} + \mathbf{G}_{zt} \cdot \mathbf{T} \cdot \mathbf{z}_\mathbf{I} + \mathbf{G}_{tt}. \tag{2.171}$$

The system of index-1 DAEs can be written as

$$\begin{bmatrix} \mathbf{M} & \mathbf{G}^T \\ \mathbf{G} & \mathbf{0} \end{bmatrix} \cdot \begin{bmatrix} \dot{\mathbf{z}}_\mathbf{I} \\ \boldsymbol{\lambda} \end{bmatrix} = \begin{bmatrix} \mathbf{f} \\ \boldsymbol{\gamma} \end{bmatrix} \tag{2.172}$$

with $\boldsymbol{\gamma} = -\mathbf{G}_z \cdot \dot{\mathbf{T}} \cdot \mathbf{z}_\mathbf{I} - \left(\mathbf{G}_z \cdot \dot{\mathbf{z}} \right)_z \cdot \mathbf{T} \cdot \mathbf{z}_\mathbf{I} - 2 \cdot \mathbf{G}_{zt} \cdot \mathbf{T} \cdot \mathbf{z}_\mathbf{I} - \mathbf{G}_{tt}$.

If the matrix of left hand side of Eq. 2.172 is invertible in a neighborhood of solution, then the system has a unique solution for the variables $\dot{\mathbf{z}}_\mathbf{I}$ and $\boldsymbol{\lambda}$. This holds if the Jacobian matrix $\mathbf{G}$ has a full rank, i.e. the constraint equations are linear independent, and the mass matrix $\mathbf{M}$ is symmetric and positive definite.

The solution of Eq. 2.172 can be found by the Gaussian elimination and it yields

$$\begin{cases} \dot{\mathbf{z}}_\mathbf{I} = \mathbf{M}^{-1} \cdot \left(\mathbf{f} - \mathbf{G}^T \cdot \boldsymbol{\lambda} \right) \\ \boldsymbol{\lambda} = \left(\mathbf{G} \cdot \mathbf{M}^{-1} \cdot \mathbf{G}^T \right)^{-1} \left(\mathbf{G} \cdot \mathbf{M}^{-1} \cdot \mathbf{f} - \boldsymbol{\gamma} \right). \end{cases} \tag{2.173}$$

Substituting the latter equation into the former leads to an ODE for the variable $\mathbf{z}_\mathbf{I}$.

The system of equations to be solved is given as

$$\begin{cases} \dot{\mathbf{z}} = \mathbf{T} \cdot \mathbf{z}_\mathbf{I} \\ \dot{\mathbf{z}}_\mathbf{I} = \mathbf{M}^{-1} \cdot \left(\mathbf{f} - \mathbf{G}_z^T \cdot \boldsymbol{\lambda} \right) \\ \boldsymbol{\lambda} = \left(\mathbf{G}_z \cdot \mathbf{M}^{-1} \cdot \mathbf{G}_z^T \right)^{-1} \left(\mathbf{G}_z \cdot \mathbf{M}^{-1} \cdot \mathbf{f} - \boldsymbol{\gamma} \right). \end{cases} \tag{2.174}$$

Assuming Lipschitz continuity of right hand side of differential equations, the unique solution for $\mathbf{z}$ and $\mathbf{z}_\mathbf{I}$ is guarantied. It follows that the Lagrange multipliers are also uniquely determined.

It is necessary to point out that the solution of Eq. 2.174 may dissatisfy the position and velocity constraints. This phenomenon is called a drift effect. Many of the methods proposed for the solution of index-1 DAEs allow small constraint violations. In order to alleviate the drift effect stabilization techniques must be used.

In contrast to solution approaches that use minimal set of coordinates, the index reduction techniques keep sparse structure of equations of motion. The sparsity of system equations is computationally advantageous because it is usually more efficient to solve a large system of sparse equations rather than a smaller system of dense equations.

The widely used methods for the solution of Eq. 2.172 are the Newmark, Runge-Kutta, Gear's, and generalized alpha methods. Gear's algorithm is particularly suited to DAEs because it can be tuned to be stable for stiff equations [89].

3 Line-fitting method of model reduction

The primary goal of model order reduction methods based on projection is to construct a coordinate transformation matrix $\mathbf{V}$, see Section 2.2.1. For this purpose, the line fitting method exploits transfer functions, which provide complete description of dynamic behavior of a system. The transfer functions can be found by applying the Laplace transformation to equations of motion of deformable body. In this thesis the equations of motion are formulated based on the floating frame of reference approach described in Section 2.1.1. According to this approach the motion of body is separated into the large rigid body motion approximated by the motion of body coordinate system and small deformations with respect to the body frame. According to Section 2.2.1, the following equations describe deformation effects of the body and have to be reduced:

$$\begin{cases} \mathbf{M}_e \cdot \ddot{\mathbf{q}}(t) + \mathbf{D}_e \cdot \dot{\mathbf{q}}(t) + \mathbf{K}_e \cdot \mathbf{q}(t) = \mathbf{B}_e \cdot \mathbf{u}(t) \\ \mathbf{y}(t) = \mathbf{C}_e \cdot \mathbf{q}(t). \end{cases} \tag{3.1}$$

The matrices $\mathbf{M}_e$, $\mathbf{D}_e$, $\mathbf{K}_e \in \mathbb{R}^{N \times N}$ denote constant mass, damping, and stiffness matrices, where N is a total number of DoFs of FE model. The terms $\mathbf{u}(t) \in \mathbb{R}^p$ and $\mathbf{y}(t) \in \mathbb{R}^r$ define input and output vectors, respectively, with p and r being numbers of input and output coordinates. The matrices $\mathbf{B}_e \in \mathbb{R}^{N \times p}$ and $\mathbf{C}_e \in \mathbb{R}^{r \times N}$ are input and output matrices that distribute loads on respective degrees of freedom of the model and select coordinates of interests from the vector $\mathbf{q}$, respectively.

The Laplace transformation of a function $f(t)$, $t \geqslant 0$ is defined as

$$\mathcal{L}\{f(t)\}(s) = \int_0^\infty e^{-st} \cdot f(t)\, dt. \tag{3.2}$$

The transformation of first and second time derivatives of $f(t)$ yields

$$\mathcal{L}\{\dot{f}(t)\}(s) = s \cdot \mathcal{L}\{f(t)\} - f(0) \tag{3.3}$$

$$\mathcal{L}\{\ddot{f}(t)\}(s) = s^2 \cdot \mathcal{L}\{f(t)\} - s \cdot f(0) - \dot{f}(0). \tag{3.4}$$

Assuming zero initial conditions, the Laplace transformation of the system of Eq. 3.1 gives

$$\mathbf{y}(s) = \mathbf{H}(s) \cdot \mathbf{u}(s). \tag{3.5}$$

The variable s is a complex number, and it takes a physically meaningful value by $s = i \cdot 2\pi f$ with f being an excitation frequency. The terms $\mathbf{y}(s) := \mathcal{L}\{\mathbf{y}(t)\}(s)$ and $\mathbf{u}(s) := \mathcal{L}\{\mathbf{u}(t)\}(s)$ define the Laplace transforms of output and input vectors. The matrix $\mathbf{H}(s)$ is a matrix of transfer functions and it is defined as

$$\mathbf{H}(s) = \mathbf{C}_e \cdot (s^2 \cdot \mathbf{M}_e + s \cdot \mathbf{D}_e + \mathbf{K}_e)^{-1} \cdot \mathbf{B}_e. \tag{3.6}$$

According to the demands to model order reduction techniques used for EMBS simulation, see Section 2.2.2, the coordinate transformation matrix $\mathbf{V}$ has to capture only deformation effects. In order to obtain the matrix $\mathbf{V}$ without rigid body modes, it is necessary to exclude the component of rigid body motion from elastic coordinates.

3.1 Elimination of rigid body motion from elastic coordinates

Slight damping insignificantly influences model eigenvectors and eigenfrequencies. For this reason, the modal analysis of slightly damped systems can be performed using modal characteristics of undamped systems. The modal representation of displacement vector for undamped system takes the form

$$\mathbf{q} = \boldsymbol{\Psi} \cdot \boldsymbol{\eta}, \tag{3.7}$$

where the matrix $\boldsymbol{\Psi} \in \mathbb{R}^{N \times N}$consists of modes of the system and $\boldsymbol{\eta}$ defines modal coordinates. Substituting Eq. 3.7 into Eq. 3.1 and premultiplying by $\boldsymbol{\Psi}^T$ yield the system of equations of motion and the transfer function matrix in terms of modal coordinates as

$$\begin{cases} \boldsymbol{\Psi}^T \cdot \mathbf{M}_e \cdot \boldsymbol{\Psi} \cdot \ddot{\boldsymbol{\eta}} + \boldsymbol{\Psi}^T \cdot \mathbf{D}_e \cdot \boldsymbol{\Psi} \cdot \dot{\boldsymbol{\eta}} + \boldsymbol{\Psi}^T \cdot \mathbf{K}_e \cdot \boldsymbol{\Psi} \cdot \boldsymbol{\eta} = \boldsymbol{\Psi}^T \cdot \mathbf{B}_e \cdot \mathbf{u}(t) \\ \mathbf{y}(t) = \mathbf{C}_e \cdot \boldsymbol{\Psi} \cdot \boldsymbol{\eta} \end{cases} \tag{3.8}$$

and

$$\mathbf{H}(s) = \mathbf{C}_e \cdot \boldsymbol{\Psi} \cdot (s^2 \cdot \boldsymbol{\Psi}^T \cdot \mathbf{M}_e \cdot \boldsymbol{\Psi} + s \cdot \boldsymbol{\Psi}^T \cdot \mathbf{D}_e \cdot \boldsymbol{\Psi} + \boldsymbol{\Psi}^T \cdot \mathbf{K}_e \cdot \boldsymbol{\Psi})^{-1} \cdot \boldsymbol{\Psi}^T \cdot \mathbf{B}_e. \tag{3.9}$$

Partition of modal matrix into rigid and deformation modes yields

$$\mathbf{\Psi} = \begin{bmatrix} \mathbf{\Psi}_0, & \mathbf{\Psi}_1 \end{bmatrix}. \tag{3.10}$$

Due to the orthogonality property of eigenvectors, see e.g. [21], the non-diagonal terms of modal mass and stiffness matrices vanish:

$$\mathbf{\Psi}_i^T \cdot \mathbf{M}_e \cdot \mathbf{\Psi}_j = \mathbf{0} \,\text{and}\, \mathbf{\Psi}_i^T \cdot \mathbf{K}_e \cdot \mathbf{\Psi}_j = \mathbf{0} \,\text{for}\, i, j = 0, 1,\ i \neq j. \tag{3.11}$$

When using the proportional representation of damping matrix $\mathbf{D}_e = \alpha \cdot \mathbf{M}_e + \beta \cdot \mathbf{K}_e$, the same conditions are satisfied for non-diagonal blocks of modal damping matrix, i.e.:

$$\mathbf{\Psi}_i^T \cdot \mathbf{D}_e \cdot \mathbf{\Psi}_j = \mathbf{0} \,\text{for}\, i, j = 0, 1,\ i \neq j. \tag{3.12}$$

Thus, the transfer function matrix

$$\mathbf{H}(s) = \mathbf{C}_e \cdot \begin{bmatrix} \mathbf{\Psi}_0, & \mathbf{\Psi}_1 \end{bmatrix} \cdot \begin{bmatrix} \mathbf{\Psi}_0^T \cdot \mathbf{P} \cdot \mathbf{\Psi}_0 & \mathbf{0} \\ \mathbf{0} & \mathbf{\Psi}_1^T \cdot \mathbf{P} \cdot \mathbf{\Psi}_1 \end{bmatrix}^{-1} \begin{bmatrix} \mathbf{\Psi}_0^T \\ \mathbf{\Psi}_1^T \end{bmatrix} \cdot \mathbf{B}_e$$

with $\mathbf{P} = s^2 \cdot \mathbf{M}_e + s \cdot \mathbf{D}_e + \mathbf{K}_e$ can be decomposed into two parts

$$\mathbf{H} \;=\; \mathbf{H}_0 + \mathbf{H}_1, \tag{3.13}$$

where

$$\mathbf{H}_j = \mathbf{C}_e \cdot \mathbf{\Psi}_j \cdot (\mathbf{\Psi}_j^T \cdot \mathbf{P} \cdot \mathbf{\Psi}_j)^{-1} \cdot \mathbf{\Psi}_j^T \cdot \mathbf{B}_e,\ j = 0, 1 \tag{3.14}$$

The component of transfer function matrix for pure deformations $\mathbf{H}_1$ can be calculated without computing deformation modes as

$$\mathbf{H}_1 = \mathbf{H} - \mathbf{H}_0 \tag{3.15}$$

where the component of rigid body motion $\mathbf{H}_0$ can be computed by the matrix of rigid body modes defined in Eq. 2.143. It follows that the solution of eigenvalue problem is not necessary for the construction of matrix $\mathbf{H}_1$. Graphically the process of eliminating of the component of rigid body motion from a transfer function can be illustrated by a magnitude plot shown in Fig. 3.1.

According to [47] the elimination of component of rigid body motion from transfer functions can be also performed by the following transformation of input matrix

$$\mathbf{B}_{mod} = \left(\mathbf{I} - \mathbf{M}_e \bar{\mathbf{V}}_\mathbf{0} \bar{\mathbf{V}}_\mathbf{0}^T\right) \mathbf{B}_e, \tag{3.16}$$

where $\bar{\mathbf{V}}_\mathbf{0}$ is a matrix of rigid-body modes normalized through the mass matrix $\mathbf{M}_e$, and

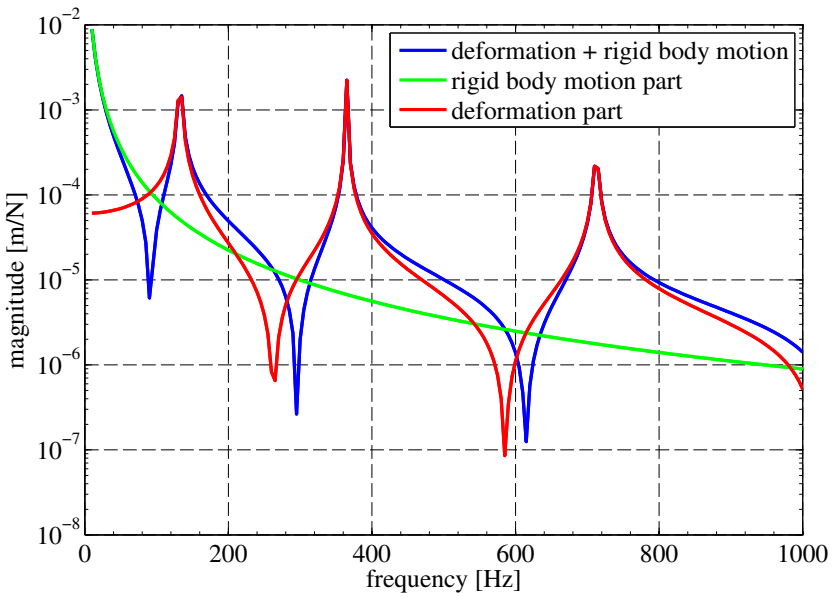

Figure 3.1: Elimination of component of rigid body motion from a transfer function.

$\mathbf{I}$ is an identity matrix of size $N \times N$. The reader interested in the physical interpretation of this transformation is referred to [21, 35].

The goal of the line fitting method is to approximate transfer functions that describe pure deformations. The eliminated rigid body motion will be taken into account in the equations of motion by the motion of floating frame.

3.2 Approximation of transfer functions

3.2.1 Method description

Multiplication of the both parts of Eq. 3.13 with the input load vector $\mathbf{u}$ yields

$$\mathbf{H} \cdot \mathbf{u} = \mathbf{H}_0 \cdot \mathbf{u} + \mathbf{H}_1 \cdot \mathbf{u} \tag{3.17}$$

that can be written in a more compact form

$$\mathbf{y} = \mathbf{y}_0 + \mathbf{y}_1, \tag{3.18}$$

where $\mathbf{y}_0$ and $\mathbf{y}_1$ correspond to a rigid body motion component and a deformation component of output coordinates $\mathbf{y}$, respectively. Let non-output coordinates be denoted as $\mathbf{y}^\perp$. Similarly to the decomposition of output coordinates $\mathbf{y}$ the vector $\mathbf{y}^\perp$ can be represented as

$$\mathbf{y}^\perp = \mathbf{y}_0^\perp + \mathbf{y}_1^\perp. \tag{3.19}$$

Using this notation the vector of nodal displacement coordinates is given as

$$\mathbf{q} = \begin{bmatrix} \mathbf{y} \\ \mathbf{y}^{\perp} \end{bmatrix} = \begin{bmatrix} \mathbf{y}_0 \\ \mathbf{y}_0^{\perp} \end{bmatrix} + \begin{bmatrix} \mathbf{y}_1 \\ \mathbf{y}_1^{\perp} \end{bmatrix} = \mathbf{q}_0 + \mathbf{q}_1. \tag{3.20}$$

As it is discussed in Section 2.2.1, the nodal elastic coordinates are approximated using reduced coordinates $\hat{\mathbf{q}}$ and the coordinate transformation matrix $\mathbf{V}$ as

$$\mathbf{q} = \mathbf{V} \cdot \hat{\mathbf{q}}. \tag{3.21}$$

Since we require the matrix $\mathbf{V}$ without rigid-body modes, we calculate it using the relation

$$\mathbf{q}_1 = \mathbf{V} \cdot \hat{\mathbf{q}}. \tag{3.22}$$

The matrix $\mathbf{V}$ obtained from this equation will be used for the reduction of $\mathbf{q}$.

Similarly to the condensation reduction approaches, the degrees of freedom of reduced order model are chosen to be output coordinates:

$$\hat{\mathbf{q}} = \mathbf{y}_1. \tag{3.23}$$

This choice of $\hat{\mathbf{q}}$ requires a proper initialization of the method, which is discussed in Section 3.2.2.

Substituting $\mathbf{q}_1$ from Eq. 3.20 and Eq. 3.23 into Eq. 3.22 yields

$$\begin{bmatrix} \mathbf{y}_1 \\ \mathbf{y}_1^{\perp} \end{bmatrix} = \mathbf{V} \cdot \mathbf{y}_1. \tag{3.24}$$

The transformation matrix $\mathbf{V}$ can be partitioned in the same way as the left hand side of Eq. 3.24, that is

$$\mathbf{V} = \begin{bmatrix} \mathbf{I} \\ \mathbf{W} \end{bmatrix} \tag{3.25}$$

with $\mathbf{I} \in \mathbb{R}^{r \times r}$ and $\mathbf{W} \in \mathbb{R}^{(N-r) \times r}$ being an identity matrix and an approximation matrix for non-output coordinates, respectively. It follows that the non-output coordinates are approximated using the input coordinates as

$$\mathbf{y}_1^{\perp} = \mathbf{W} \cdot \mathbf{y}_1. \tag{3.26}$$

The vectors $\mathbf{y}_1^{\perp}$ and $\mathbf{y}_1$ are connected with the transfer function matrices as

$$\mathbf{y}_1(s) = \mathbf{H}_1(s) \cdot \mathbf{u}(s) \tag{3.27}$$

$$\mathbf{y}_1^{\perp}(s) = \mathbf{H}_1^{\perp}(s) \cdot \mathbf{u}(s). \tag{3.28}$$

Analogous to $\mathbf{H}_1$ and $\mathbf{H}_1^{\perp}$ for the full order model, let $\hat{\mathbf{H}}_1$ and $\hat{\mathbf{H}}_1^{\perp}$ denote transfer function

matrices of reduced order model.

The idea is to fit the transfer functions $\hat{\mathbf{H}}_1$ by fitting adjacent to them transfer functions contained in $\mathbf{H}_1^{\perp}$. The error of adjacent transfer functions is reduced by minimizing an error of transfer functions from $\mathbf{H}_1^{\perp}$:

$$\Delta\mathbf{H}_1^{\perp}(s) = \mathbf{H}_1^{\perp}(s) - \mathbf{W} \cdot \mathbf{H}_1(s). \tag{3.29}$$

This results in the relation

$$\mathbf{H}_1^{\perp}(s) = \mathbf{W} \cdot \mathbf{H}_1(s). \tag{3.30}$$

Next, the matrix $\mathbf{W}$ is constructed as a compromise between different points $s_k = i \cdot 2\pi f_k$, $k = 1..z$ of the frequency range of interest, where z defines a number of frequency points. Eq. 3.30 is turned into

$$\left[\ \mathbf{H}_1^{\perp}(s_1),\ \ \cdots,\ \ \mathbf{H}_1^{\perp}(s_z)\ \right] = \mathbf{W} \cdot \left[\ \mathbf{H}_1(s_1),\ \ \cdots,\ \ \mathbf{H}_1(s_z)\ \right]. \tag{3.31}$$

In order to avoid working with complex numbers, Eq. 3.31 is decomposed into real and imaginary parts as

$$\begin{aligned} &\left[\ \Re(\mathbf{H}_1^{\perp}(s_1),\ \ \cdots,\ \ \mathbf{H}_1^{\perp}(s_z)\ ),\ \Im(\mathbf{H}_1^{\perp}(s_1),\ \ \cdots,\ \ \mathbf{H}_1^{\perp}(s_z))\ \right] = \\ &\mathbf{W} \cdot \left[\ \Re(\mathbf{H}_1(s_1),\ \ \cdots,\ \ \mathbf{H}_1(s_z)\ ),\ \Im(\mathbf{H}_1(s_1),\ \ \cdots,\ \ \mathbf{H}_1(s_z))\ \right] \end{aligned} \tag{3.32}$$

that can be written in more simple form as

$$\mathbf{T}_n = \mathbf{W} \cdot \mathbf{T}_o.$$

Transposing the last equation we get

$$\mathbf{T}_o^T \cdot \mathbf{W}^T = \mathbf{T}_n^T. \tag{3.33}$$

The matrices $\mathbf{T}_o^T \in \mathbb{R}^{2pz \times r}$ and $\mathbf{T}_n^T \in \mathbb{R}^{2pz \times (N-r)}$, where p, r, and z are the numbers of input coordinates, output coordinates, and reference frequency points, respectively; N is the total number of finite element model. The matrix $\mathbf{W}$ can be found as a least-squares solution of Eq. 3.33. After that, the coordinate transformation matrix $\mathbf{V}$ is obtained using Eq. 3.25. The number of reduced coordinates n is equal to the number of outputs r.

The obtained matrix $\mathbf{V}$ can be used for the reduction of coordinates in the time domain

because $\mathbf{V}$ is constant and the inverse Laplace transformation is a linear operator, i.e.

$$\mathbf{q}_1(t) = \mathcal{L}^{-1}\{\mathbf{q}_1(s)\}(t) = \mathcal{L}^{-1}\{\mathbf{V}\cdot\hat{\mathbf{q}}(s)\}(t) = \tag{3.34}$$

$$\mathbf{V}\cdot\mathcal{L}^{-1}\{\hat{\mathbf{q}}(s)\}(t) = \mathbf{V}\cdot\hat{\mathbf{q}}(t). \tag{3.35}$$

Further we discuss under which conditions the described method leads to an accurate approximation of transfer functions of interest $\mathbf{H}_1$.

3.2.2 Method initialization

The accuracy of reduced order model is limited among other factors by a number of reduced coordinates. There is a certain number of reduced coordinates by which an accurate approximation of limited frequency range can be gained. In case of the line-fitting method, the order of reduced model is defined by a number of output DoFs. In order to improve accuracy of transfer functions of interest, the set of input-output coordinates for the construction of matrix $\mathbf{V}$ can differ from the set of coordinates defined by a user. The optimal number of reduced coordinates for a certain model is difficult to estimate a priori. We found that a number of DoFs equal to a double number of eigenfrequencies contained in the frequency range of interest is usually enough to achieve high accuracy of important transfer functions. These DoFs have to be distributed thought the model including the user defined inputs and outputs. Let this set of DoFs be referred to as *interface coordinates*. The interface coordinates serve as input and output coordinates for the method initialization. The important for the user transfer functions are contained in the set of transfer functions originated by the interface coordinates, therefore tuning of interface transfer functions leads to the reduction of error of user defined transfer functions.

The error $\Delta\mathbf{H}_1^{\perp}$ from Eq. 3.29 can be decreased not only by solving Eq. 3.30 for the matrix $\mathbf{W}$, but also by including in $\mathbf{H}_1$ additional transfer functions that enable more accurate approximation of $\mathbf{H}_1^{\perp}$. The correction transfer functions can be inserted in $\mathbf{H}_1$ by proper distribution of interface coordinates.

Another issue of the initialization process is related to the choice of reference frequency points. These points can be defined by analyzing the transfer functions $\mathbf{H}_1$. The set of frequency points is common for all transfer functions in $\mathbf{H}_1$, therefore it is sufficient to assign frequency points only for several of them. The question concerning the proper choice of reference frequencies is considered in the next section.

3.3 Reference frequency points

Resonance and antiresonance frequencies determine important dynamic characteristics of deformable bodies. For this reason, the reference frequency points that are used for the initialization of line-fitting method have to include the resonance and antiresonance points. Besides, the set of reference frequency points can contain additional frequencies to enhance the quality of reduced models in special ranges of spectrum.

The resonance and antiresonance frequencies can be identified by frequency response functions or by finite element mass and stiffness matrices.

3.3.1 Identification of resonance frequencies

Resonances correspond to poles of transfer function. They are associated with peaks in the magnitude of transfer function and with the simultaneous change of phase on $-180°$. The weak damping has a negligible influence on the resonance frequencies, therefore the resonances can be determined using an undamped system. The transfer function matrix of undamped system is obtained as

$$\mathbf{H} = \left(\mathbf{K}_e - \omega^2 \cdot \mathbf{M}_e\right)^{-1} = \frac{\mathrm{adj}(\mathbf{K}_e - \omega^2 \cdot \mathbf{M}_e)}{\det(\mathbf{K}_e - \omega^2 \cdot \mathbf{M}_e)}. \tag{3.36}$$

The element c_{lk} of adjugate matrix $\mathbf{C} = \mathrm{adj}(\mathbf{A})$ takes the form

$$c_{lk} = (-1)^{k+l} \det(\mathbf{A}_{[kl]}), \tag{3.37}$$

where $\mathbf{A}_{[kl]}$ is obtained from the matrix $\mathbf{A}$ by the elimination of k-th row and l-th column.

The poles of transfer functions in the system are defined by the solution of the following equation

$$\det(\mathbf{K}_e - \omega^2 \cdot \mathbf{M}_e) = 0. \tag{3.38}$$

The resonance frequencies f_k are connected with the values $\boldsymbol{\omega}_k^2$ by the relation

$$f_k = \frac{\sqrt{\boldsymbol{\omega}_k^2}}{2 \cdot \pi}, k = 1..N. \tag{3.39}$$

3.3.2 Identification of antiresonance frequencies

Antiresonances correspond to zeros of transfer functions. These frequencies are determined by dips in the magnitude of transfer function and simultaneous change of phase on $+180°$. The slight damping affects antiresonance frequencies to a small extent [24]. The antiresonance frequencies are characteristics of transfer functions. The transfer function with a given input k and output l is defined as an element $\mathbf{H}_{lk}$ of transfer function matrix.

The zeros of $\mathbf{H}_{lk}$ are those ω for which the numerator of $\mathbf{H}_{lk}$ vanishes. Using Eq. 3.37 the zeros of transfer function $\mathbf{H}_{lk}$ are specified by the solution of the eigenvalue problem

$$\det(\mathbf{K}_{[kl]} - \omega^2 \cdot \mathbf{M}_{[kl]}) = 0. \tag{3.40}$$

The antiresonance frequencies are obtained from the values ω_j^2 as

$$f_j = \frac{\sqrt{\boldsymbol{\omega}_j^2}}{2 \cdot \pi}, j = 1..N-1. \tag{3.41}$$

3.4 Preservation of stability

The preservation of stability is an important property of reduction approaches because it ensures that the reduced model does not cause any type of failure (e.g., instability, excessive vibrations, large stresses) to the EMBS.

In this thesis, the stability concept is considered for a system of linear second order equations of motion of Eq. 2.139. The stability means that for any limited initial values $\hat{\mathbf{q}}_0, \dot{\hat{\mathbf{q}}}_0$ there is a limited solution of the system of equations $\hat{\mathbf{q}}(t)$, $t > 0$, see [6]. The stability is determined by eigenvalues of the generalized eigenvalue problem. The asymptotic stability presents if all eigenvalues possess only negative real parts. In [59] a special criterion is proposed to ascertain whether this property is preserved. The system is asymptotic stable if and only if the system matrices have the following properties:

$$\hat{\mathbf{M}}_e = \hat{\mathbf{M}}_e^T > 0,\ \hat{\mathbf{D}}_e = \hat{\mathbf{D}}_e^T > 0,\ \hat{\mathbf{K}}_e = \hat{\mathbf{K}}_e^T > 0. \tag{3.42}$$

The coordinate transformation matrix of line fitting method possesses no rigid body modes because the matrix is constructed for the system with suppressed rigid body motion. In addition, the columns of the coordinate transformation matrix are linear independent because of identity matrix in $\mathbf{V}$, see Eq. 3.25.

It follows that the reduced system matrices $\hat{\mathbf{M}}_e, \hat{\mathbf{K}}_e$ are positive definite. In case of using a proportional damping matrix, the reduced damping matrix has the same property $\hat{\mathbf{D}}_e > 0$. Besides, considering the symmetric property of original finite element matrices the reduced system matrices are also symmetric:

$$\hat{\mathbf{M}}_e^T = \left(\mathbf{V}^T \cdot \mathbf{M}_e \cdot \mathbf{V}\right)^T = \mathbf{V}^T \cdot \mathbf{M}_e^T \cdot (\mathbf{V}^T)^T = \mathbf{V}^T \cdot \mathbf{M}_e \cdot \mathbf{V} = \hat{\mathbf{M}}_e. \tag{3.43}$$

It follows that the line fitting method preserves model stability.

4 Application examples

This chapter is devoted to the comparison of the line fitting reduction approach proposed in Chapter 3 and the classical Craig-Bampton method described in Section 2.3.3. The comparison is carried out based on two models: an elastic bar and a bearing cage. The model of bar was developed for academic purposes to test different order reduction approaches. It has a simple form and a relative small number of degrees of freedom, which significantly simplifies its analysis and interpretation of results. The second model is a part of needle roller bearing (Fig. 4.1) used in rear swinging forks. Due to the complex geometry and large number of DoFs the model is referred to as a complex model.

Figure 4.1: Bearing design.
Source: [85]

The comparison of reduction techniques is performed using the validation methods presented in Section 2.4: eigenfrequency and eigenvector related tests, frequency response analysis, as well as validation in the time domain using different simulation setups. The dynamic properties of finite element non-reduced models developed in Ansys serve as reference characteristics for the assessment of reduction approaches. Ensuring of compliance of FE models with real items is a task of FE-engineers, therefore this point is not considered in the thesis. Section 4.1 covers the comparison of reduction methods based on the model of elastic bar, while Section 4.2 is devoted to the analysis of more challenging model - the elastic cage.

4.1 Simple model

4.1.1 Model description

The finite element model of elastic rod is illustrated in Fig. 4.2.

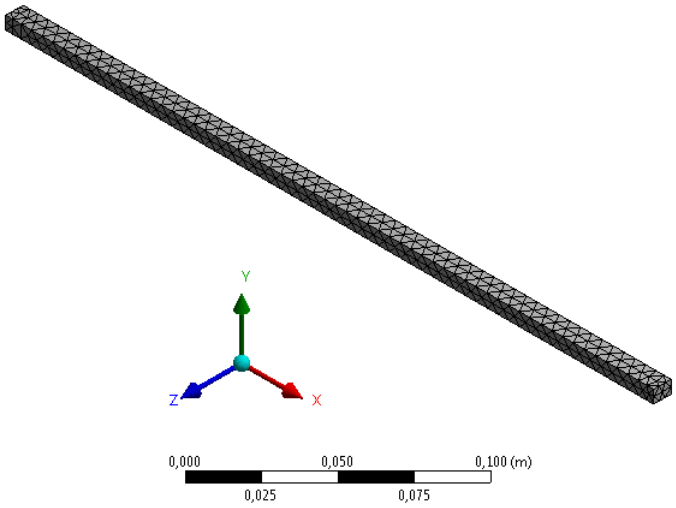

Figure 4.2: Flexible bar.

The bar has the following characteristics:

- Size: $6 \times 8 \times 300$ mm,
- Mass: 0,1 kg,
- Young's modulus: 2e+10 Pa,
- Damping factor beta: 10e-5,
- Number of degrees of freedom: 1656.

The modal analysis of free bar yields the eigenfrequencies shown in Table 4.1.

Table 4.1: Nonzero eigenfrequencies of free bar.

Mode	7	8	9	10	11	12	13	...
Frequency, Hz	133,06	171,78	364,45	469,75	714,94	917,99	1173,7	...

The bar is subjected to the influence of three external forces applied at the middle point, left and right ends of the model. The operating conditions of the bar are illustrated in Fig. 4.3.

We define the interval [0, 1000] Hz as a frequency range of interest. It is necessary to point out that this interval contains six deformation eigenfrequencies.

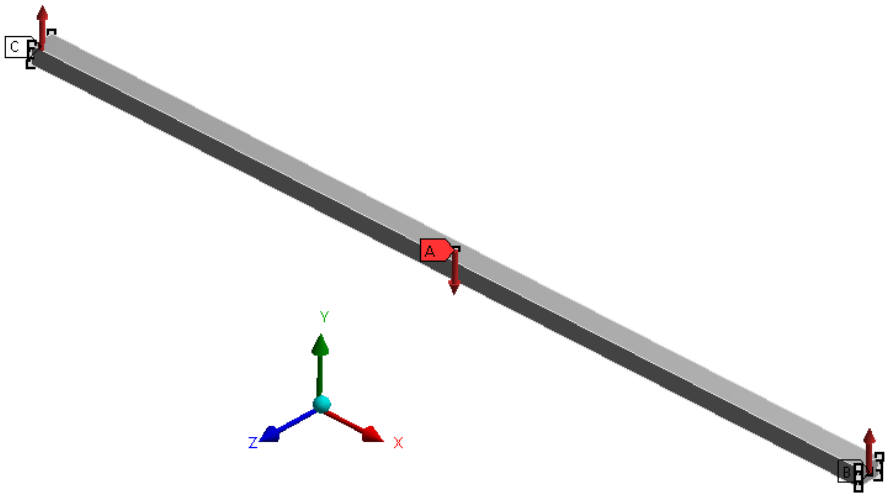

Figure 4.3: Operating conditions of the bar.

The set of input coordinates includes 9 DoFs of 3 nodes where external forces are applied, see Fig. 4.4. The set of output coordinates coincides with the set of input parameters.

Figure 4.4: Input and output coordinates of the bar.

4.1.2 Initialization of reduction methods

Craig-Bampton method

The initialization of Craig-Bampton method is carried out in a standard way. The set of interface (boundary) nodes consists of the nodes where external forces are applied. The interface nodes for the Craig-Bampton method are shown in Fig. 4.5. The initial estimation of sufficient number of dynamic modes is usually made using a rule of thumb for this method: double number of eigenfrequencies contained in a frequency range of interest. In order to enhance accuracy of model reduced by the Craig-Bampton method, we increase the number of retained normal modes to 19, which is more than three times larger than the number of eigenfrequencies in the frequency rage of interest. It follows that the number of constrained and dynamic modes is equal to 9 and 19, respectively. In order to use the obtained modes in the context of elastic multibody simulation, they must be adapted to demands discussed in Section 2.2.2. Since none of the used modes are mass orthogonal to a subspace spanned by the rigid body modes, the generated modes have to be projected onto a subspace of deformation modes. This can be performed using Eq. 2.142 and subsequent elimination of depended modes. As it is discussed in Section 2.2.2 these operations do not damage dynamic properties of a reduced model. The column dimension

of coordinate transformation matrix $\mathbf{V}$ after the execution of described procedure becomes $9 + 19 - 6 = 22$. It follows that the dimension of reduced order model is 22.

Figure 4.5: Interface nodes of the bar for the Craig-Bampton method.

Line-fitting method

The frequency range of interest and input and output coordinates are considered as a given information for the initialization of line-fitting method. The task of engineer is to choose an appropriate order of reduced model, to define interface degrees of freedom, and to allocate reference frequency points. The order of reduced model depends on a number of transfer functions that need to be tuned and a number of eigenfrequencies contained in a frequency range of interest. As it is discussed in Section 3.2.2, the order equal to a double number of eigenfrequencies in the frequency range of interest is usually enough to achieve high accuracy of reduced model. In the case of the bar model, we define the order of reduced model to be 14. After that the same number of interface DoFs must be determined. Nine interface degrees of freedom are assigned to nine user defined input and output coordinates, while the remaining five coordinates are distributed thought the model. The interface coordinates are located as it is shown in Fig. 4.6. The choice of an optimal order of reduced model and efficient allocation of interface coordinates are the topics of further research.

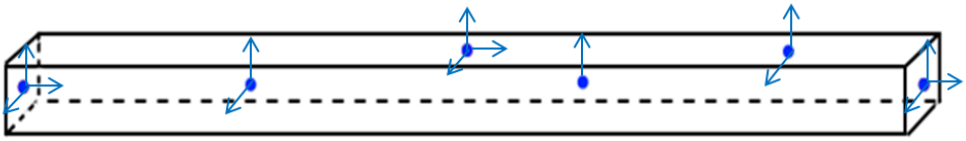

Figure 4.6: Interface degrees of freedom for the line-fitting reduction method.

In order to chose reference frequency points, we compute transfer functions specified by the interface DoFs. As it is considered in Section 3.2.2, the set of reference frequency points is common for all interface transfer functions, therefore it is possible to obtain a complete set of frequency points analyzing only several transfer functions. The reference points are defined at resonance, antiresonance and some intermediate frequencies of the interval [0,1000] Hz, see Fig. 4.7. For this model 20 frequency points of interest are assigned.

After the coordinate transformation matrices for the Craig-Bampton and line-fitting methods are generated, we perform the tests aimed at the evaluation of quality of reduced order models.

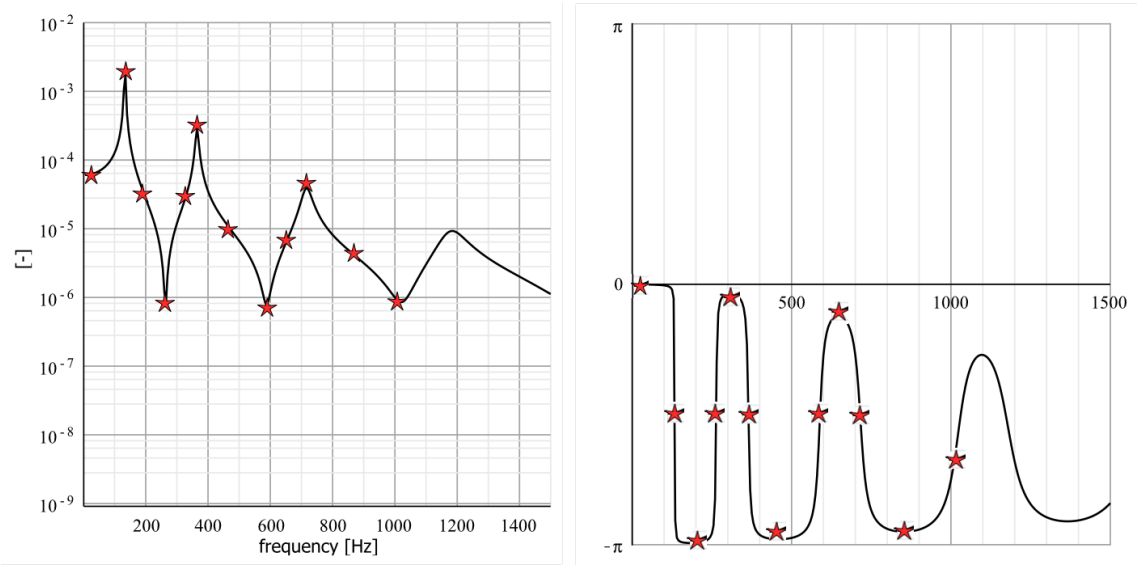

Figure 4.7: Choice of reference frequency points for the line-fitting reduction method.

4.1.3 Validation of reduced order models

For the comparison of the reduced order models we employ three criteria from Section 2.4: relative eigenfrequencies difference, modal assurance criterion, and relative error of transfer functions.

Normalized Relative Eigenfrequency Difference

Fig. 4.8 represents the result of NRED test for the eigenfrequencies in the predefined range of interest [0, 1000] Hz, as well as for all eigenfrequencies of the reduced models.

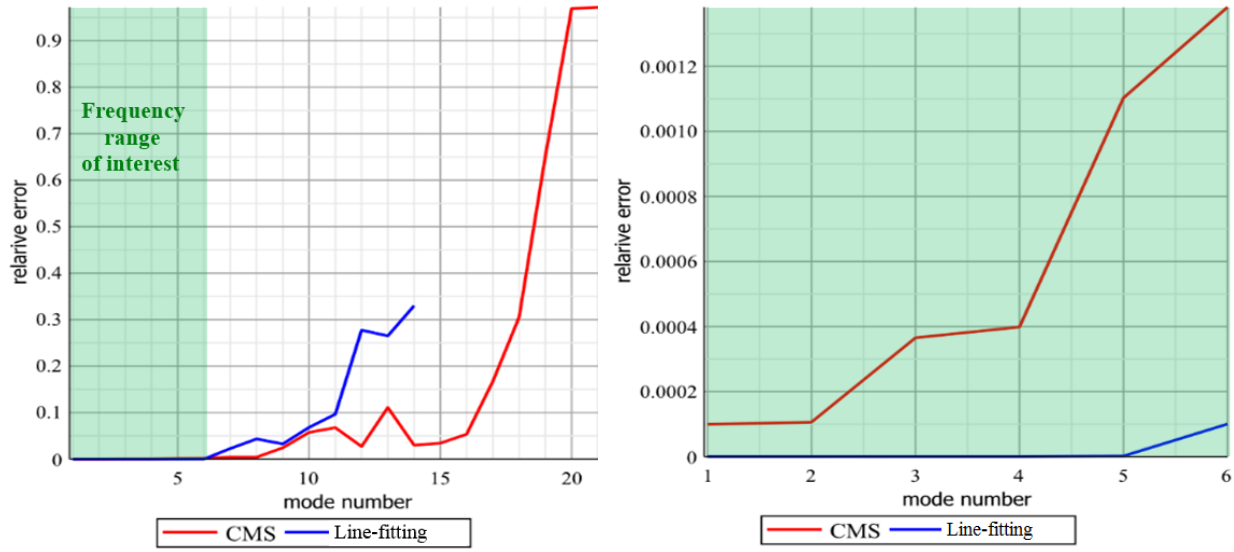

Figure 4.8: Relative error of non-zero eigenfrequencies for reduced models.

The diagrams show that the eigenfrequencies in the predefined frequency range are accurately approximated by the both methods, but the precision is considerably better for the

line-fitting model. The error of eigenfrequencies outside the interval of interest is more significant. In the case of line-fitting method, it is explained by the fact that the reference frequency points are allocated only in the frequency rage of interest. Besides, the diagrams show that the number of incorrect values for the line-fitting model is small, which keeps the order of reduced model close to minimum and eliminates the problems with an erroneous high-frequency spectrum: ill-conditioned matrices and the need of using a small integration step.

Modal Assurance Criterion

Fig. 4.9 illustrates the results of MAC test. The diagrams show that MAC values for all modes in the predefined frequency range are higher than 0.8. This implies a high correlation of deformation forms of the reduced and full models and, as a result, a qualitative successful approximation.

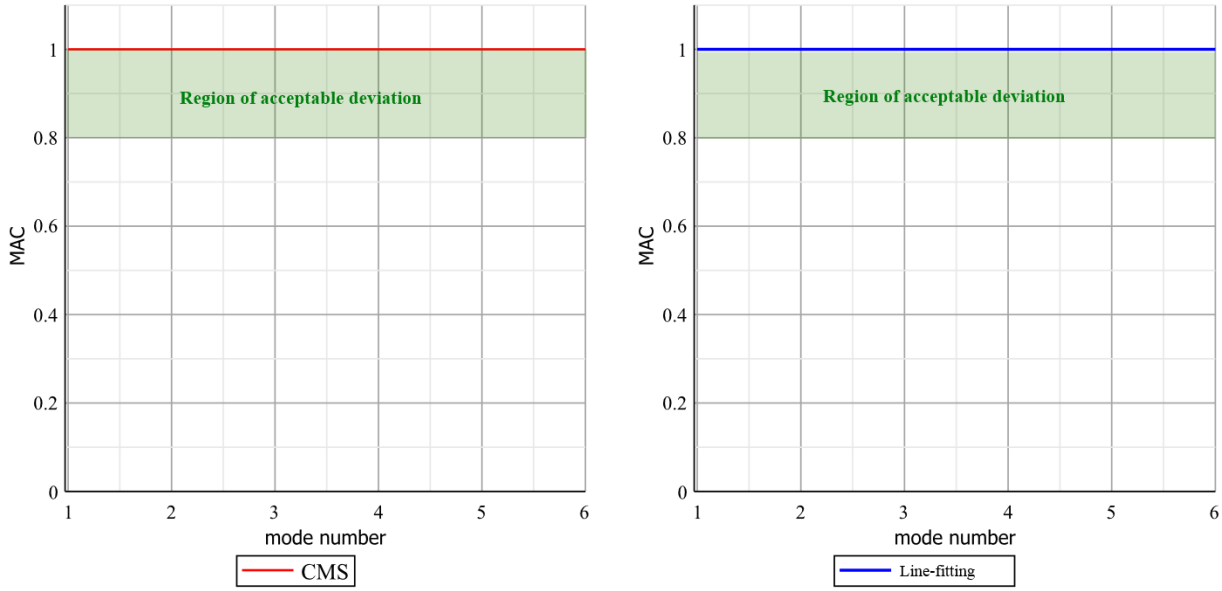

Figure 4.9: Validation of deformation modes using MAC test.

The quality of reduction can be evaluated more precisely if modes that are active under operating conditions are known.

Frequency response analysis

The preservation of important dynamic properties in a reduced order model can be examined using transfer functions of original and reduced models. For multi-input multi-output systems the error of transfer functions is usually evaluated using Eq. 2.158. The function $\epsilon(\omega)$ can be treated as a total error introduced by a model reduction approach to certain transfer functions in a certain frequency range.

The transfer functions of interest for the model of bar are specified by the coordinates shown in Fig. 4.10.

Figure 4.10: Input and output coordinates of transfer functions of interest.

The relative error $\epsilon(\omega)$ for the Craig-Bampton and line-fitting reduced order models is compared in Fig. 4.11.

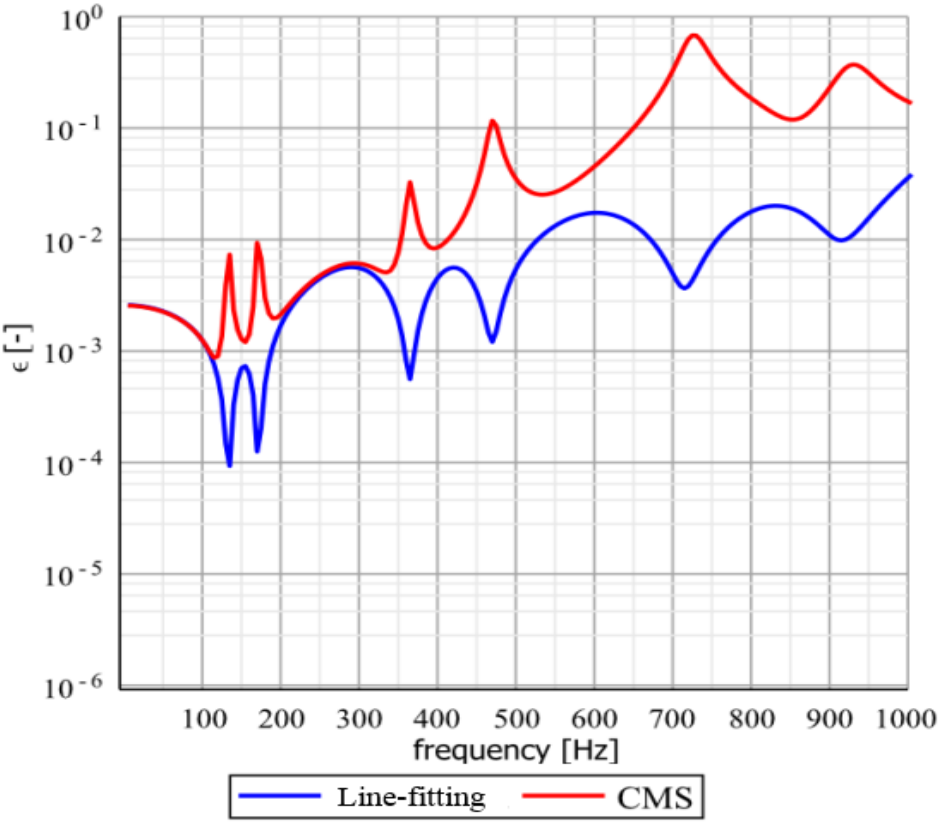

Figure 4.11: Relative error of frequency response for different reduced models of the bar.

The plot of Fig. 4.11 shows that the line-fitting method approximated the relevant transfer functions more accurately than the Craig-Bampton approach, especially at the resonance points. The error of line-fitting model does not exceed 3%. The Craig-Bampton method provides acceptable results only until 400 Hz. After that the error increases up to 70%.

4.1.4 Simulation

The use of reduced order models in the context of elastic multibody systems implies that reduction techniques provide a meaningful approximation not only for the elastic part of

equations of motion of Eq. 2.136, but also for the complete set of equations from Eq. 2.140. In order to verify the complete set of equations of motion, as well as to gain information about a proper time step of integration and the total time of simulation of reduced order models, we perform the following simulation test.

The body is subjected to three constant forces as it is shown in Fig. 4.12.

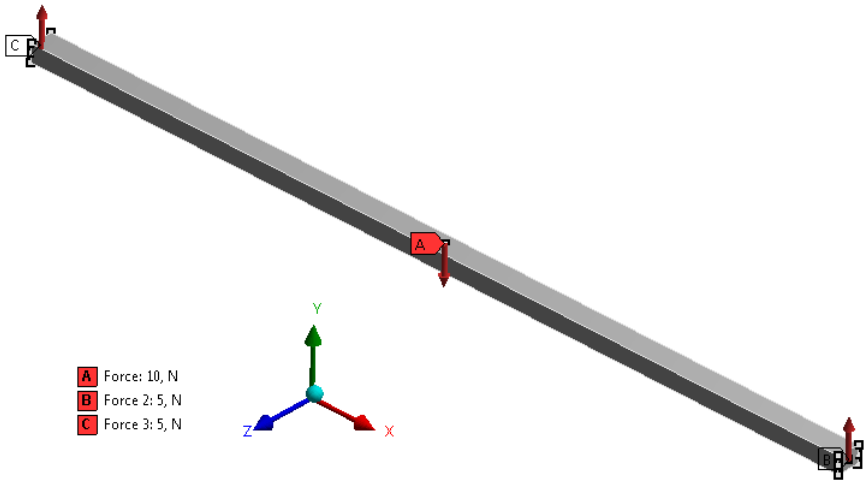

Figure 4.12: External forces applied to the bar.

The value of end-forces is

$$F_y^C = F_y^B = 5\,\mathrm{N},$$

while the middle-force acts in the opposite direction with a magnitude

$$F_y^A = -2F_y^C = -10\,\mathrm{N}.$$

The resultant force is equal to $F_y^A + F_y^B + F_y^C = 0$. The interest is focused on the displacement of the middle point along the vertical axis Y. The interval of simulation equals $3 \cdot 10^{-2}$ s and covers several periods of bar oscillation. As the body floating frame is chosen the Buckens coordinate system described in Section 2.1.6. In order to solve the system of equations, we exploit the implicit Backward-Euler method. The simulation is performed in Maple.

Fig. 4.13 compares the response of original FE model with the response of models reduced by the Craig-Bampton and line-fitting methods. The simulation of reduced order models yields nearly the same results. The accuracy of simulation is high for the both methods, but the erroneous high-frequency spectrum of Craig-Bampton model significantly decreases a suitable step of integration and, consequently, slows down the simulation. The simulation time of Craig-Bampton model is 3,5 hours, while the simulation of line-fitting model takes 15 minutes, which is 14 times faster.

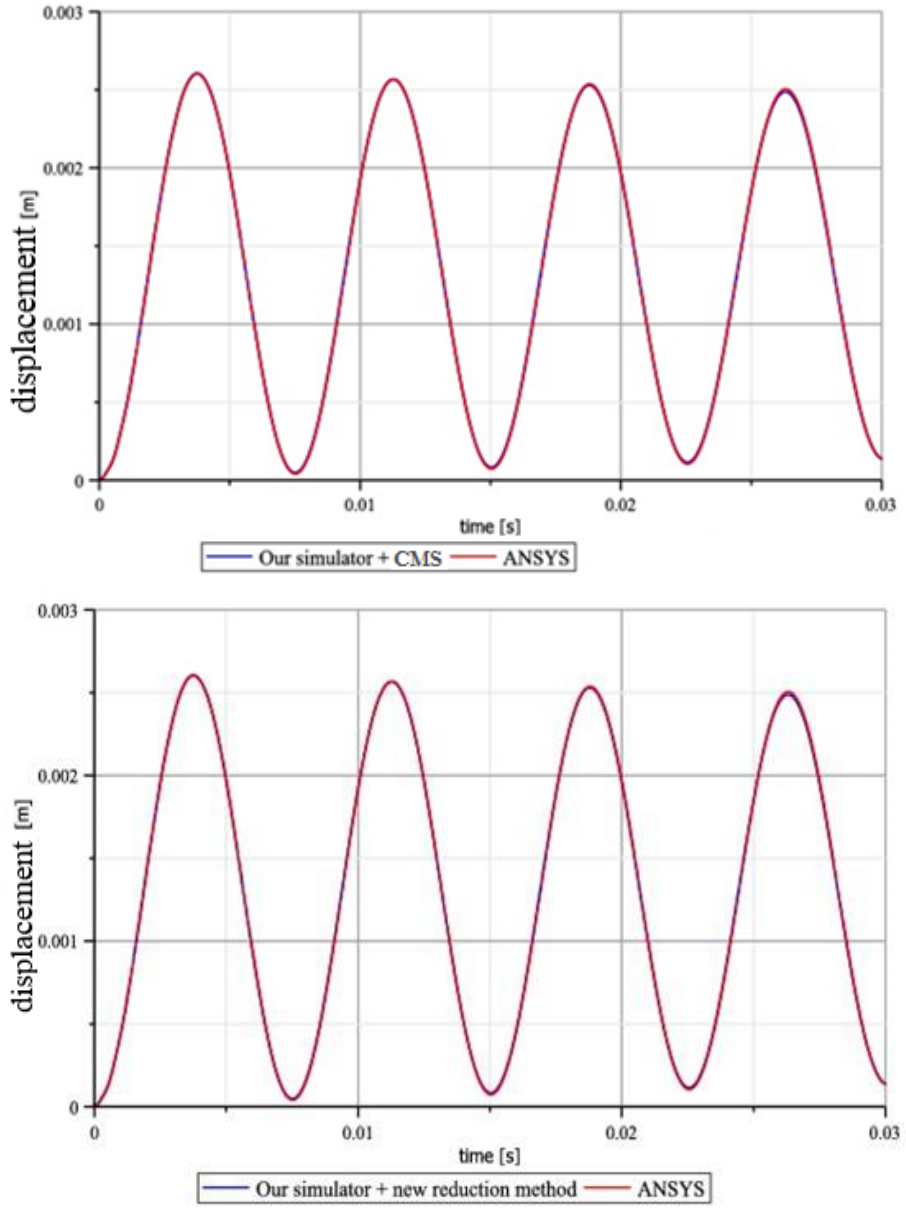

Figure 4.13: Simulation results of reduced models.

4.1.5 Comparison of reduced order models

Table 4.2 summarizes the results of analysis of the line-fitting method and compares them with the corresponding results of the classical Craig-Bampton method based on CMS approach.

The data show that the method proposed in this thesis constructed the reduced order model with the lower order, higher accuracy and better condition properties of system matrices. The cost of coordinate transformation matrix generation is higher as compared to the Craig-Bampton approach, but it remains acceptable for moderately dimensional FE models. In addition, the coordinate transformation matrix has to be calculated only once before the beginning of simulation process.

Table 4.2: Comparison of reduced order models of the bar.

Parameters	Craig-Bampton	Line-fitting
Order	22	14
Highest eigenfrequency, (Hz)	$2 \cdot 10^5$	$4.5 \cdot 10^3$
Suitable step of integration, (s)	$2.5 \cdot 10^{-7}$	10^{-5}
Time of simulation, (h)	3.5	0.25
Relative error of eigenfrequencies in [0,1000] Hz	$< 1.4 \cdot 10^{-3}$	$< 10^{-4}$
Correlation of eigenvectors in [0,1000] Hz	high	very high
Relative error of transfer functions in [0,1000] Hz	$0.1 - 70\%$	$0,01 - 3\%$
Time of projection matrix generation, (min)	5	10

4.2 Complex model

In this section we reduce a model of bearing cage by the Craig-Bampton method and the line-fitting method, perform validation tests, and compare the results.

4.2.1 Model description

The model under consideration is shown in Fig. 4.14 and has the following characteristics:

- size: 1.8 × 1.8 × 2.4 cm,
- mass: 3.3 g,
- Young's modulus: $2.1 \cdot 10^5$ MPa,
- number of degrees of freedom: 54000.

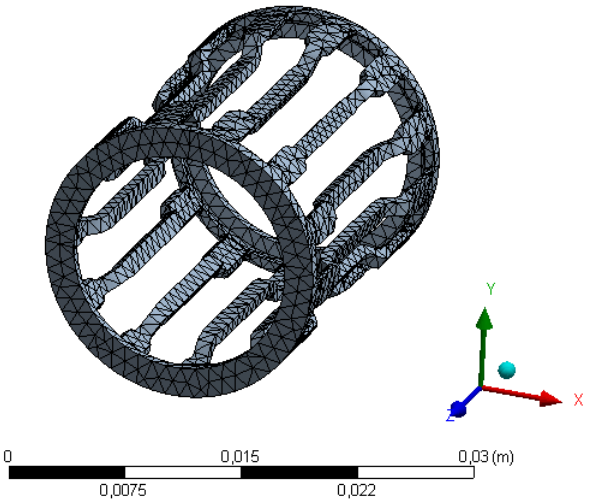

Figure 4.14: Flexible cage.

The modal analysis of free system yields the eigenfrequencies illustrated in Table 4.3.

Table 4.3: Nonzero eigenfrequencies of free cage.

Mode	7	8	9	10	11	12	13	14	15	16
Frequency, Hz	3985	4430	4966	4969	5087	5088	5738	5738	5858	5861
...	17	18	19	20	21	22	23	24	25	26	27
...	7077	7079	8511	8516	9076	9079	9819	9819	10860	10863	11635
...	28	29	30	31	32	33	34	35	36	...
...	11639	12208	12214	12501	12510	12646	12651	12694	12695	...

Damping initialization

The damping matrix of real system is rarely known in advance. The damping results from looseness of joints and material damping, therefore the damping matrix is usually defined by experimental results. For this model the damping matrix is assumed to be proportional to the FE mass and stiffness matrices, see Section 2.1.8. In order to specify values of damping coefficients, we examine a transfer function defined by an input-output coordinate shown in Fig. 4.15.

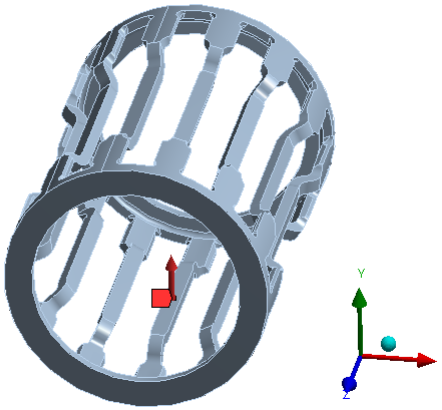

Figure 4.15: Input-output coordinate of transfer function used for initialization of beta coefficient of damping.

Fig. 4.16 illustrates Bode plots built in Ansys with beta damping 10^{-7} and 10^{-6} respectively. Based on the recommendations of Schaeffler company we have chosen the value 10^{-6} for further model analysis.

Definition of frequency range of interest

The reduced order model can be generated with the emphasis of different frequency ranges. The choice of frequency interval depends on the system operating conditions. The analysis of transfer functions provides better insight into a certain problem, therefore the frequency response analysis can be employed for the estimation of frequency range of interest.

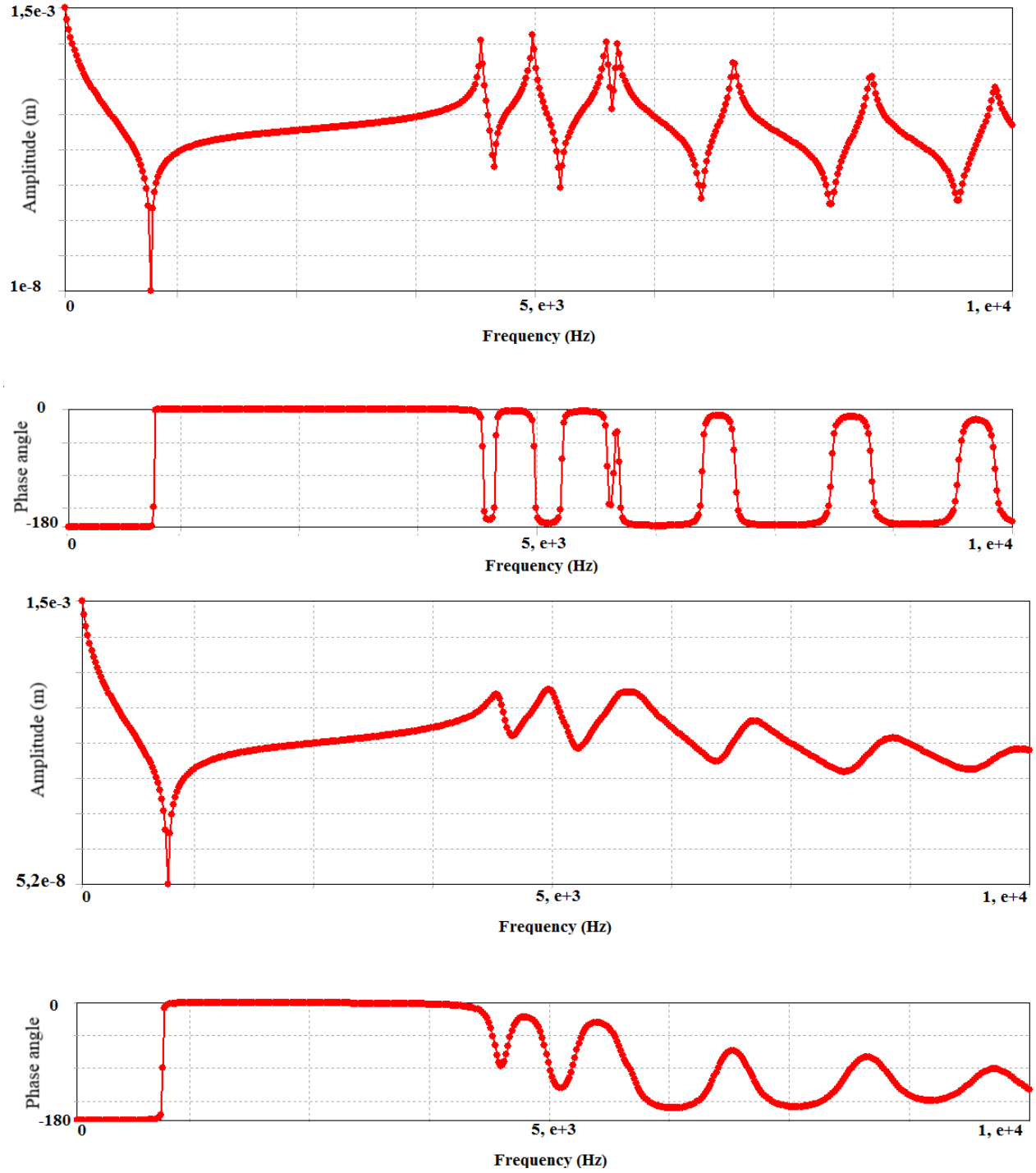

Figure 4.16: Bode plots for beta coefficients of damping 10^{-7} and 10^{-6}.

According to the recommendations of Schaeffler's engineers, we limited the frequency range of interest by 13000 Hz. There is a gap between the model eigenfrequencies and the amplitudes of resonance peaks are small. In order to have information about the reduced model behavior near the boundary of the defined interval, we generate transfer functions until 15000 Hz.

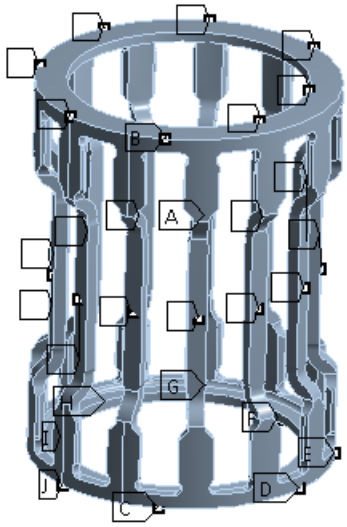

Figure 4.17: Set of input coordinates of the cage.

Initialization of input and output coordinates

The choice of input and output degrees of freedom is task-dependent. In the case of cage model, the exact positions of contact forces acting on the body are unknown. However, the set of possible input coordinates can be defined as it is shown in Fig. 4.17.

In this model we are interested in the response of the same nodes, therefore the set of output coordinates coincides with the set of input parameters. The goal of model order reduction is to accurately approximate the dynamic behavior of the defined nodes in the frequency range of interest.

4.2.2 Initialization of reduction methods

Craig-Bampton method

In order to construct a coordinate transformation matrix of Craig-Bamton method, one has to define a set of interface nodes and a number of fixed interface dynamic modes.

The choice of interface coordinates is crucial for the quality of the reduced order model. The choice is model-dependent and requires advanced engineering experience. The common criteria that specify positions of interface degrees of freedom are discussed in Section 2.3.3.

Positions of interface coordinates for the cage model are shown in Fig. 4.18. The number of interface nodes is 29, which results in 87 interface degrees of freedom.

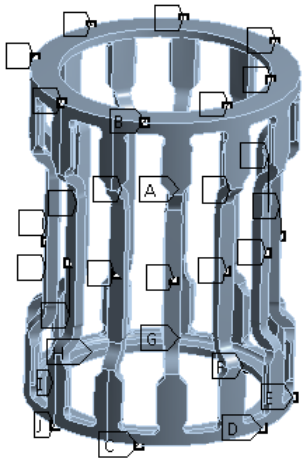

Figure 4.18: Interface nodes for the Craig-Bampton method.

The quantity of dynamic modes is usually chosen experimentally. We tuned the model for the given frequency range and determined that 59 dynamic modes result in a very accurate reduced order model. The size of reduced order model equals 146.

Line-fitting method

The principle of initialization of line-fitting method for the cage model is the same as it is described in Section 4.1.2 for the elastic bar. We consider the frequency range of interest and input-output coordinates as a given information for the initialization process. The next initialization steps include the choice of an appropriate order of reduced model, definition of interface degrees of freedom, allocation of reference frequency points.

The order of reduced model depends on a number of transfer functions that need to be tuned and a number of eigenfrequencies contained in a frequency range of interest. As it is discussed in Section 3.2.2, the order equal to a double number of eigenfrequencies in the frequency range of interest is usually enough to achieve high accuracy of reduced model. In case of the cage model, the number of eigenfrequencies in the frequency range of interest is 30. In order to make the generation of accurate results more difficult for the line-fitting method, we define the order of reduced model to be 55.

Further, 55 DoFs must be spread throughout the body. The model is stiff in Z direction (see Fig. 4.14), therefore the interface coordinates are mainly assigned to X and Y coordinates of the nodes shown in Fig. 4.18.

The main positions of reference frequency points are points of resonances and antiresonances of transfer functions specified by the interface DoFs. The total set of frequency points is the union of sets for the different transfer functions. Usually it is necessary to allocate reference points for a few transfer functions with highest amplitudes to obtain accurate approximation of the remaining functions. The frequency rage of the cage is

wide and it includes 30 nonzero eigenfrequencies. For this model we defined 70 reference frequency points.

4.2.3 Validation of reduced order models

Normalized Relative Eigenfrequency Difference

The frequency interval of interest [0,13000] Hz contains 30 nonzero eigenfrequencies. In Fig. 4.19 we compare a relative error of eigenfrequencies for the models reduced by the Craig-Bampton and line-fitting methods.

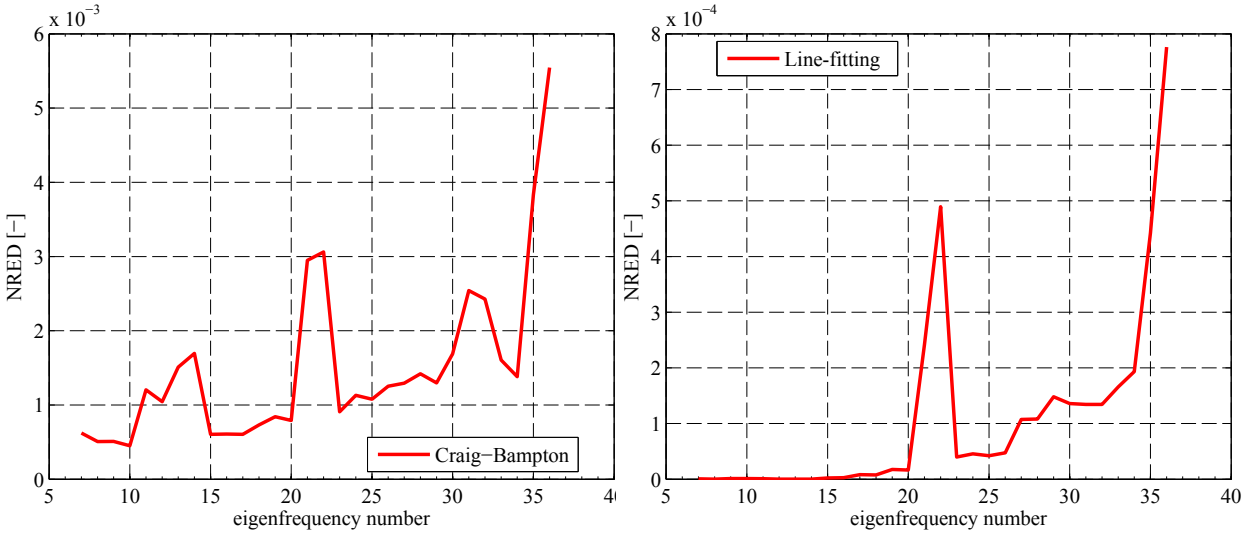

Figure 4.19: Relative error of non-zero eigenfrequencies of reduced models.

The data show that the line-fitting method approximates the model spectrum about ten times better than the Craig-Bampton procedure. However, the Craig-Bampton model is still accurate enough, as the relative error of eigenfrequencies does not exceed 0.6 %.

Modal Assurance Criterion

The cage model is symmetric relative to the X and Y axis. This leads to the repetition of certain eigenfrequencies of the model. In Section 2.4.2 we have pointed out that eigenvectors corresponded to repeated eigenfrequencies are not uniquely defined. This makes the result of MAC test ambiguous and complicated for interpretation, therefore we omit this test for the model of cage.

Frequency response analysis

In this section we analyze errors of transfer functions specified by different inputs and outputs. Without loss of generality, we chose three interface nodes shown in Fig. 4.20 in

yellow and a non-interface node marked in green for the analysis of transfer functions. In scopes of this section the interface and non-interface nodes are referred to as master and slave nodes, respectively.

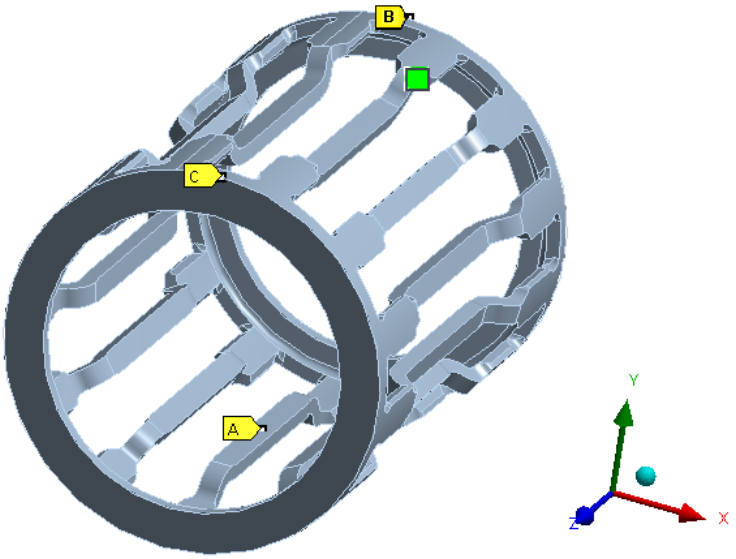

Figure 4.20: Positions of interface nodes and a non-interface node.

Further, we consider transfer functions that correspond to master-master, master-slave, and slave-slave inputs and outputs. Fig. 4.21 presents comparison of Bode plots for the master-master transfer function. In this case, the input and output are the Y-coordinate of the node at the middle of the model.

Both methods provide the accurate approximation of transfer function in the given interval [0,13000] Hz. The increasing error of line-fitting transfer function in the range [13000-15000] Hz is explained by the absence of reference frequency points in this region. The Craig-Bampton method captures intervals of antiresonances and the high frequency range slightly better, but small amplitudes of magnitude in these ranges make the error less critical. The diagrams demonstrate that the Craig-Bampton method generated the results comparable with the line-fitting results by the model of three times larger size.

Fig. 4.22 shows the comparison of Bode plots for master input slave output coordinates. The input coordinate is X degree of freedom at the middle node, while the output is X coordinate of the slave node. In this case, the responses of reduced models are still accurate.

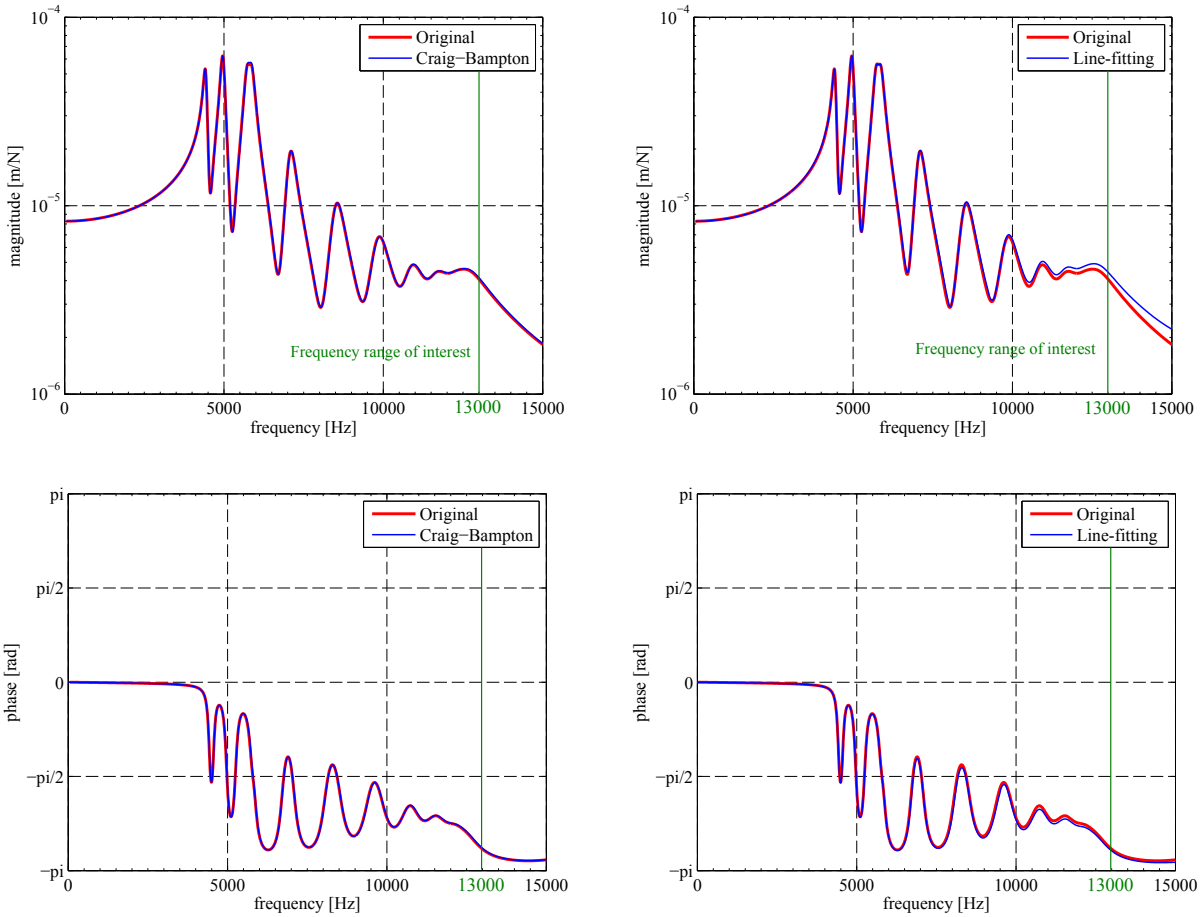

Figure 4.21: Comparison of transfer functions for master input master output coordinates.

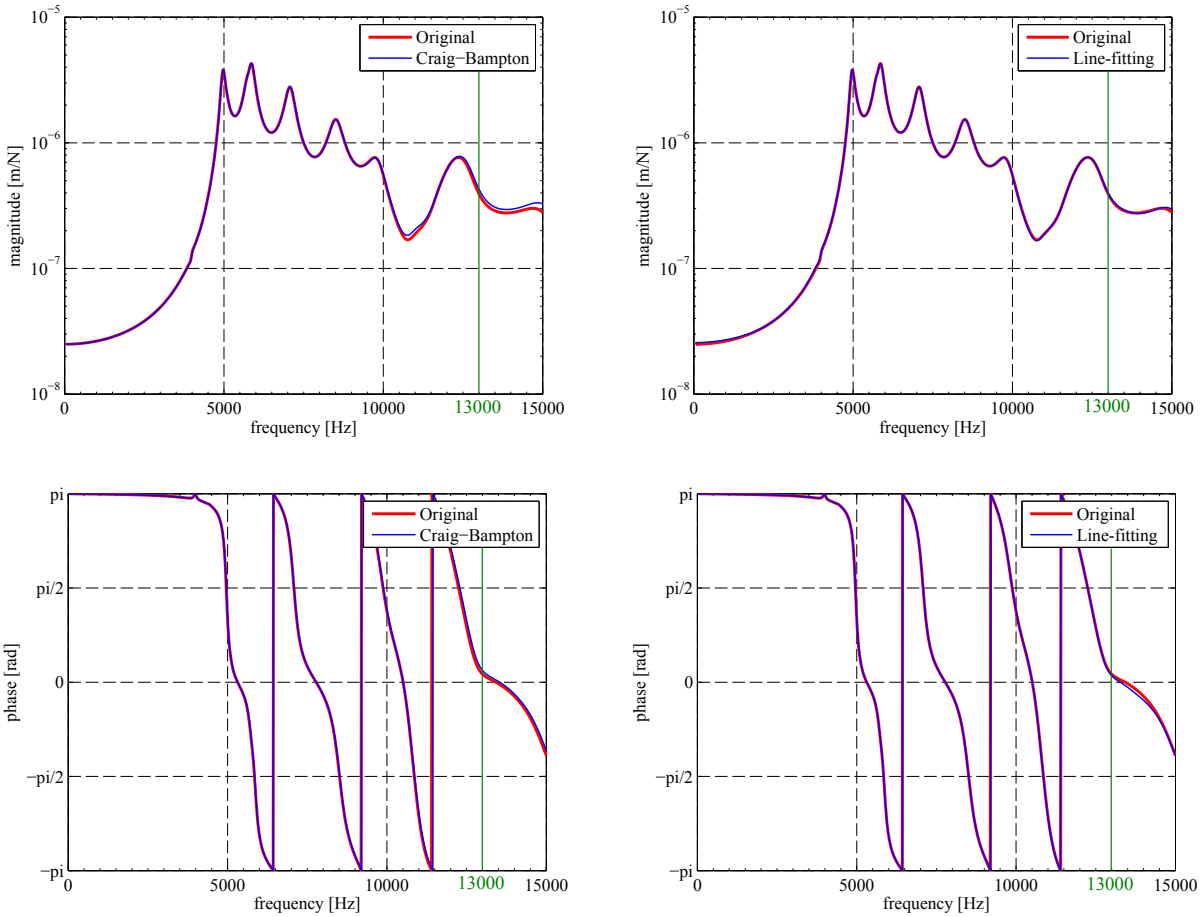

Figure 4.22: Comparison of transfer functions for master input slave output coordinates.

Finally, Fig. 4.23 provides the comparison of results for the slave-slave case, where the input and output are Y degree of freedom for the slave node. The diagrams show that the error of slave-slave transfer function is larger as compared with previous tests, but it remains acceptable because slave DoFs represent unimportant for user coordinates. Although the line-fitting method tunes only the master-master transfer functions and reduces the error of master-slave transfer paths, the error of slave-slave transfer function is turned out to be comparable with the result of Craig-Bampton model.

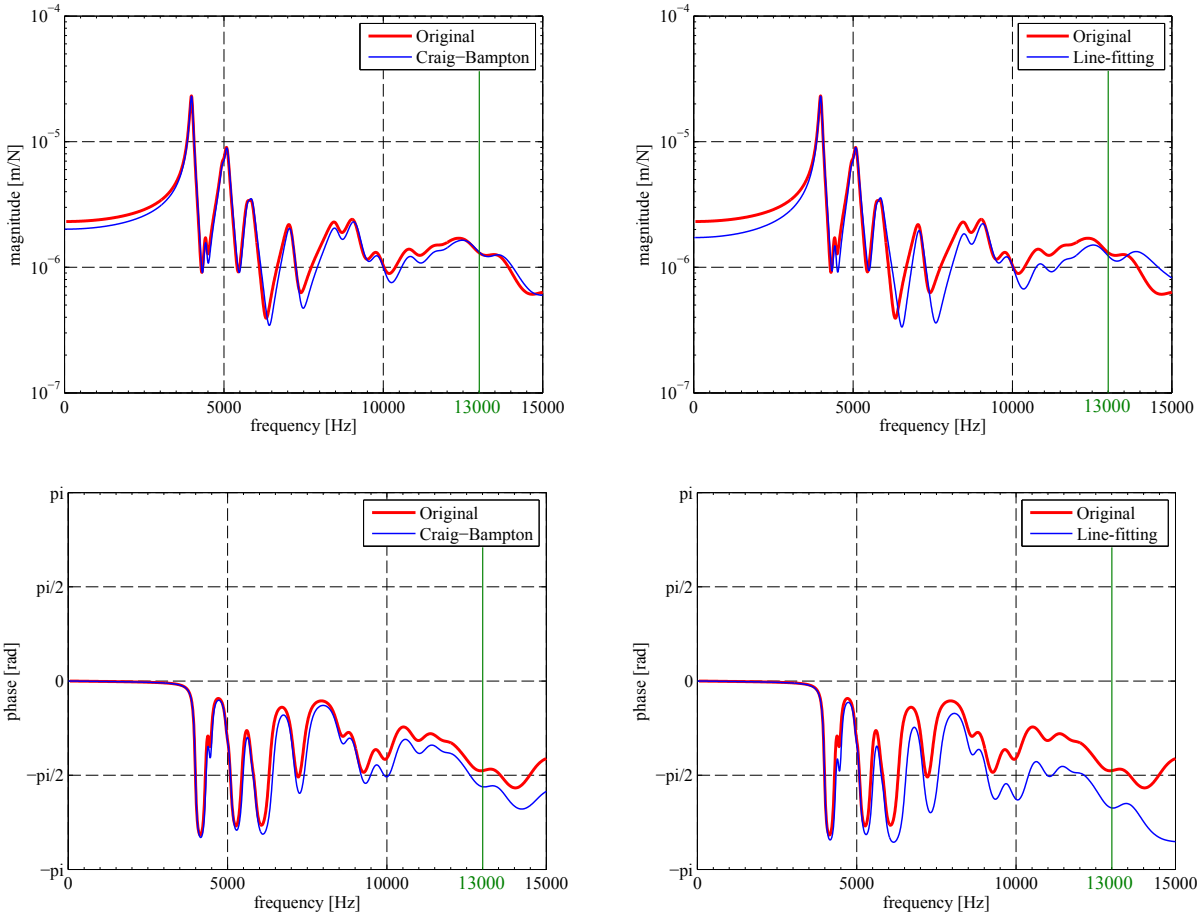

Figure 4.23: Comparison of transfer functions for slave input slave output coordinates.

Next, we deal with a relative error of transfer functions for all interface nodes shown in Fig. 4.18. The error is calculated using the formula from Eq. 2.158. Fig. 4.24 compares the relative error of transfer functions for the both reduced models.

The plot of Fig. 4.24 shows that the low frequency range is accurately approximated by the both methods. In the interval [3500-6500] Hz the line-fitting model demonstrates significantly better results than the Craig-Bampton model. In the range [6500-13000] Hz the errors are comparable and they possess the following peculiarity: the resonance frequencies are better approximated by the line-fitting method, while the Craig-Bampton approach captures better amplitudes of antiresonances. Within the frequency range [0-12000] Hz the error of line-fitting model does not exceed 3%, while the error of Craig-

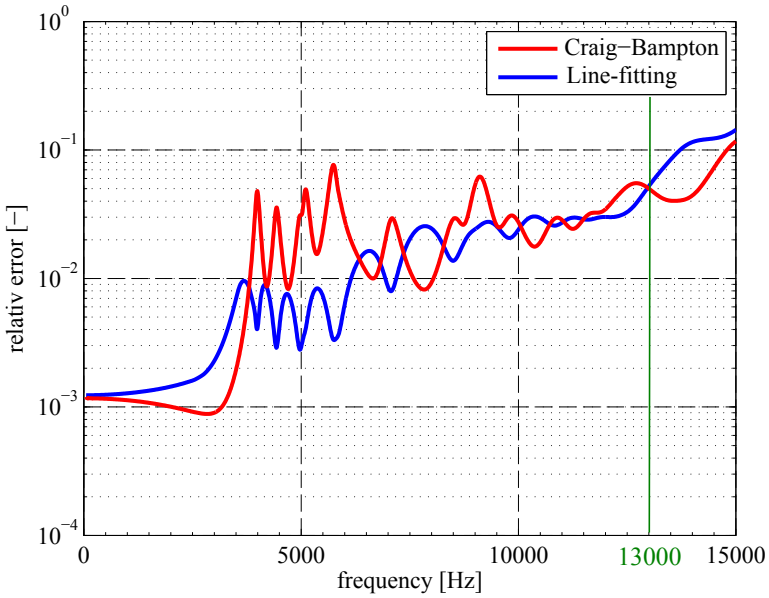

Figure 4.24: Relative error of transfer functions specified by the interface nodes.

Bampton model reaches 8%.

4.2.4 Simulation

The goal of simulation test described in this section is to validate the equations of motion of reduced order models in the time domain, as well as to obtain information about the total time of simulation.

At the initial moment the body is undeformed and it starts to rotate with the angular velocity $\boldsymbol{\omega} = \begin{bmatrix} 0, & 0, & 10 \end{bmatrix}^T$. Two longitudinal rods of the cage are connected by a stretched spring, whose influence can be treated as contact forces. The spring is attached to the points shown in Fig. 4.25. These points are contained in the sets of interface nodes for the both reduction techniques. The simulation of original FE model is carried out in Ansys, while the reduced models are simulated in Maple.

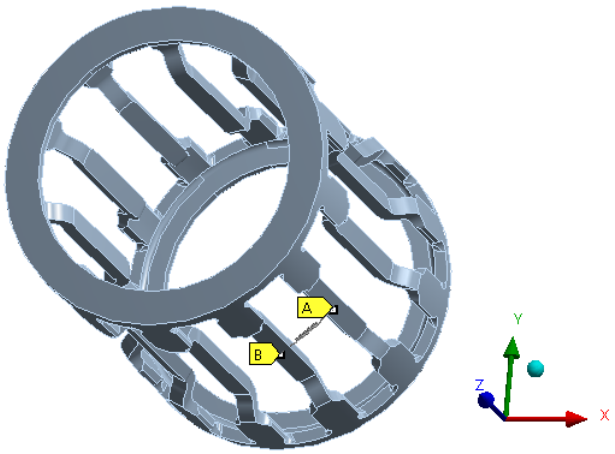

Figure 4.25: Stretched spring attached to the cage.

The interest is focused on the spring elongation. In Ansys the elongation is measured by a spring probe feature, while in Maple it is calculated using absolute coordinates of the nodes where the spring is attached. The spring is defined as follows:

- undeformed length: 3.65 mm,
- initial elongation: 0.2 mm,
- stiffness:10^4 N/m.

The period of simulation is defined to be 10^{-3}s. The system of equations of motion are solved by the implicit Backward-Euler method. The step of integration is initialized using a rule of thumb as $h = \frac{1}{20 \cdot f_{max}}$, where f_{max} defines the maximal eigenfrequency of reduced model. This results in the time steps 10^{-7}s and $6 \cdot 10^{-7}$s for the Craig-Bampton and line-fitting models, respectively.

Fig. 4.26 represents the comparison of spring elongation for the both reduced order models.

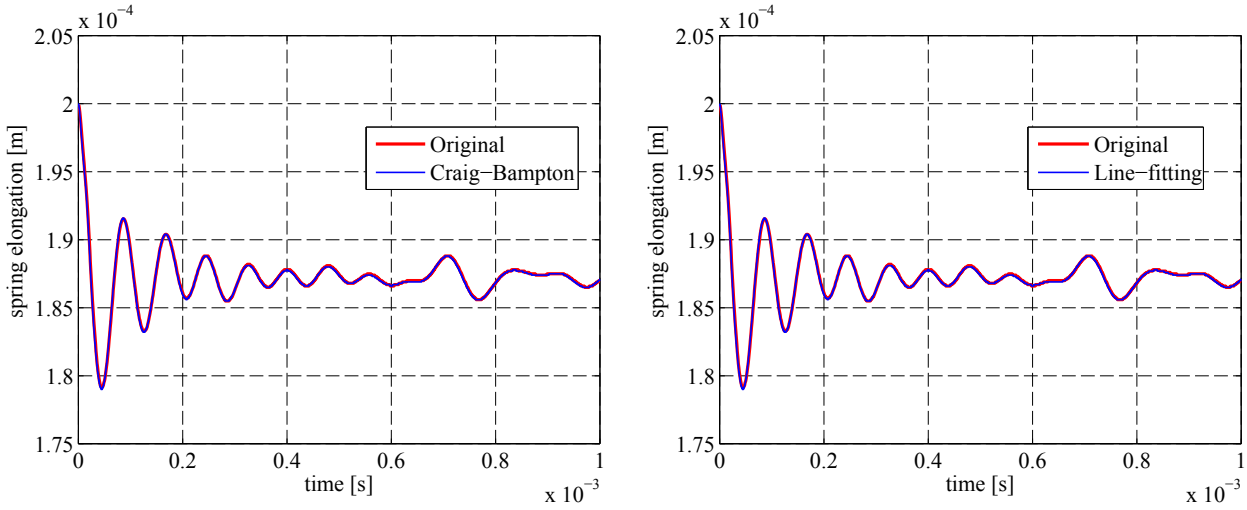

Figure 4.26: Comparison of spring elongation for the reduced models.

As can be seen, the spring elongation for each reduced order model is in the perfect agreement with the reference result. This gives reason to assert that equations of motion are correctly implemented. In addition, the test reveals a significant drawback of the Craig-Bampton model, namely, the large time of simulation. The problem is caused by the relative large number of DoFs of the reduced order model and the small time step of integration. The step is affected by the erroneous high-frequency spectrum of Craig-Bampton model. These factors considerably slow down the simulation process. The simulation of Craig-Bampton model takes 8 hours, while for the line-fitting model it is 0.8 hours, which is 10 times faster. The simulation time of the both models can be reduced by using Matlab, C++ programs, and in some cases by explicit integration schemes.

4.2.5 Comparison of reduced order models

Table 4.4 summarizes the results of analysis of the line-fitting reduction method and compares them with the corresponding results of the classical Craig-Bampton approach.

Table 4.4: Comparison of reduced order models of the cage.

Criteria\Methods	Craig-Bampton	Line-fitting
Order	140	55
Highest eigenfrequency, (Hz)	$4{\cdot}10^5$	$8 \cdot 10^4$
Suitable step of integration, (s)	$1 \cdot 10^{-7}$	$6 \cdot 10^{-7}$
Time of simulation, (h)	8	0.8
Relative error of eigenfrequencies	$< 6 \cdot 10^{-3}$	$< 8 \cdot 10^{-4}$
Relative error of transfer functions	$< 8\%$	$< 4\%$
Time of projection matrix generation, (h)	direct import from FE software	1

The data show that the line-fitting method generated the reduced order model having the lower order, higher accuracy of eigenfrequencies and important transfer functions, and better condition properties of system matrices. The advantage of Craig-Bampton approach lies in the smaller time of coordinate transformation matrix generation. In addition, there is a possibility to import the Craig-Bampton transformation matrix from existing FE software, while the generation of line-fitting matrix requires using of additional preprocessor module.

5 Discussion

The goal of this chapter is comprehensive evaluation of the line-fitting method. The analysis is performed based on the theoretical description of the approach in Chapter 3 and the numerical results presented in Chapter 4. At the beginning we examine whether the proposed method solves the problem of traditional order reduction approaches: the lack of possibility to tune a reduced order model for certain transfer functions and certain frequency ranges. After that the method is evaluated based on the demands from Section 1.3 to model order reduction techniques. Further, the proposed method is compared to the existing reduction approaches described in Section 1.2. Finally, advantages and limitations of the line-fitting method are considered.

Transfer functions comprise complete information about the behavior of points of the model. Among traditional reduction approaches the component mode synthesis method is the most suitable for the accurate approximation of transfer functions. The method is based on the modal representation in which a set of normal modes and a set of correction modes are used. The correction modes allow tuning of transfer functions for a certain frequency. However, tuning of reduced order model for certain transfer paths and frequency ranges using CMS methods is not feasible. First, important modes for the predefined transfer functions are unknown. Second, the quality of approximation depends on the choice of interface coordinates used for the method initialization. Third, the reduced model can be tuned only for a one frequency (static case for the Craig-Bampton method).

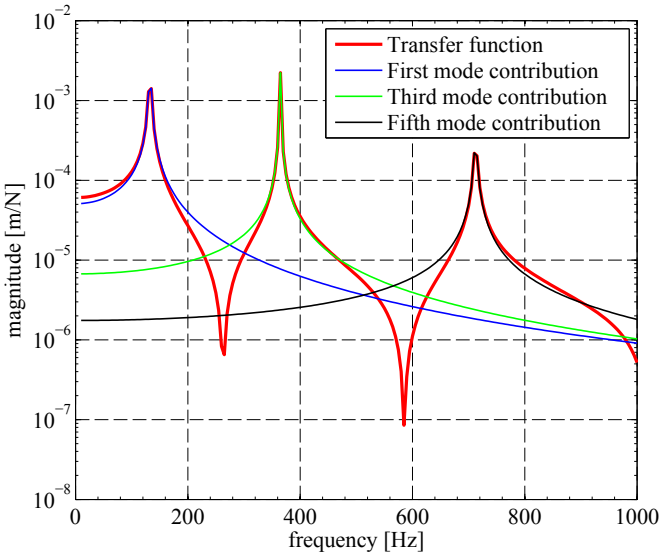

Figure 5.1: Decomposition of transfer function into modes contributions.

The contributions of several modes to a transfer function are shown in Fig. 5.1. The combination of modes leads to the results illustrated in Fig. 5.2.

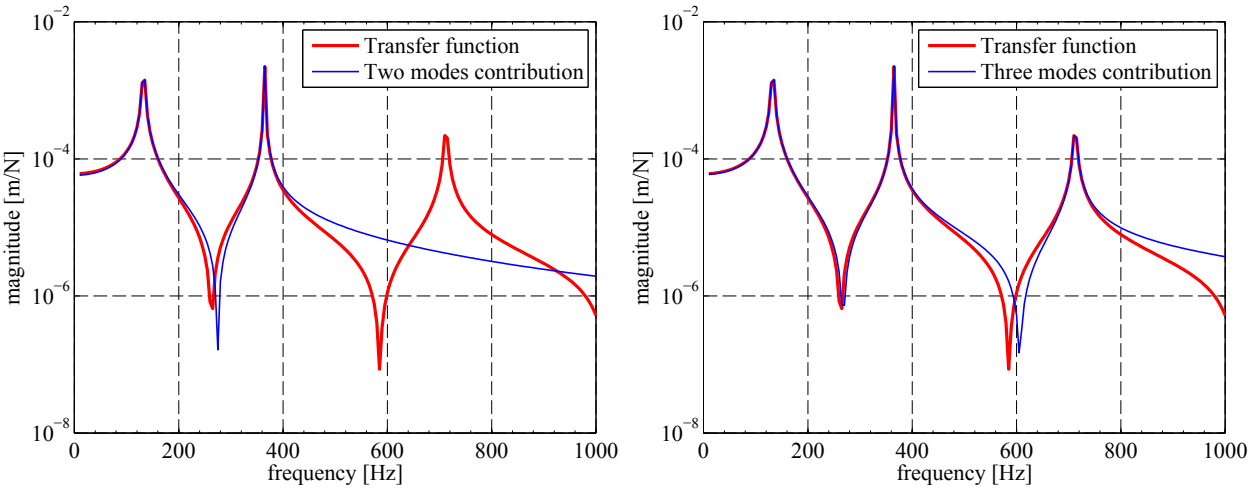

Figure 5.2: Combined contribution of several modes to a transfer function.

The modal reduction requires using of all modes to obtain exact values of transfer functions in a limited frequency range. However, the exact values of transfer functions in the limited frequency range can be obtained using much smaller number of coordinates. This idea is used in the line-fitting method. In the proposed approach all DoFs of reduced order model contribute to the improvement of predefined transfer functions in the frequency interval of interest.

The next idea that stands behind the line-fitting method is connected with the approximation of predefined transfer functions by minimizing an error of adjacent transfer functions. In Fig. 5.3 positions of important transfer functions are shown in red, while outputs of adjacent transfer functions are contained in a blue hemisphere with a small radius. The curves of adjacent and important functions are almost identical. Since the line fitting method expresses transfer functions with non-interface outputs through the important transfer functions, the adjacent transfer functions are accurately approximated. This forces important transfer functions to be precise as well. The assertion is confirmed by the results of several numeric examples in Chapter 4. It follows that the line-fitting method solves the problem of classical reduction approaches.

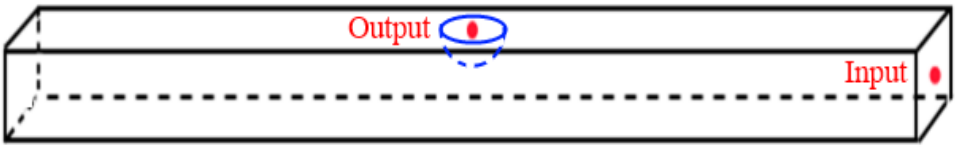

Figure 5.3: Approximation of important transfer functions using adjacent transfer functions.

Further we dwell on the compliance of the line-fitting method with the requirements to

model order reduction techniques. The requirements are formulated in Section 1.3 and repeated in this section for the discussion:

- accuracy of reduced model,
- computational efficiency of reduction method,
- preservation of model stability,
- estimation of error introduced by the reduction process,
- possibility to automate the reduction process,
- fast simulation of reduced model.

In addition, using of model order reduction methods in the context of EMBS imposes on them additional restrictions:

- preservation of second order structure of equations of motion,
- coordinate transformation matrix excludes rigid body modes.

The accuracy of line-fitting method is ensured by its ability of tuning important for the user transfer functions. Local accuracy of transfer functions can be improved by additional reference frequency points, whereas the quality over a whole frequency range of interest is enhanced by increasing an order of reduced model.

The main computational burdens of the proposed reduction approach consist in the calculation of transfer function matrices for several frequency points and the solution of large least-squares problem. The most of reduction approaches require performing of frequency response analysis to evaluate accuracy of reduced order model in the frequency domain. This analysis needs calculating of transfer function matrices for all points in a discrete frequency range of interest, therefore the calculation of transfer matrices at several points for the line-fitting method is considered as an uncritical issue. The total computational cost of the line-fitting method is larger in comparison with the Craig-Bampton approach, but it remains acceptable for moderately dimensional FE models.

The preservation of stability is an important property of reduction approaches because it ensures that a reduced model does not cause any type of failure to elastic multibody systems. It was proven in Section 3.4 that the line-fitting technique meets this essential requirement.

Along with the classical reduction approaches and the methods based on Krylov subspaces, the line-fitting reduction method lacks of possibility to specify in advance a permissible error introduced by the reduction process. In this case, generation of admissible reduced order model becomes an iterative process where each iteration corrects the quality of reduced order model.

The current version of the line-fitting reduction method requires user's involvement in some steps of the method initialization: the choice of reference frequency points and

distribution of redundant interface coordinates. These steps of the method can be automated. The complete automation of line-fitting reduction approach is possible, but it is easier to realize, if a reduction error estimator is available.

Simulation speed in addition to other factors depends on a number of coordinates of reduced order model and system stiffness. According to the results presented in Chapter 4, the time of simulation of line-fitting models is 10-14 times smaller in comparison with the Craig-Bampton models under the same conditions. This is achieved due to much smaller number of DoFs and smaller stiffness of line-fitting models. All coordinates of line-fitting models are involved in improving the accuracy of reduction, which allows using of smaller number of DoFs as against the number of coordinates of Craig-Brampton models. The stiffness is determined by the highest eigenfrequency of the system. The line-fitting method can influence accuracy of eigenfrequencies contained in the predefined frequency range, but the spectrum of model beyond this range is uncontrolled. For this reason, no statements about the limits of the spectrum can be made. However, the both numeric examples show that the stiffness of line-fitting models remains considerably lower than the stiffness of Craig-Bampton models.

The systems reduced by the line-fitting method preserve the second order structure of equations of motion. This enables integration of reduced order models into a multibody system of second order type.

Since a projection matrix of line-fitting method is calculated based on transfer functions without a component of rigid body motion, the rigid body modes can not be captured by this matrix. This property allows the line-fitting method to satisfy the last requirement in the list above.

The advantages of line-fitting approach in comparison with the classical methods are high accuracy, low order, and small stiffness of reduced systems. In addition, the proposed method makes it possible to emphasize certain transfer functions and certain frequency ranges. The new approach produced significantly more accurate results for systems with slight damping than the Craig-Bampton method.

The modern reduction methods based on Krylov subspaces are to some extent comparable to what this thesis proposes and might even outperform it. However, for the Krylov subspace method stability of reduced model is not guaranteed even if the full order model is stable. In addition, transfer functions for non-interface DoFs are uncontrolled, which can lead to artificial and undesired effects in the motion of non-interface nodes of the model. In contrast, the line-fitting methods ensures that the error of transfer functions having non-interface outputs is limited. As concerns the modern Balanced truncation method, high computational burdens make the reduction feasible only for small dimensional FE models.

Along with a number of advantages, the line-fitting method has several limitations as compared to classical and modern reduction techniques. The main drawback of the method

is computational cost of projection matrix generation. Besides, the modern methods can excel the line-fitting method in tuning of reduced order models for antiresonance frequencies. Formulation of weighted least squares problem can help to address this issue for the proposed reduction approach.

The common problem of reduction techniques is processing of a large number of interface coordinates. Since the set of DoFs of line-fitting model includes interface DoFs, the size of reduced order model can be redundant. This can result in producing stiff reduced order systems. One of the solutions of the problem is the interface reduction where the motion of interface surface is approximated by the motion of several nodes. Another approach is to omit unnecessary interface DoFs, but this requires much experience and insight into a specific problem.

6 Summary and further work

The main scientific contribution of the thesis is a new linear model order reduction method for elastic multibody simulation. The set of classical reduction approaches consists of modal truncation, condensation, and component mode synthesis techniques. The category of modern reduction methods includes the techniques based on the singular value decomposition using Gramian matrices and moment matching via Krylov subspaces. The proposed method allows solving of problem of classical reduction approaches: the lack of possibility to tune a reduced order model for certain transfer functions and frequency ranges. In addition, the new method satisfies the following requirements: high accuracy of reduced order models, preservation of stability, fast simulation of reduced order models, and the possibility of using the method in the context of elastic multibody systems. The new method differs from the modern reduction approaches and it has its own advantages.

The research topic belongs to the area of computational dynamics and relates to such disciplines as multibody dynamics, finite element analysis, and model order reduction. Chapter 2 of this work covers fundamentals of elastic multibody system simulation. The fundamentals include the modeling of multibody dynamics using a floating frame approach, finite element discretization, model order reduction approaches, validation of reduced order models, and schemes of numerical solution of equations of motion. Chapter 3 is devoted to the novel reduction technique proposed by the author of the thesis: line-fitting reduction technique. In Chapter 4 we apply the new method to the bar and the bearing cage models, perform validation tests of the reduced order models in the time and frequency domains, and compare the results with results of classical Craig-Bampton approach. Chapter 5 includes comprehensive evaluation of the line-fitting method and its comparison with the classical and modern reduction procedures.

The advantages of line-fitting approach in comparison with the classical methods are higher accuracy, lower order, and usually smaller stiffness of reduced systems. Low order and small stiffness lead to considerable gains in computational speed for practical EMBS. In addition, the proposed method makes it possible to emphasize certain transfer functions and certain frequency ranges. It is also necessary to point out that line-fitting approach produces significantly more accurate results for systems with slight damping than the Craig-Bampton method. The main drawback of the method is computational cost of projection matrix generation. However, the computational burdens remain small for moderately dimensional systems.

The line-fitting method can be used as an alternative to modern Krylov subspace based methods, if the preservation of stability of reduced model is important or it is necessary to limit an error of non-interface nodes. In addition, the proposed approach is an appropriate choice for the systems where the application of modern Balanced truncation method is not feasible due to high computational costs.

The reduction method proposed in this work is developed in scopes of a project "Elastic bodies in Caba3D" of the Otto von Guericke University and the Schaeffler Technologies AG & Co. KG. The primary goal of the project was to develop software that can take into account deformation effects arisen in mechanical systems under operating conditions. The line-fitting reduction technique is implemented in the commercial simulation software Caba3D as an alternative to other reduction approaches. Within the project the author of the thesis et al. published several international articles devoted to the topic of model order reduction:[53, 54, 52].

Looking ahead, there are a number of points that can improve the current version of line-fitting reduction. The first issue is the enhancement of computational efficiency. The solution of this task needs additional investigation. The second aspect relates to the improvement of accuracy. The unanswered questions remain how to chose an optimal number of coordinates for a reduced order model and where to allocate interface coordinates to obtain the most accurate approximation. Another issue concerning the accuracy is better approximation of transfer function in regions with small magnitudes. Next, the user's involvement in the initialization of method can be decreased by automating the choice of reference frequency points and the allocation of interface coordinates. The range of application of the method can be extended by adopting the line-fitting approach for models with six degrees of freedom per node. Besides, the correct work of the method for different types of constraints imposed on the model needs to be confirmed.

Appendix

Rotation matrix using Euler parameters

Let's denote a unit vector of axis of rotation as $\mathbf{v}$ and an angle of finite rotation as α, see Fig. A.1.

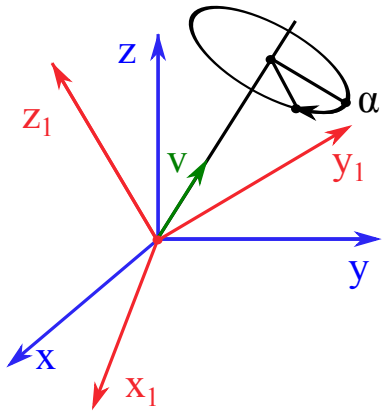

Figure A.1: Finite rotation.

A set of Euler parameters is defined as

$$\begin{cases} \theta_0 = \cos\frac{\alpha}{2}, & \theta_1 = v_1 \cdot \sin\frac{\alpha}{2}, \\ \theta_2 = v_2 \cdot \sin\frac{\alpha}{2}, & \theta_3 = v_3 \cdot \sin\frac{\alpha}{2} \end{cases}. \tag{A.1}$$

From the definition follows that $\sum_{k=0}^{3}(\theta_k)^2 = 1$.

According to [79], the body rotation matrix $\mathbf{A}$ can be expressed in terms of Euler parameters as

$$\mathbf{A}(\theta) = \begin{bmatrix} 1-2(\theta_2)^2-2(\theta_3)^2 & 2(\theta_1\theta_2-\theta_0\theta_3) & 2(\theta_1\theta_3+\theta_0\theta_2) \\ 2(\theta_1\theta_2+\theta_0\theta_3) & 1-2(\theta_1)^2-2(\theta_3)^2 & 2(\theta_2\theta_3-\theta_0\theta_1) \\ 2(\theta_1\theta_3-\theta_0\theta_2) & 2(\theta_2\theta_3+\theta_0\theta_1) & 1-2(\theta_1)^2-2(\theta_2)^2 \end{bmatrix}. \tag{A.2}$$

The angular velocity vector $\boldsymbol{\omega}$ in the global frame and the vector of time derivatives of Euler parameters are related as

$$\boldsymbol{\omega} = 2 \cdot \boldsymbol{\Theta}(\boldsymbol{\theta}) \cdot \dot{\boldsymbol{\theta}} \tag{A.3}$$

where $\boldsymbol{\Theta} \in \mathbb{R}^{3\times 4}$ is given by

$$\boldsymbol{\Theta}(\boldsymbol{\theta}) = \begin{bmatrix} -\theta_1 & \theta_0 & -\theta_3 & \theta_2 \\ -\theta_2 & \theta_3 & \theta_0 & -\theta_1 \\ -\theta_3 & -\theta_2 & \theta_1 & \theta_0 \end{bmatrix}, \tag{A.4}$$

see, e.g. [79].

Bibliography

[1] O. P. Agrawal and A. A. Shabana. Dynamic analysis of multibody systems using component modes. *Computers & Structures*, 21(6):1303–1312, 1985.

[2] O. P. Agrawal and A. A. Shabana. Application of deformable-body mean axis to flexible multibody system dynamics. *Computer Methods in Applied Mechanics and Engineering*, 56(2):217–245, 1986.

[3] J. Ambrosio. Dynamics of structures undergoing gross motion and nonlinear deformations: A multibody approach. *Computers & Structures*, 59(6):1001–1012, 1996.

[4] J. Ambrosio. Efficient kinematic joint descriptions for flexible multibody systems experiencing linear and non-linear deformations. *International Journal for Numerical Methods in Engineering*, 56(12):1771–1793, 2003.

[5] A. Antoulas and D. Sorensen. Approximation of large-scale dynamical systems: an overview. *International Journal of Applied Mathematics and Computer Science*, 11(5):1093–1121, 2001.

[6] A. C. Antoulas. *Approximation of Large-Scale Dynamical Systems*. Society for Industrial and Applied Mathematics, 2005.

[7] K. Atkinson and W. Han. Finite difference method. In W. Han and K. Atkinson, editors, *Theoretical Numerical Analysis*, volume 39 of *Texts in Applied Mathematics*, pages 253–275. Springer New York, New York, NY, 2009.

[8] Z. Bai and Y. Su. Dimension reduction of large-scale second-order dynamical systems via a second-order arnoldi method. *SIAM Journal on Scientific Computing*, 26(5):1692–1709, 2005.

[9] M. Bampton and R. Craig. Coupling of substructures for dynamic analyses. *AIAA Journal*, 6(7):1313–1319, 1968.

[10] A. Banerjee and J. M. Dickens. Dynamics of an arbitrary flexible body in large rotation and translation. *Journal of Guidance, Control, and Dynamics*, 13(2):221–227, 1990.

[11] K.-J. Bathe. *Finite element procedures*. Prentice Hall, Englewood Cliffs, N.J, 1996.

[12] J. W. Baumgarte. A new method of stabilization for holonomic constraints. *Journal of Applied Mechanics*, 50(4a):869, 1983.

[13] G. Beer, I. Smith, and C. Duenser. *The boundary element method with programming: For engineers and scientists*. Springer, Wien and New York, 2008.

[14] P. Benner, P. Kürschner, and J. Saak. An improved numerical method for balanced truncation for symmetric second-order systems. *Mathematical and Computer Modelling of Dynamical Systems*, 19(6):593–615, 2013.

[15] P. Benner and J. Saak. Efficient balancing-based mor for large-scale second-order systems. *Mathematical and Computer Modelling of Dynamical Systems*, 17(2):123–143, 2011.

[16] B. Besselink, U. Tabak, A. Lutowska, van de Wouw, N., H. Nijmeijer, D. J. Rixen, M. E. Hochstenbach, and W.H.A. Schilders. A comparison of model reduction techniques from structural dynamics, numerical mathematics and systems and control. *Journal of Sound and Vibration*, 332(19):4403–4422, 2013.

[17] J. R. Canavin and P. W. Likins. Floating reference frames for flexible spacecraft. *Journal of Spacecraft and Rockets*, 14(12):724–732, 1977.

[18] T. K. Caughey. Classical normal modes in damped linear dynamic systems. *Journal of Applied Mechanics*, 27(2):269, 1960.

[19] K. Changizi and A. A. Shabana. A recursive formulation for the dynamic analysis of open loop deformable multibody systems. *Journal of Applied Mechanics*, 55(3):687, 1988.

[20] J. Chaskalovic. *Finite element methods for engineering sciences*. Springer, New York and London, 2008.

[21] R. Craig. *Structural dynamics: An introduction to computer methods*. Wiley, New York, 1981.

[22] R. Craig. Coupling of substructures for dynamic analyses - an overview. In *41st Structures, Structural Dynamics, and Materials Conference and Exhibit*, April 2000.

[23] R. Craig and A. Kurdila. *Fundamentals of structural dynamics*. John Wiley, Hoboken, N.J., 2nd ed. edition, 2006.

[24] W. D'Ambrogio and A. Fregolent. Robust dynamic model updating using point antiresonances.

[25] Dassault Systemes SolidWorks Corp. Understanding of nonlinear analysis. http://files.solidworks.com/whitepapers/2010/nonlinear_analysis_2010_eng_final.pdf.

[26] S. Dietz. *Vibration and fatigue analysis of vehicle systems using component modes: Techn. Univ., Diss–Berlin*, volume 401 of *Fortschritt-Berichte VDI Reihe 12, Verkehrstechnik/Fahrzeugtechnik*. VDI-Verl, Düsseldorf, als ms. gedr edition, 1999.

[27] E. Eich-Soellner and C. Führer. *Numerical methods in multibody dynamics*. European Consortium for Mathematics in Industry. Stuttgart, 1998.

[28] J. Fehr and P. Eberhard. Simulation process of flexible multibody systems with non-modal model order reduction techniques. *Multibody System Dynamics*, 25(3):313–334, 2011.

[29] M. Fischer and P. Eberhard. Linear model reduction of large scale industrial models in elastic multibody dynamics. *Multibody System Dynamics*, 31(1):27–46, 2014.

[30] R. W. Freund. Model reduction methods based on krylov subspaces. *Acta Numerica*, 12:267–319, 2003.

[31] O. Friberg. A method for selecting deformation modes in flexible multibody dynamics. *International Journal for Numerical Methods in Engineering*, 32(8):1637–1655, 1991.

[32] W. Gawronski. *Dynamics and control of structures: A modal approach*. Mechanical engineering series. Springer, New York, 1998.

[33] C. W. Gear. Differential-algebraic equation index transformations. *SIAM Journal on Scientific and Statistical Computing*, 9(1):39–47, 1988.

[34] M. Geradin and A. Cardona. *Flexible multibody dynamics: A finite element approach*. John Wiley, New York, 2001.

[35] M. Géradin and D. Rixen. *Mechanical vibrations: Theory and application to structural dynamics*. John Wiley, Chichester and New York, 2nd ed. edition, 1997.

[36] E. J. Grimme. *Krylov Projection Methods For Model Reduction*. PhD thesis, University of Illinois at Urbana-Champaign, Urbana-Champaign, 1997.

[37] R. J. Guyan. Reduction of stiffness and mass matrices. *AIAA Journal*, 3(2):380, 1965.

[38] E. Hairer and G. Wanner. *Solving Ordinary Differential Equations II: Stiff and Differential-Algebraic Problems*. Springer Berlin Heidelberg, second revised edition edition, 1996.

[39] Heirman, G. H. K. and W. Desmet. Interface reduction of flexible bodies for efficient modeling of body flexibility in multibody dynamics. *Multibody System Dynamics*, 24(2):219–234, 2010.

[40] W. C. Hurty. Dynamic analysis of structural systems using component modes. *AIAA Journal*, 3(4):678–685, 1965.

[41] T. Kane, R. Ryan, and A. Banerjee. Dynamics of a cantilever beam attached to a moving base. *Journal of Guidance, Control, and Dynamics*, 10(2):139–151, 1987.

[42] K. Kim. A review of mass matrices for eigenproblems. *Computers & Structures*, 46(6):1041–1048, 1993.

[43] P. Koutsovasilis. *Model order reduction in structural mechanics: Coupling the rigid and elastic multi body dynamics*, volume Nr. 712 of *Fortschrittberichte VDI / 12*. VDI-Verl., Düsseldorf, als ms. gedr edition, 2009.

[44] P. Koutsovasilis and M. Beitelschmidt. Comparison of model reduction techniques for large mechanical systems. *Multibody System Dynamics*, 20(2):111–128, 2008.

[45] A. Kurdila, J. G. Papastavridis, and M. P. Kamat. Role of maggi's equations in computational methods for constrained multibody systems. *Journal of Guidance, Control, and Dynamics*, 13(1):113–120, 1990.

[46] H. Lai and B. Dopker. Influence of lumped rotary inertia in flexible multibody dynamics. *Mech. Struct. Mach.*, 18:47–59, 1990.

[47] M. Lehner. *Modellreduktion in elastischen Mehrkörpersystemen*, volume Bd. 2007,10 of *Schriften aus dem Institut für Technische und Numerische Mechanik der Universität Stuttgart*. Shaker, Aachen, 2007.

[48] M. Lehner and P. Eberhard. On the use of moment-matching to build reduced order models in flexible multibody dynamics. *Multibody System Dynamics*, 16(2):191–211, 2006.

[49] A. Leung. An accurate method of dynamic condensation in structural analysis. *International Journal for Numerical Methods in Engineering*, 12(11):1705–1715, 1978.

[50] B. Lohmann and B. Salimbahrami. Ordnungsreduktion mittels krylov-unterraummethoden. *Automatisierungstechnik 52*, pages 30–38, 2004.

[51] A. Love. *A treatise on the mathematical theory of elasticity*. Cambridge University Press, Cambridge, 4th ed edition, 2013.

[52] V. Makhavikou and R. Kasper. Choice of a modal reduction method in the context of modular simulation of flexible multibody dynamics. *Selected Works of international conference on mechanics VI Polyahov's Readings*, pages 27–33, 2012.

[53] V. Makhaviou, R. Kasper, and D. Vlasenko. Method of model reduction for elastic multibody systems. *Proceedings of 11th World Congress on Computational Mechanics (WCCM XI), 5th European Conference on Computational Mechanics (ECCM V), July 20-25*, pages 475–486, 2014.

[54] V. Makhaviou, D. Vlasenko, and R. Kasper. Alternative method of model reduction for flexible multibody systems. *Effizienz, Praezision, Qualitaet: 11. Magdeburger Maschinenbau-Tage*, page 10, 2013.

[55] D. Mangler. *Die Berechnung geometrisch nichtlinearer Probleme der Dynamik unter Nutzung linearer FEM-Programme*. PhD thesis, Otto-von-Guericke University, Magdeburg, 1994.

[56] F. Melzer. Symbolic computations in flexible multibody systems. *Nonlinear Dynamics*, 9(1-2):147–163, 1996.

[57] D. G. Meyer and S. Srinivasan. Balancing and model reduction for second-order form linear systems. *IEEE Transactions on Automatic Control*, 41(11):1632–1644, 1996.

[58] B. Moore. Principal component analysis in linear systems: Controllability, observability, and model reduction. *IEEE Transactions on Automatic Control*, 26(1):17–32, 1981.

[59] P. C. Müller. *Stabilität und Matrizen: Matrizenverfahren in der Stabilitätstheorie linearer dynamischer Systeme*. Springer-Verlag, Berlin and New York, 1977.

[60] P. Nikravesh. Understanding mean-axis conditions as floating reference frames. In J. Ambrosio, editor, *Advances in Computational Multibody Systems*, volume 2 of *Computational Methods in Applied Sciences*, pages 185–203. Springer-Verlag, Berlin/Heidelberg, 2005.

[61] P. Nikravesh and J. Ambrosio. Systematic construction of equations of motion for rigid-flexible multibody systems containing open and closed kinematic loops. *International Journal for Numerical Methods in Engineering*, 32(8):1749–1766, 1991.

[62] P. Nikravesh and Y.-S. Lin. Use of principal axes as the floating reference frame for a moving deformable body. *Multibody System Dynamics*, 13(2):211–231, 2005.

[63] N.N. Ansys® academic research, release 14.5, help system, mechanical user guide, ansys, inc.

[64] C. Nowakowski, J. Fehr, and P. Eberhard. Einfluss von Schnittstellenmodellierungen bei der Reduktion elastischer Mehrkörpersysteme. *Automatisierungstechnik*, 59(8):512–519, 2011.

[65] C. Nowakowski, J. Fehr, M. Fischer, and P. Eberhard, editors. *Model Order Reduction in Elastic Multibody Systems using the Floating Frame of Reference Formulation*, 2012.

[66] C. Nowakowski, P. Kürschner, P. Eberhard, and P. Benner. Model reduction of an elastic crankshaft for elastic multibody simulations. *ZAMM - Journal of Applied Mathematics and Mechanics / Zeitschrift für Angewandte Mathematik und Mechanik*, 93(4):198–216, 2013.

[67] W. Pan and E. Haug. Flexible multibody dynamic simulation using optimal lumped inertia matrices. *Comput. Methods Appl. Mech.*, 173:189–200, 1999.

[68] M. S. Pereira and P. Nikravesh. Impact dynamics of multibody systems with frictional contact using joint coordinates and canonical equations of motion. *Nonlinear Dynamics*, 9(1-2):53–71, 1996.

[69] J. Pfister. *Elastic multibody systems with frictional contacts*. Schriften aus dem Institut für Technische und Numerische Mechanik der Universität Stuttgart. Shaker, Aachen, 2006.

[70] Z.-Q. Qu. *Model Order Reduction Techniques: With Applications in Finite Element Analysis*. Springer London, London, 2004.

[71] J. Ryu, Sang-S. Kim, and Sung-S. Kim. A general approach to stress stiffening effects on flexible multibody dynamic systems. *Mechanics of Structures and Machines*, 22(2):157–180, 1994.

[72] Y. Saad. *Iterative methods for sparse linear systems*. SIAM, Philadelphia, 2nd ed edition, 2003.

[73] B. Salimbahrami and B. Lohmann. Order reduction of large scale second-order systems using krylov subspace methods. *Linear Algebra and its Applications*, 415(2-3):385–405, 2006.

[74] W. Schilders, Vorst, H. A. van der, and J. Rommes. *Model order reduction: Theory, research aspects and applications*, volume 13 of *Mathematics in industry The European Consortium for Mathematics in Industry*. Springer, Berlin, 2008.

[75] R. von Schwerin. *Multibody system simulation: Numerical methods, algorithms, and software*, volume 7 of *Lecture notes in computational science and engineering*. Springer-Verlag, Berlin and New York, 1999.

[76] R. Schwertassek and O. Wallrapp. *Dynamik flexibler Mehrkoerpersysteme: Methoden der Mechanik zum rechnergestützten Entwurf und zur Analyse mechatronischer Systeme*. Grundlagen und Fortschritte der Ingenieurwissenschaften. Vieweg, Braunschweig [u.a.], 1999.

[77] R. Schwertassek, O. Wallrapp, and A. A. Shabana. Flexible multibody simulation and choice of shape functions. *Nonlinear Dynamics*, 20(4):361–380, 1999.

[78] A. A. Shabana. Flexible multibody dynamics: Review of past and recent developments. *Multibody System Dynamics*, 1(2):189–222, 1997.

[79] A. A. Shabana. *Dynamics of multibody systems*. Cambridge University Press, Cambridge and New York, 3rd ed edition, 2005.

[80] A. A. Shabana and R. A. Wehage. A coordinate reduction technique for dynamic analysis of spatial substructures with large angular rotations. *Journal of Structural Mechanics*, 11(3):401–431, 1983.

[81] K. Sherif, H. Irschik, and W. Witteveen. Transformation of arbitrary elastic mode shapes into pseudo-free-surface and rigid body modes for multibody dynamic systems. *Journal of Computational and Nonlinear Dynamics*, 7(2):021008, 2012.

[82] P. Sokol. *Kinematik und Dynamik von Mehrkörperschleifen mit elastischen Körpern*. PhD thesis, Universität-Gesamthochschule-Duisburg, 1990.

[83] D. Sorensen and A. Antoulas. Gramians of structured systems and an error bound for structure-preserving model reduction, 2004.

[84] K. Sorge. *Mehrkörpersysteme mit starr-elastischen Subsystemen*, volume Nr. 184 of *Fortschrittberichte VDI : Reihe 11, Schwingungstechnik*. VDI-Verl, Düsseldorf, als ms. gedr edition, 1993.

[85] The Schaeffler Technologies AG and Co. KG. http://www.schaeffler.de/ content.schaeffler.de/ en/ branches/ industry/ motorcycles_specvehicles/ product/ chassis_system/ rear_swinging_fork/ rear_swinging_fork.jsp.

[86] F. E. Udwadia and R. E. Kalaba. Explicit equations of motion for mechanical systems with nonideal constraints. *Journal of Applied Mechanics*, 68(3):462, 2001.

[87] Veubeke, B. F. de. The dynamics of flexible bodies. *International Journal of Engineering Science*, 14(10):895–913, 1976.

[88] O. Wallrapp. Standardization of flexible body modeling in multibody system codes, part i: Definition of standard input data*. *Mechanics of Structures and Machines*, 22(3):283–304, 1994.

[89] T. M. Wasfy and A. K. Noor. Computational strategies for flexible multibody systems. *Applied Mechanics Reviews*, 56(6):553, 2003.

[90] R. A. Wehage and E. J. Haug. Generalized coordinate partitioning for dimension reduction in analysis of constrained dynamic systems. *Journal of Mechanical Design*, 104(1):247, 1982.

[91] W. Yoo and E. Haug. Dynamics of articulated structures. part i. theory. *Journal of Structural Mechanics*, 14(1):105–126, 1986.

[92] Z.-H. Zhong and J. Mackerle. Contact-impact problems: A review with bibliography. *Applied Mechanics Reviews*, 47(2):55, 1994.